



THE HONG KONG
POLYTECHNIC UNIVERSITY

香港理工大學

Pao Yue-kong Library

包玉剛圖書館

Copyright Undertaking

This thesis is protected by copyright, with all rights reserved.

By reading and using the thesis, the reader understands and agrees to the following terms:

1. The reader will abide by the rules and legal ordinances governing copyright regarding the use of the thesis.
2. The reader will use the thesis for the purpose of research or private study only and not for distribution or further reproduction or any other purpose.
3. The reader agrees to indemnify and hold the University harmless from and against any loss, damage, cost, liability or expenses arising from copyright infringement or unauthorized usage.

IMPORTANT

If you have reasons to believe that any materials in this thesis are deemed not suitable to be distributed in this form, or a copyright owner having difficulty with the material being included in our database, please contact lbsys@polyu.edu.hk providing details. The Library will look into your claim and consider taking remedial action upon receipt of the written requests.

THE USE OF PULSED ELECTROMAGNETIC FIELD
TO PROMOTE DIABETIC WOUND HEALING IN DIFFERENT WOUND MODELS

RACHEL LAI-CHU KWAN

PhD

The Hong Kong Polytechnic University

2019

The Hong Kong Polytechnic University

Department of Rehabilitation Sciences

The Use of Pulsed Electromagnetic Field
to Promote Diabetic Wound Healing in Different Wound Models

Rachel Lai-Chu Kwan

A thesis submitted in partial fulfilment of the requirements
for the degree of Doctor of Philosophy

January 2019

CERTIFICATE OF ORIGINALITY

I hereby declare that this thesis is my own work and that, to the best of my knowledge and belief, it reproduces no material previously published or written, nor material that has been accepted for the award of any other degree or diploma, except where due acknowledgement has been made in the text.

(Signed)

KWAN LAI CHU

(Name of student)

All of my work is dedicated to Henry, Cheryl and Chloe.

I couldn't have done it without you.

Abstract of thesis entitled “The Use of Pulsed Electromagnetic Field to Promote Diabetic Wound Healing in Different Wound Models” submitted by Rachel Lai-Chu Kwan for the degree of Doctor of Philosophy at The Hong Kong Polytechnic University in January 2019.

ABSTRACT

Wound healing involves complex processes and people with diabetes mellitus (DM) often present with a delay in wound healing. Microvascular changes are common DM-related complications that may lead to foot oedema that is associated with a reduction in oxygen delivery to the tissues that results in foot ulceration. *Pseudomonas aeruginosa* (PAO1) is a common pathogen found in ulcers among people with DM. Photoacoustic measurement is an advanced technology that allows quantitative measurement of the oxyhemoglobin concentration on plantar skin or wound site in human or small animals. An effective treatment for infected DM ulcer may result in restoring normal oxyhemoglobin concentration, which can prevent lower limb amputation. Pulsed electromagnetic field (PEMF) is a potential non-invasive intervention that might be able to control inflammation, enhance tissue perfusion in wound area and promote healing of infected cutaneous wounds. In this thesis, we adopted several animal models to determine whether pulsed electromagnetic field (PEMF) would enhance healing of chronic wound model infected with PAO1.

Therefore, this thesis consists of four inter-related studies. In terms of treatment, a systematic review was conducted to evaluate the effectiveness of biophysical energies in promoting wound healing *in vivo* and *in vitro* diabetic wound models. Then in Study I, we first examined the skin morphology and oxyhemoglobin concentration of plantar soft tissue in people with type 2 DM with or without neuropathy and ulceration. Study II examined the efficacy and underlying biological mechanism of PEMF on restoring oxyhemoglobin concentration and promoting acute dermal wounds healing in Streptozotocin-induced DM rat models. Since DM

wound healing is a complex process that might be contributed by the underlying pathology or exogenous bacteria, we set off to study whether pulsed electromagnetic field would promote healing of infected wound with PAO1 in non-DM model. Subsequently, we examined the efficacy of PEMF in promoting dermal wounds healing with or without PAO1 in a chronic wound model in Study III. In the last part of this thesis (study IV), we further examined the efficacy of PEMF in promoting dermal wounds healing in acute and chronic wounds with or without PAO1 in a transgenic DM mice model.

Chronic wound is a major complication of DM. A positive correlation between the subepidermal oedema and the oxyhemoglobin concentration was found at the heel region of people with DM. People with DM tend to develop subepidermal oedema as compared to their non-DM counterpart. However, epidermal thinning occurs in those people who have already developed DM complications and skin break down may lead to ulceration. Our animal studies demonstrated that PEMF was effective in promoting dermal wounds healing in a streptozotocin-induced DM rat in terms of oxyhemoglobin concentration and wound size, and in non-diabetic chronic wound model in terms of wound size. Moreover, histological analyses showed that PEMF might potentially enhance wound closure, angiogenesis and tissue remodeling in a DM chronic wound model. Yet, large scale clinical trials are warranted to translate the current findings into clinical practice.

PUBLICATIONS ARISING FROM THE THESIS

Publication in peer-reviewed journal

KWAN, R. L. C., LU, S., CHOI, H. M. C., KLOTH, L. C., CHEING, G. L. Y. 2019. Efficacy of Biophysical Energies on Healing of Diabetic Skin Wounds in Cell Studies and Animal Experimental Models: A Systematic Review. *International Journal of Molecular Sciences*, 20(2), 368.

Conference paper

KWAN, R. L. C., CHEING, G. L. Y. Efficacy of Biophysical Energies on Healing of Diabetic Wounds. *International Conference on Dermatology and Cosmetology*. Tokyo, Japan, May 2019.

KWAN, R. L. C., CHEING, G. L. Y. Effects of Pulsed Electromagnetics Field on Oxyhemoglobin Concentration During Diabetic Wound Healing. *22nd Regional Conference of Dermatology (Asian-Australasian)*. Singapore, April 2016.

ACKNOWLEDGEMENTS

Undertaking this PhD has been a truly life-challenging experience for me and it would not have been possible to do without support and guidance that I received from many people.

I would like to first give my deepest gratitude to my supervisor Prof. Gladys Cheing for her kind guidance and earnest encouragement not only in the research study, but also to my personal growth. Without her guidance and constant feedback, this PhD would not have been achievable.

Many thanks also to Prof Luther Kloth, who provided me with professional guidance and invaluable advice for writing the systematic review. Thanks to Prof. Yong-Ping Zheng's research team and technical support. Also, my deep appreciation goes out to the research team members: Dr. Alex Cheung, Dr. Song Lu, Dr. Harry Choi, Dr. Rosanna CHAU, Dr. Clare CHAO, Dr. Kevin Yu, Mr. Thomas NG and Ms. Carmen Ng for their friendship and the warmth they extended to me during my hard time and for always making me feel so welcome.

I would like to thank Dr. Siu-Leung Yip, Dr. Wing-Cheung Wong and the physiotherapy colleague of Kwong Wah Hospital for providing space, patient source and expert opinion for the study. I would also like to thank Dr. Louis Cheung's team, Dr. Chris Lai, Angels of Diabetes, and Community Rehabilitation Network for helping with patient recruitment.

I am also grateful to the general rat-keeping service provided by the Centralized Animal Facilities of the Hong Kong Polytechnic University. This project was supported by the General Research Fund provided by the Research Grants Council of the Hong Kong SAR Government (PolyU 5600/11M).

Lastly, I must thank my husband, Cheryl and Chloe for giving me a happy family; for their kind understanding, spiritual support and sustained encouragement unconditionally all the time.

Table of Contents

ABSTRACT.....	iii
PUBLICATIONS ARISING FROM THE THESIS.....	v
ACKNOWLEDGEMENTS.....	vi
LIST OF FIGURES	xiii
LIST OF TABLES.....	xix
LIST OF APPENDICES.....	xx
LIST OF ABBREVIATIONS.....	xxi
CHAPTER 1	
INTRODUCTION.....	1
1.1 BACKGROUND AND RATIONALE.....	2
CHAPTER 2	
LITERATURE REVIEW	5
2.1 DIABETES MELLITUS (DM)	6
2.2 PATHOLOGIES OF DIABETIC ULCERS.....	6
2.3 PULSED ELECTROMAGNETIC FIELD.....	8
2.3.1 Effects of pulsed electromagnetic fields (PEMF) on wound healing	8
2.3.2 Effects of pulsed electromagnetic fields on <i>Pseudomonas aeruginosa</i>	10
2.4 OBJECTIVES	11

CHAPTER 3

INSTRUMENTATION	13
3.1 MEASUREMENT OF SKIN MORPHOLOGY	14
3.2 MEASUREMENT OF TISSUE OXYHEMOGLOBIN	15
3.3 ASSESSMENT OF WOUND HEALING.....	18
3.4 BIOMECHANICAL TESTING OF THE SKIN WOUND TISSUE	19
3.5 TREATMENT MODALITY: PULSED ELECTROMAGNETIC FIELD	20

CHAPTER 4

THE ASSOCIATION BETWEEN OXYHEMOGLOBIN CONCENTRATION WITH EPIDERMAL OEDEMA IN THE DIABETIC FOOT	22
4.1 INTRODUCTION	23
4.2 METHODS	24
4.2.1 Study Design.....	24
4.2.2 Subjects.....	25
4.2.3 Outcome Measures.....	26
4.2.4 Statistical Analysis.....	28
4.3 RESULTS	28
4.3.1 Demographic characteristics.....	28
4.3.2 Epidermal thickness in plantar skin	30
4.3.3 Subepidermal low echogenic band in the plantar skin.....	31

4.3.4	Oxyhemoglobin concentrations of the plantar skin	32
4.3.5	Deoxyhemoglobin concentrations of the plantar skin	33
4.3.6	Oxygen saturation of the plantar skin	34
4.3.7	Relationship between the oxyhemoglobin concentration and epidermal oedema	35
4.4	DISCUSSION	36
4.5	CONCLUSIONS.....	38

CHAPTER 5

THE EFFECTS OF PULSED ELECTROMAGNETIC FIELD ON

OXYHEMOGLOBIN CONCENTRATION AND WOUND HEALING IN DIABETIC

ACUTE WOUND MODEL.....39

5.1	INTRODUCTION	40
5.2	METHODS	42
5.2.1	Diabetic rat model.....	42
5.2.2	Wound induction.....	42
5.2.3	Treatment protocol.....	43
5.2.4	Outcome measures	45
5.2.5	Statistical Analysis.....	46
5.3	RESULTS	47
5.3.1	Demographic Characteristics	47
5.3.2	Wound area	47

5.3.3	Oxyhemoglobin at the wound sites.....	48
5.3.4	Deoxyhemoglobin of at the wound sites.....	51
5.3.5	Oxygen saturation of at the wound sites	54
5.3.6	Biochemical analysis	57
5.4	DISCUSSION	57
5.5	CONCLUSIONS.....	59

CHAPTER 6

	EFFICACY OF PULSED ELECTROMAGNETIC FIELD IN PROMOTING NON- DIABETIC DERMAL WOUND HEALING WITH OR WITHOUT PSEUDOMONAS AERUGINOSA	60
6.1	INTRODUCTION	61
6.2	METHODS	62
6.2.1	Animal model.....	62
6.2.2	Wound induction.....	62
6.2.3	<i>P.aeruginosa</i> biofilm.....	63
6.2.4	Biofilm application and animal care	63
6.2.5	Treatment protocols	64
6.2.6	Outcome measures	64
6.2.7	Statistical Analysis.....	65
6.3	RESULTS	66
6.4	DISCUSSION	69

CHAPTER 7**EFFICACY OF PULSED ELECTROMAGNETIC FIELD IN PROMOTING
DIABETIC WOUND HEALING WITH OR WITHOUT PSEUDOMONAS**

AERUGINOSA IN TRANSGENIC MICE	71
7.1 INTRODUCTION	72
7.2 METHODS	73
7.2.1 Animal model.....	73
7.2.2 Wound induction.....	74
7.2.3 <i>P.aeuginosa</i> biofilm.....	74
7.2.4 Biofilm application and animal care	75
7.2.5 Treatment protocols	75
7.2.6 Outcome measures	77
7.2.7 Statistical Analysis.....	80
7.3 RESULTS	80
7.3.1 Demographic Characteristics	80
7.3.2 Gross morphology.....	82
7.3.3 Angiogenesis.....	88
7.3.4 Tissue repair.....	94
7.3.5 Biomechanical parameters for the wound specimen	102
7.4 DISCUSSION	103

CHAPTER 8

CONCLUSIONS AND SUGGESTIONS FOR FUTURE RESEARCH 106

APPENDICES 113

REFERENCES 158

LIST OF FIGURES

Figures		Page
3.1	Ultrasound image showing the epidermal and subepidermal low echogenic band thickness at the first metatarsal head of a healthy subject	13
3.2	The sensor consisted of a black plastic baseplate, eight 400 μm -diameter core emitter fibers and a collecting 3 mm-diameter fiber bundle. The fiber tips are inserted through the holes in the plastic baseplate, so the protruding fiber tips length could be adjusted to fit the shape of the human foot or rats wounds	14
3.3	Schematic diagram of the near infrared spectroscopy probe used in this study	14
3.4	Absorption characteristics of oxyhemoglobin (HbO_2) and deoxyhemoglobin (Hb). The yellow box indicated the measuring window of the NIRS	15
3.5	The VeV wound measurement system. The software automatically detects the 3x3 cm target plate in a correct orientation, and then the margin, length and width of the wound were traced on the image of the screen	16
3.6	Hydraulic load frames for tension test by using a piston to apply force to the specimens for preventing wound tissues being destroyed	18
3.7	The rats were placed on top of the applicator for pulsed electromagnetic field exposure	19
4.1	Comparisons of epidermal thicknesses measured at different foot regions between groups	28

Figures		Page
4.2	Subepidermal low echogenic band (SLEB) thickness measured at different foot regions were compared among groups	30
4.3	Oxyhemoglobin concentrations measured at different foot regions were compared among groups	31
4.4	Deoxyhemoglobin concentrations measured at different foot regions were compared among groups	32
4.5	Oxygen saturation measured at different foot regions were compared among groups	33
4.6	Correlation between (A) oxyhemoglobin concentrations and (B) deoxyhemoglobin concentrations, with subepidermal low echogenic band thickness	34
5.1	The full-thickness wound excised by the 6mm biopsy punch	41
5.2	Flow chart showing the samples during the experiment	42
5.3	Change in percentage wound closure in the PEMF and sham PEMF groups over time	46
5.4	The mean oxyhemoglobin concentration of the PEMF and sham PEMF group, as measured by the near-infrared spectroscopy at the (A) wound center and (B) wound edge over time	47
5.5	Scatter plot on oxyhemoglobin concentration of the PEMF and sham PEMF group, as measured by the near-infrared spectroscopy at the (A) wound center and (B) wound edge over time	48

Figures	Page	
5.6	The mean deoxyhemoglobin concentration of the PEMF and sham PEMF group, as measured by the near-infrared spectroscopy at the (A) wound center and (B) wound edge over time	50
5.7	Scatter plot on deoxyhemoglobin concentration of the PEMF and sham PEMF group, as measured by the near-infrared spectroscopy at the (A) wound center and (B) wound edge over time	51
5.8	The mean oxygen saturation of the PEMF and sham PEMF group, as measured by the near-infrared spectroscopy at the (A) wound center and (B) wound edge over time	53
5.9	Scatter plot on oxygen saturation percentage of the PEMF and sham PEMF group, as measured by the near-infrared spectroscopy at the (A) wound center and (B) wound edge over time	54
5.10	Nitrite concentration of the rats in PEMF and sham PEMF group over time	55
6.1	Flow chart showing the samples obtained during the study period	62
6.2	Wound size recorded in various treatment groups on Day 7	64
6.3	Wound percentage change recorded in various treatment groups on Day 7	65
6.4	Oxyhemoglobin and deoxyhemoglobin as measured by near infrared spectroscopy at baseline and post-wounding in C57 mice	66
6.5	Oxygen saturation as measured by near infrared spectroscopy at baseline and post-wounding in C57 mice	66
7.1	Flow chart showing the samples obtained during the study period	74

Figures		Page
7.2	Body weight (mean±SD) measurement in the PEMF-PAO1 and sham PEMF-PAO1 groups throughout the study period	79
7.3	Blood glucose level (mean±SD) measurement in the PEMF-PAO1 and sham PEMF-PAO1 groups on post-wounding Day 23 and 32	79
7.4	Representative macro photographs of acute and chronic wounds taken from 0 to 32 days post-wounding of db/db mice in PEMF and sham groups	81
7.5	Percentage of mice achieving 100% wound closure in the PEMF-PAO1 and Sham PEMF-PAO1 groups	82
7.6	Percentage of wound closure (mean±SD) of the 6 mm diameter circular wound was monitored throughout the study period until day 32.	83
7.7	H&E stained sections of wound tissue obtained on day 14, 23 and 32 in PEMF-PAO1 and shame PEMF-PAO1 group	84
7.8	Re-epithelization percentage of chronic wound in PEMF-PAO1 and sham PEMF-PAO1 group on day 23 and 32	84
7.9	Granulation tissue thickness of PEMF-PAO1 and sham PEMF-PAO1 group measured in hematoxylin and eosin-stained cryosections on day 23 and 32	85
7.10	Effects of PEMF on angiogenesis assessed by the endothelial cell marker CD31. Representative CD31 of PEMF-PAO1 and sham PEMF-PAO1 group on day 23 and 32 post wounding, respectively	86
7.11	Density of vessels in the chronic wound bed in diabetic mice in PEMF-PAO1 and sham PEMF-PAO1 group on day 23 and 32	87

Figures		Page
7.12	Immunohistochemical staining for VEGF expressions in PEMF-PAO1 and sham PEMF-PAO1 groups on day 23 and 32 post wounding	88
7.13	VEGF mean staining intensity of PEMF-PAO1 and sham PEMF-PAO1 groups on day 23 and 32	88
7.14	The mean oxyhemoglobin concentration of the PEMF-PAO1 and sham PEMF-PAO1 group, as measured by the near-infrared spectroscopy on different days of wound healing	89
7.15	The mean deoxyhemoglobin concentration of the PEMF-PAO1 and sham PEMF-PAO1 group, as measured by the near-infrared spectroscopy on different days of wound healing	90
7.16	The mean oxygen saturation of the PEMF-PAO1 and sham PEMF-PAO1 group, as measured by the near-infrared spectroscopy on different days of wound healing	91
7.17	The population of α -SMA measured in PEMF-PAO1 and sham PEMF-PAO1 groups on day 23 and 32	92
7.18	Graph showing the α -SMA staining area fraction of the PEMF-PAO1 and sham PEMF-PAO1 wounds on post-wounding day 23 and 32.	93
7.19	The α -SMA mean staining intensity (arbitrary unit) of the PEMF-PAO1 and sham PEMF-PAO1 wounds	94
7.20	Representative picro-sirius red stained sections form PEMF-PAO1 and sham PEMF-PAO1 groups on days 23 and 32	96

Figures		Page
7.21	Thick mature (red) to thin immature (green) collagen ratio of chronic wound tissues in PEMF-PAO1 and sham PEMF-PAO1 groups on day 23 and 32	97
7.22	Type I collagen fibril deposition of samples from PEMF-PAO1 and Sham PEMF-PAO1 groups on days 23 and 32	98
7.23	Type I collagen fibril alignment of samples from PEMF-PAO1 and Sham PEMF-PAO1 groups on days 23 and 32	99
7.24	Type I collagen fibre anisotropy of samples from PEMF-PAO1 and sham PEMF-PAO1 on days 23 and 32	99
7.25	Type I collagen fibre orientation angle measured form the epidermis between PEMF-PAO1 and sham PEMF-PAO1 groups on day 23 and 32	100

LIST OF TABLES

Table		Page
4.1	Demographic characteristics of the participants	27
7.1	Biomechanical parameters to the healing mice skin wounds of db/db mice as measured by the material testing system ex vivo	101

LIST OF APPENDICES

Appendix		Page
I	Patient Information Sheet and Consent Form (English version) for Study I	111
II	Patient Information Sheet and Consent Form (Chinese version) for Study I	113
III	Subject recruitment leaflet for Study I	115
IV	Published peer-reviewed article	117
V	Conference abstract	154

LIST OF ABBREVIATIONS

α -SMA	Alpha-smooth muscle actin
ANOVA	Analysis of variance
DM	Diabetes mellitus
DPN	Diabetic polyneuropathy
DU	Diabetic ulceration
H&E	Hematoxylin and eosin
Hb	Deoxyhemoglobin
HbA1c	Glycated hemoglobin
HbO ₂	Oxyhemoglobin
ICC	Intraclass correlation
LB	Lysogeny broth
LSD	Least significant difference
NHS	Normal horse serum
NIRS	Near infrared spectroscopy
NO	Nitric oxide
PEMF	Pulsed electromagnetic field
PAO1	<i>Pseudomonas aeruginosa</i>
PBS	Phosphate-buffered saline
SD	Sprague Dawley
SLEB	Subepidermal low echogenic band
STZ	Streptozotocin
VEGF	Vascular endothelial growth factor

CHAPTER 1

INTRODUCTION

1.1 BACKGROUND AND RATIONALE

Foot ulcer is a serious complication that could lead to lower limb amputation among people with diabetes. Identification on the risk factors of chronic foot ulceration is crucial for limb salvage. Microvascular disturbance is commonly found in people with diabetes mellitus (DM), it may cause foot oedema and lead to reduction in oxygen delivery to the tissues, which subsequently results in foot ulceration. Exogenous factors including bacteria infection is frequently found in DM ulcer. Previously, there is a lack of quantitative methods to measure the oxyhemoglobin concentration in the plantar soft tissues and wound tissues in people with diabetes. Transcutaneous partial pressure of oxygen has been a common method for measuring oxygen perfusion in persons with diabetes. However, the measurement procedures require the heating the electrode that causing dermal capillary dilation, oxyhemoglobin dissociation and enhancement (Hurley, 2008). There is an urgent need to identify a quantitative assessment of DM ulcer. Measurement of oxyhemoglobin concentration on plantar skin maybe a potential clinical assessment of DM ulcer that provides useful information on the prognosis of foot ulcer. With the advanced near infrared spectroscopy, the oxyhemoglobin, deoxyhemoglobin concentrations and oxygen saturation in the plantar soft tissues and wound tissues could be measured. An objective monitoring of chronic wound healing is vital to assist clinicians making optimal treatment strategies in a timely manner.

Our earlier research work found that subepidermal oedema occurs in the foot of people with diabetes without neuropathy and people with diabetic ulceration (Chao et al., 2012). However, relationship between skin morphological changes and the oxyhemoglobin concentration in foot of people with diabetic neuropathy were not known. As the people with diabetic peripheral neuropathy are at higher risk of ulceration, the information on the changes of the skin morphology and oxyhemoglobin concentration is crucial for screening risk of foot ulceration. The use of near infrared spectroscopy can provide information on the unexplored relationship

between the oxyhemoglobin concentration and the skin morphological changes in people with diabetic complications. This can also allow a better understanding of the pathophysiological mechanisms of the diabetic ulcer formation.

Pulsed electromagnetic field (PEMF) has been used for improving venous ulcer and diabetic wound healing. It was also shown to increase microvascular blood flow and nerve conduction in people with diabetes. However, the underlying biological mechanisms of the pulsed electromagnetic field towards the oxyhemoglobin concentration changes and skin morphology are unclear. The PEMF is a potential therapy that may restore oxyhemoglobin concentration and foot oedema in people with DM foot ulceration. Since DM wound healing is a complex process that might be contributed by the underlying pathology or exogenous bacteria, we set off to examine whether PEMF would promote wound healing with *Pseudomonas aeruginosa* (PAO1) without diabetes.

Therefore, we hypothesized that people with advance diabetic foot complications might represented increase foot oedema and poor oxygenation of skin. Moreover, we hypothesized that pulsed electromagnetic field might be effective in promoting dermal wounds healing in streptozotocin-induced diabetic rat model, non-diabetic dermal wounds in mice and chronic wound healing in transgenic diabetic mice.

Detailed literature review will be provided in Chapter 2. The instrumentation used in this study is described in Chapter 3. Chapter 4 compare the skin morphology and the oxyhemoglobin concentration of plantar soft tissue in people with type 2 diabetes mellitus with or without neuropathy and ulceration. Chapter 5 examines the efficacy of pulsed electromagnetic field on restoring of the oxyhemoglobin concentration and its related biological mechanisms in promoting dermal wound healing in Streptozotocin-induced diabetic rata. Chapter 6 reports the efficacy of PEMF in promoting wound healing of non-diabetic dermal wounds with or without *Pseudomonas aeruginosa* in mice. Chapter 7 demonstrates the efficacy of PEMF in promoting

dermal wounds healing with or without *Pseudomonas aeruginosa* in a transgenic diabetic mice.

The last chapter will conclude the present study and provide insight in future research direction.

CHAPTER 2

LITERATURE REVIEW

2.1 DIABETES MELLITUS (DM)

Diabetes is a lifelong metabolic condition. The number of diabetic cases worldwide is continuously increasing. In year 2018, 500 million people were estimated with diabetes worldwide (Kaiser et al., 2018), and this number is expected to rise continuously (Guariguata et al., 2014). In China, the estimated prevalence of diabetes was 11.6%, suggested that 113.9 million Chinese adults suffer from diabetes (Xu et al., 2013). Diabetic foot complications result in huge costs for both society and individual patients worldwide. Lower limb amputation results in a significant economic problem particularly for those required prolonged hospitalization. Diabetes mellitus are classified as type 1 and type 2. Type 1 is characterized by absolute insulin deficiency. In contrast, type 2 diabetes is a combination of insulin resistance and a relative of insulin deficiency, and is frequently not diagnosed until complications appear. Many people with diabetes develop complications that seriously affect the life expectancy and quality of life.

2.2 PATHOLOGIES OF DIABETIC ULCERS

Chronic foot ulcer is a common diabetes complication, and is the leading cause of non-traumatic lower limb amputation. The causes of diabetic foot ulcers are multifactorial including peripheral neuropathy, vascular disturbance and biomechanical alteration. Diabetes imposes impact on complex wound healing. Hyperglycemia, neuropathy, ischemia, foot deformities or infections are high risk factors for DM foot ulcers (Alavi et al., 2014). Excessive oxidant production and repeated inflammation at the wound makes it difficult to heal.

Autonomic, motor and sensory neuropathies are all correlated, and are commonly seen at the foot region of people with diabetes. Autonomic neuropathy causing absence of sweating, thus callosities without hydration tend to fissure and serving as a portal for infection. The

arteriovenous shunts controlled by the autonomic nerves that located at the sole of the foot were inappropriately dilated and causing dry feet. Motor neuropathy causing interosseous foot muscles wasting and also stiffen up the plantar soft tissues in people with diabetes (Chao et al., 2011), thus altering the biomechanical function over the foot and the abnormal weight bearing skin. The fat pad over the metatarsal heads were moved distally, leaving the metatarsal head press on the tissue during walking, and eventually causing ulceration at these weight bearing points. Sensory neuropathy causing inadequate sensation over the foot of people with diabetes allows trauma go unnoticed, resulting from traumatic ulceration (Sumpio, 2012).

People with long history of diabetes are more likely to develop angiopathy in both macro- and microvascular systems (Cheing et al., 2013). Microvascular disturbance results from glycosylation contribute to the diabetic neuropathy and non-healing wound. The sympathetic nerves that control blood flow to the feet were damaged by high blood glucose. The vasoconstrictive response to standing is substantially reduced (Chao and Cheing, 2009), so the blood flow to the skin of the foot remains high at weight bearing position. In addition, the autonomic neuropathy causing a decrease in nutritional flow in the skin relative to arteriovenous shunt for people with diabetes (Chao and Cheing, 2009), and this may lead to diffuse soft tissue oedema in the foot.

The capillary permeability, vasoconstriction and vasodilation were controlled by the endothelium-derived factor which was later determined to be the free radical species nitric oxide (NO) (Soneja et al., 2005). Nitrogen oxide level in tissue is proinflammatory that accounts for leaky blood vessels associated with swelling (Levy et al., 2005). There are numerous factors that may influence either the production of NO or the diffusion of NO to its cellular targets. Reduced bioavailability of NO contributes to the changes in vascular tone. Acute hyperglycemia found in people with diabetes attenuates endothelium-dependent vasodilatation (Akbari et al., 1998, Williams et al., 1998). In addition, hyperglycemia

accelerates the glycation of hemoglobin affecting its affinity towards NO (Milsom et al., 2002), and was directly correlated to the increase in prevalence of amputation (Klein, 1995). Hyperglycemia increase NO release by enhancing endothelium isoform of NO synthase through increased intracellular concentrations (Taubert et al., 2004), but also influence the transport of NO to its cellular targets and thus affect its bioavailability. Several pathways were proposed for NO metabolism for transporting from the producing region downstream to the microcirculation. First, by oxidizing the oxyhemoglobin to form methemoglobin and nitrate ion. Second, combining with deoxyhemoglobin to form nitrosyl hemoglobin. Third, nitrosylation of the thio groups of the hemoglobin to form S-nitrosothiols (Moncada et al., 1991). However, plasma concentrations of NO in people with diabetes were found increased (Chien et al., 2005). Highly glycated oxyhemoglobin impairs the nitric oxide mediated responses by superoxide ions (Vallejo et al., 2000). The excessive and prolonged production of the superoxide radicals in wounds combined with the NO produces the toxic peroxynitrite and peroxynitrous acid that cause tissue hypoxia and impair the wound healing process (Soneja et al., 2005).

2.3 PULSED ELECTROMAGNETIC FIELD

2.3.1 Effects of pulsed electromagnetic fields (PEMF) on wound healing

Foot oedema is commonly found in people with diabetes. The oedema would affect the local tissue tension that impose risk of tissue breakdown and ulceration, and may impair the oxygen saturation of wound during healing process. Early management on foot oedema and diabetic ulcers is crucial to save the limb from amputation. Pulsed electromagnetic field has been used in clinical setting to promote diabetic wound healing, and is a potential treatment in reducing foot oedema and restore oxygen concentrations in people with diabetes. Our team conducted a systematic review and demonstrated that electrophysical therapy can bring beneficial effects

that promote the diabetic ulcers healing (Kwan et al., 2013). Pulsed electromagnetic field (PEMF) is a useful non-thermal adjunctive therapy for treatment of chronic wounds. The device can be applied over dressings, braces, or clothing. PEMF was shown to increase peripheral blood flow and oxygen perfusion of ischemic feet for people with diabetes (Webb et al., 2003). In addition, PEMF could relieve symptoms and nerve conductive dysfunction caused by diabetic neuropathy (Musaev et al., 2003). Moreover, our earlier study found that PEMF produces positive results in promoting ulcer healing by means of improving the microcirculation of diabetic foot (Kwan et al., 2015).

In our recently published pre-clinical systematic review (Kwan et al., 2019), we found five studies compared PEMF with sham treatment (Callaghan et al., 2008, Cheing et al., 2014, Choi et al., 2016, Goudarzi et al., 2010, Choi et al., 2018). The studies conducted by our research team compared 2 mT, 5 mT and 10 mT of 25 Hz sinusoidal PEMF in male SD rats with sham treatment (Cheing et al., 2014, Choi et al., 2016, Choi et al., 2018). Another study compared 8 mT, 20 Hz PEMF in male Wistar rats with sham treatment (Goudarzi et al., 2010). Moreover, one study involved both *in vitro* and *in vivo* studies using human umbilical vein endothelial cells, db/db mice, C57BL6 mice and FGF-2 knockout mice (Callaghan et al., 2008). Previous studies have reported significant between-group difference in the percentage of original wound size, and the experimental groups in all these studies demonstrated improved wound healing compared to the control groups (Callaghan et al., 2008, Cheing et al., 2014, Goudarzi et al., 2010, Choi et al., 2018).

PEMF has also been used for managing postoperative lymphedema (Heden and Pilla, 2008). Endothelium isoform of NO cascade is dependent on the binding of calcium and calmodulin. It was proposed that PEMF could accelerate calcium ions binding to calmodulin when homeostasis is interrupted (Weissman et al., 2002), that contributes to initial oedema, blood vessel growth, tissue regeneration and remodeling (Bruckdorfer, 2005) in the wound model

(Strauch et al., 2007). PEMF can be configured to modulate calcium-binding kinetics to calmodulin, then activates nitric oxide synthase and the relevant cascade ensues dependent for pain relieve and edema control. Moreover, PEMF demonstrated a positive effect on edema by acting on sodium-potassium pump in the cell membrane (Strauch et al., 2009). In addition, PEMF appears to enhance the release of oxygen from hemoglobin, that has been shown to reduce inflammation and enhance tissue repair (Muehsam et al., 2013). Therefore, PEMF might bring beneficial effects to healing of diabetic ulcers.

2.3.2 Effects of pulsed electromagnetic fields on *Pseudomonas aeruginosa*

Biofilm formation is a significant factor contributing to non-healing chronic wound to people with diabetes. The common clinical management of wound infection is the prescription of antibiotics and frequent debridement. However, the control of biofilm persistence and growth become difficult due to the development of resistance to antibiotics in patients. Therefore, researchers have tried to use biophysical agents to eradicate biofilm. *Pseudomonas aeruginosa* is a common pathogen associated with diabetic foot infections. In previous studies, *Pseudomonas aeruginosa* showed differences in DNA, growth rate and antibiotic sensitivity when exposed to pulsed electromagnetic field, while *S. aureus* and *S. epidermidis* did not differ in DNA, growth rate and antibiotic sensitivity following such exposure (Inhan-Garip et al., 2011, Fijalkowski et al., 2015, Salmen et al., 2018). Moreover, 60 minutes exposure to the pulsed electromagnetic field showed significant inhibition on *Pseudomonas aeruginosa* metabolic activity and biofilm formation, but not in Gram positive pathogens (Fijalkowski et al., 2015). *In vitro*, pulsed electric fields can eradicate *Pseudomonas aeruginosa* and disrupt biofilms in mesh implants without damaging the mesh (Khan et al., 2016). Moreover, addition of pulsed electric fields to antibiotics can inactivate *Pseudomonas aeruginosa in vitro* (Rubin et al., 2018). Other than pulsed electric fields, Segatore and colleagues showed that there was

significantly decreased in bacteria after the exposure of *Pseudomonas aeruginosa* to extremely low frequency electromagnetic fields although the antibiotic susceptibility was not comparable in exposed groups and control groups (Segatore et al., 2012). Unpublished pilot study in our research team showed that 20 Hz PEMF augments the antibiotic effect of gentamicin and significantly suppresses the viability of *Pseudomonas aeruginosa*. Morphological changes in *Pseudomonas aeruginosa* were seen after exposure to pulsed electromagnetic field under 0.75 MIC of gentamicin. In contrast, PEMF delivered at 72 Hz appear to enhance the survival of *Pseudomonas aeruginosa*, suggesting the effects of PEMF towards *Pseudomonas aeruginosa* is dose-specified (Choi, 2016).

Unfortunately, all previous studies of PEMF on *Pseudomonas aeruginosa* were performed *in vitro*. There was no study done to evaluate the effects of biophysical agents on diabetic chronic wounds due to lack of an appropriate model. However, human diabetic wounds usually presents with a combination of circulation impairment, chronic inflammation and bacteria biofilm. Recently, Zhao and his colleagues (2010, 2012) successfully developed a chronic diabetic wound model by inoculating the wound with *Pseudomonas aeruginosa* in transgenic db/db mice. Therefore, there is a research gap that the efficacy of PEMF on enhancing chronic wound healing and the underlying mechanisms can be investigated.

2.4 OBJECTIVES

Therefore, the specific aims of the studies embedded in the present thesis were as follows:

- To compare the extent of foot oedema and oxygenation of skin in people who are at different stages of diabetic foot complications (Study I)
- To examine the association of foot oedema and oxygenation of skin in people with diabetes (Study I)

- To evaluate the efficacy of pulsed electromagnetic field for promoting dermal wounds healing in a streptozotocin-induced diabetic rat model (Study II)
- To investigate the underlying biological mechanisms of pulsed electromagnetic field for restoring oxyhemoglobin in the healing of dermal wound in a diabetic rat model (Study II)
- To examine the effectiveness of pulsed electromagnetic fields in promoting wound healing of non-diabetic dermal wounds in mice (Study III)
- To determine the efficacy of pulsed electromagnetic field in promoting chronic wound healing using transgenic diabetic mice (Study IV).

CHAPTER 3

INSTRUMENTATION

This chapter describes the instrumentation and treatment modalities used in the studies of this thesis. High frequency ultrasound was used to measure the skin morphology in terms of epidermal thickness and subepidermal oedema; near infrared spectroscopy was used to examine the oxyhemoglobin and deoxyhemoglobin concentration in the plantar skin and at the wound site; material testing system was used to examine the biomechanical properties of the wound tissues. In addition, wound size measurement was used to monitor the wound healing.

3.1 MEASUREMENT OF SKIN MORPHOLOGY

A high-frequency ultrasound scanner with a Vevo model 708 scanhead (VisualSonics Inc, Toronto, ON, Canada) was used for imaging skin morphology. The ultrasound system consists of a transducer, which emits ultrasound beams with a central frequency of 55 MHz that gives an axial resolution of 30 μm and a lateral resolution of approximately 70 μm , producing high-resolution images to a maximum depth of 8 mm. The system displays the information obtained in the form of a B-scan in a gray scale image. The ultrasound biomicroscopy scans were performed on the big toe, first metatarsal head, third metatarsal head, fifth metatarsal head, medial foot arch and the heel of the right foot. After ultrasound gel was applied over the measuring sites, the Vevo model 708 probe was placed perpendicular to the surface of the skin during the capturing of the image. The pressure of the transducer on the surface of the skin was minimized to avoid compressing the surface of the skin. By using fractal geometry, quantitative data on the epidermal thickness were measured by analyzing the change in the echogenicity of the ultrasound image on each sonogram. The first entry echo corresponds to the interface between the coupling gel and surface of the skin, followed by a broad echo-rich band underneath corresponding to the epidermis. Then it is followed by a thin echolucent band, the subepidermal low echogenic band, which corresponds to the upper dermis (Figure 3.1). After boundaries of different layers were identified, the thickness of the skin at various layers, as

defined as the distance between the demarcation echo lines, was then calculated by the in-house Vevo image analysis software. The mean of the measurements for the two images obtained at each testing point was used to analyze the data.

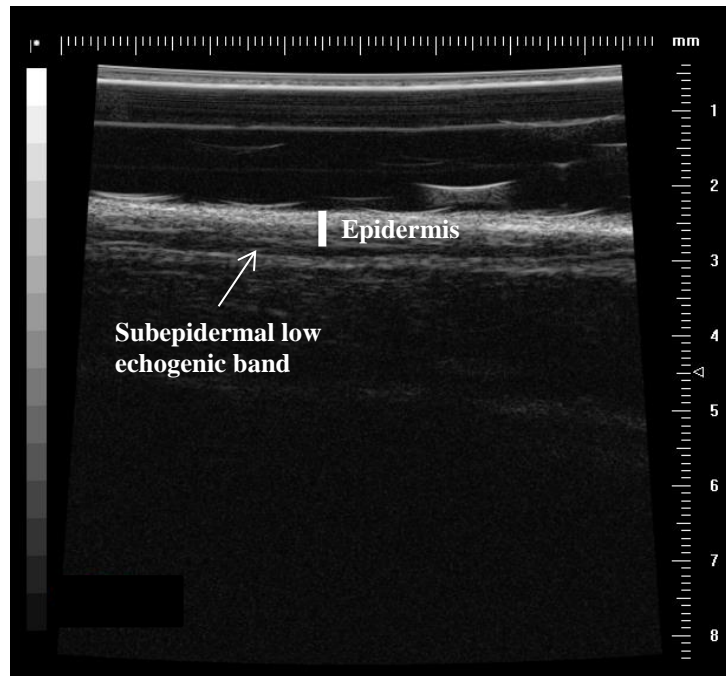


Figure 3.1 Ultrasound image showing the epidermal and subepidermal low echogenic band thickness at the first metatarsal head of a healthy subject.

3.2 MEASUREMENT OF TISSUE OXYHEMOGLOBIN

Near infrared optical measurements were performed on the intact skin of the human plantar foot and wound, or at the incised wound on rodents by a frequency-domain tissue spectrometer (Imagent®, ISS Inc., Champaign, IL). The amplitude and phase data from the four source-detector distances (ranging from 0.7, 1.0, 1.3 and 1.6 cm) were analyzed using the frequency-domain multi-distance method to calculate absorption and reduced scattering coefficients at two wavelengths (690 and 830 nm) at a frequency of 110 MHz (Figure 3.2 and 3.3). The

chromophores in the wound that absorb light delivered at the two wavelengths are primarily oxyhemoglobin and deoxyhemoglobin.



Figure 3.2 The sensor consisted of a black plastic baseplate, eight 400 μm -diameter core emitter fibers and a collecting 3 mm-diameter fiber bundle. The fiber tips are inserted through the holes in the plastic baseplate, so the protruding fiber tips length could be adjusted to fit the shape of the human foot or rodents' wounds.

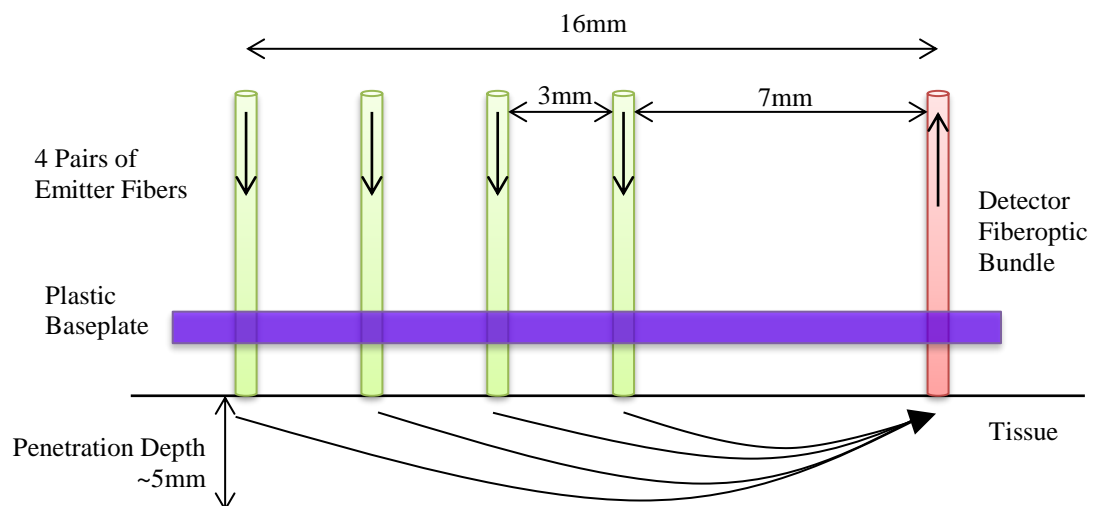


Figure 3.3 Schematic diagram of the near infrared spectroscopy probe used in this study.

This device measures the amplitude and phase shift of light as it transverses through the tissues. The light passes through tissue is being absorbed and scattered. The absorption of the hemoglobin by near infrared light increases below 650 nm to the point that no measurable light can pass through the tissue. Alternately, the absorption of water makes detection of light passing through tissue difficult above 900 nm. Thus, there is a unique window within which tissues can be probed by near infrared light between 670 and 900 nm. From these coefficients, the absolute values of oxyhemoglobin, deoxyhemoglobin concentration and percentage oxygen saturation were calculated (see Figure 3.4).

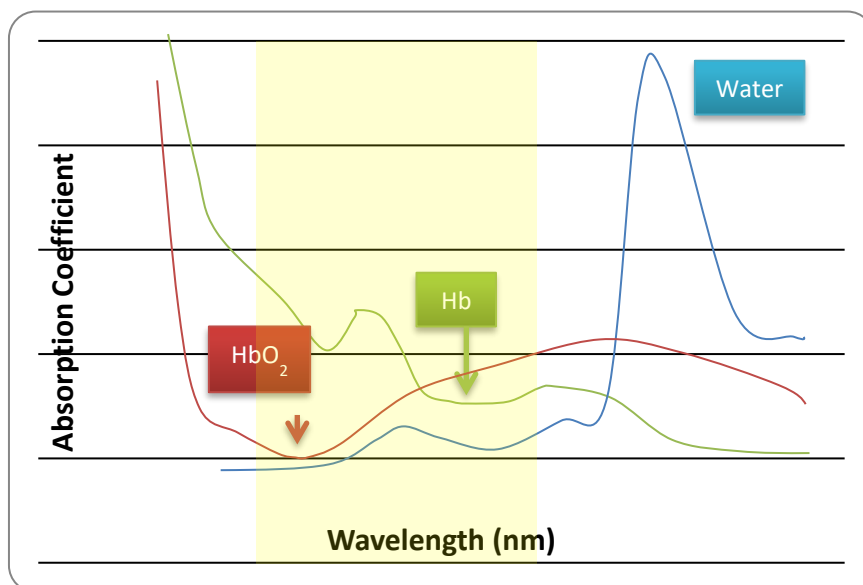


Figure 3.4 Absorption characteristics of oxyhemoglobin (HbO₂) and deoxyhemoglobin (Hb). The yellow box indicated the measuring window of the NIRS.

The near infrared collected a single data point in every 0.04 ms, and at all measurement points the probe was hand-held in continuous parallel to the wound or plantar skin tissue for a period of approximately 120 seconds. Two measurements were made at each site to ensure reproducibility, and the average of these two measurements was calculated for subsequent analysis.

3.3 ASSESSMENT OF WOUND HEALING

Digital images of the wound were obtained by one assessor after the wound cleansing, by using a compact digital camera (Nikon Coolpix P5100, Nikon, Tokyo, Japan). A square-shape target plate (VeV Measurement Documentation, Vista Medical, Winnipeg, Manitoba, Canada) of 3x3 cm was positioned adjacent to, and in the plane of the wound before capturing the image (Figure 3.5). The distance of the camera was fixed by a stand and the light supply of the room was kept constant across days. The images of the ulcers together with a paper square of 3x3 cm² were taken by the digital camera. The photos were taken with standard settings and output as Joint Photographic Experts Group (JPEG) format. The width, length and the size of the ulcers were calculated by tracing the boundaries with VeV wound measurement system (VeV Measurement Documentation, Vista Medical, Winnipeg, Manitoba, Canada). Excellent intrarater reliability (ICC_{3,1}=0.99) and interrater reliability (ICC_{2,1}=0.94) of the VeV wound measurement system was demonstrated in previous study (Thawer et al., 2002). In addition, the computerized technique is comparable with the well-established manual tracing technique when used by equally trained assessors (ICC_{2,1}=0.94; ICC_{2,2}=0.98) (Thawer et al., 2002).

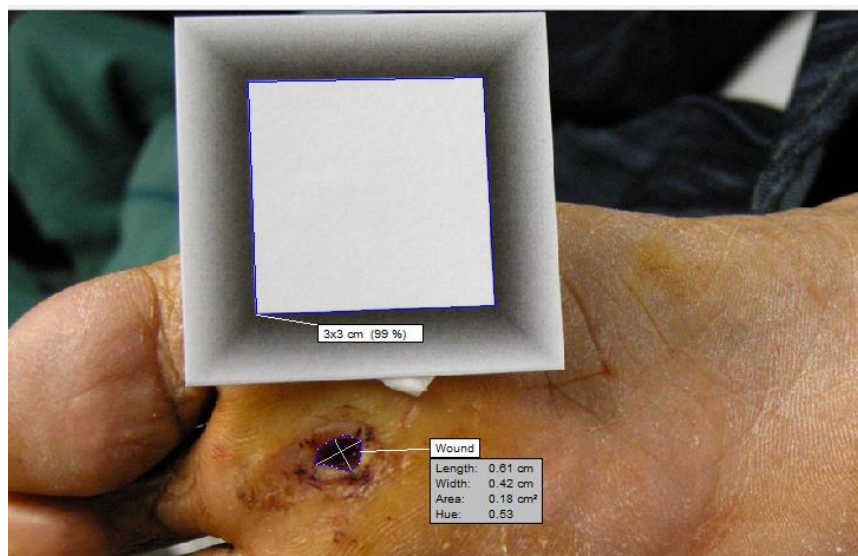


Figure 3.5 The VeV wound measurement system. The software automatically detects the 3x3 cm target plate in a correct orientation, and then the margin, length and width of the wound were traced on the image of the screen.

3.4 BIOMECHANICAL TESTING OF THE SKIN WOUND TISSUE

The biomechanical properties of healing skin wound tissues in terms of maximum load, maximum stress, Young's modulus and energy absorption capacity were collected via Bluehill 3 Systems (Instron Corporation, Norwood, MA, USA) *ex vivo* using a material testing system (Instron ElectroPuls E1000 manufactured by Instron Corporation, Norwood, MA, USA) (Figure 3.6). Seven mice were randomly selected and sacrificed by cervical dislocation under anesthesia on day 24 and day 32 post-wounding, and the animal bodies were stored in a -80 °C freezer until use. At least 6 h prior to biomechanical testing, the bodies were thawed in room temperature and the skin wound specimens on back were carefully dissected from the wound site to remove all surrounding soft tissues. The remaining skin layer was cut into strips with the dimension of 6.0 mm x 25.0 mm. The specimen geometry, including the length, width, and thickness, was measured using Vernier digital calipers before biomechanical testing. The skin strips were then mounted on the clamps of the material testing system. The room temperature was controlled at around 25 °C and the wound specimen was kept moist by wrapping with plastic film until the experiment started. The specimens were tested with the same protocols adopted in our previous study (Choi et al., 2018). The tissue specimen was elongated to a 2.5% strain position at 0.167 mm/s for 10 preconditioning oscillation cycles to minimize the deep freeze effect on the wound tissue. After preconditioning, the specimen was elongated to 2.5% strain for 5 min and viscoelasticity testing was conducted accordingly (Ng et al., 2004). Unloading then took place for another 5 min to allow the specimen to return to its original length. Tensile biomechanical properties were measured by elongating the specimen at a speed

of 8.33 mm/s until failure. Load and deformation were recorded at 100 Hz. The load relaxation property was measured by subtracting the final load by the initial load, then dividing by the initial load times 100%. The failure test was conducted according to the protocol of a previous study (Ng et al., 2011). A load-deformation curve was plotted to examine the structural properties of the specimen and the curve was transformed into a stress-strain curve by dividing the load with the cross-sectional area (stress) and the elongation with the original length (strain) to examine the biomechanical properties.

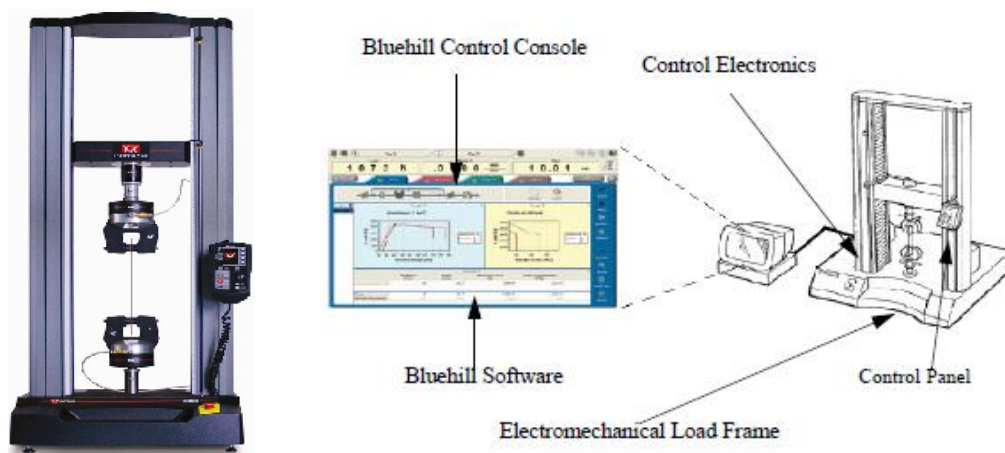


Figure 3.6 Hydraulic load frames of the material testing system for tension test by using a piston to apply force to the specimens for preventing wound tissues being destroyed (Instron, 2009).

3.5 TREATMENT MODALITY: PULSED ELECTROMAGNETIC FIELD

Several species of rodents have been used in the present thesis including streptozotocin-induced diabetic SD rats, C57 mice or transgenic db/db mice. Rodents were randomly allocated into either the PEMF group or the sham PEMF groups. The PEMF treatment was given on post-wounding day 1. The rats in the PEMF group were fixed in the rodent restraint bags (BS4 72-6408, Harvard Apparatus, Holliston, MA), while the mice were fixed in the plastic cage

placed on top of the disc applicator of the PEMF device (BTL-4000, Magnet, BTL Industries Ltd., UK). The wound was placed at the central space area close to the wall of the applicators to ensure the delivery of a maximum uniform magnetic field was distributed (Figure 3.7). For the study with SD rats (Study II), the PEMF generator produced a train of sinusoidal pulses with a width of 3 ms, giving an overall frequency of 25 Hz. The maximum field applied to the sample was 2 mT and was measured by the hand-held Gauss/Tesla meter (Model 4048, F.W. Bell, Milwaukie, OR). For the studies with mice (Study III and IV), the maximum field applied was 5 mT with an overall frequency of 20 Hz. The wounds were exposed to active PEMF for 60 min on a daily basis until the rats were sacrificed. The rodents in the sham PEMF group were handled in the same manner but without exposing to PEMF.

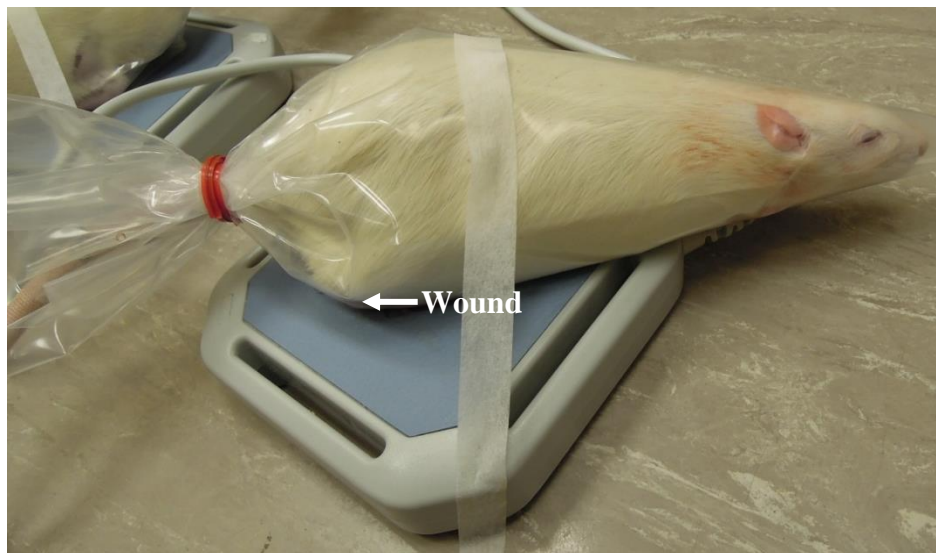


Figure 3.7 The rats were placed at the top of the PEMF applicator during intervention.

CHAPTER 4

**THE ASSOCIATION BETWEEN OXYHEMOGLOBIN CONCENTRATION WITH
EPIDERMAL OEDEMA IN THE DIABETIC FOOT**

An earlier study conducted by our research team showed that the epidermal layer of people with diabetes (DM) without complications is thicker than that in healthy control, but people with diabetic neuropathy presented with thinnest epidermal layer among the three groups (Chao et al., 2011). In addition, the subepidermal low echogenic band thickness was increased in people with diabetic complications (Chao et al., 2012), which reflects subepidermal edema. The oxyhemoglobin concentration can be an important indicator to predict the prognosis of DM wound healing, but the relationship between the oxyhemoglobin concentration and subepidermal oedema remained unclear in DM subjects with or without complications. Thus, the present chapter conducted a cross sectional study that examines the oxyhemoglobin concentration among DM subjects with or without complications; and the relationship between oxyhemoglobin concentration and subepidermal oedema was explored.

4.1 INTRODUCTION

Impaired peripheral blood flow (Delbridge et al., 1985) and microcirculation (Chao and Cheing, 2009) is the main predisposing factors for diabetic foot ulceration. For persons with diabetic polyneuropathy, the vasoconstrictive response to standing is substantially reduced (Chao and Cheing, 2009) and so the skin blood flow remains high with gravity. An increase in capillary filtration may cause thickening of capillary basement membranes, also increases the oxygen and nutrient diffusion distance travel from capillaries to tissues, and impair oxygen diffusion (Gibbons, 2003).

It is well known that tissue oxygenation is important for wound healing. Transcutaneous partial pressure of oxygen is a common method for measuring oxygen perfusion in persons with diabetes. However, the measurement procedures require the heating the electrode that causing dermal capillary dilation, oxyhemoglobin dissociation and enhancement (Hurley, 2008). Subsequently, near infrared spectroscopy was developed to measure the absolute

oxyhemoglobin, deoxyhemoglobin concentrations and oxygen saturation in superficial tissues. Measurements of these parameters provide regional information that indicative for microvascular changes, and can also provide useful information in differentiate the stages of vascular damages on the lower limbs that contributes to ulcer development. Papazoglou and colleagues found that higher average value of oxyhemoglobin and deoxyhemoglobin concentration in the wound tissues of the diabetic rats as compared to the control rats (Papazoglou et al., 2006). The authors postulated that continued inflammation at the wound (Weingarten et al., 2008) with higher density of vasculature and low oxygen delivery might be the reasons that contribute to higher value of oxyhemoglobin concentration in the diabetic rats. Clinically, it is common to observe foot oedema in people with DM. Foot oedema reflects distortion in skin microcirculation, which usually occurs precede the development of chronic foot ulceration, early detection of foot oedema may prevent subsequent foot complication for people with diabetes. However, there was a lack of precise measurement for foot oedema. Until recently, our research team first identified the subepidermal foot oedema in persons with diabetes by using the high frequency ultrasonography (Chao et al., 2012). No study has investigated the relationship between foot oedema and skin oxygenation, and their subsequent impact on the delayed in wound healing remains unclear. Therefore, the present study evaluated the skin morphology and oxyhemoglobin concentration of plantar soft tissue in people with type 2 DM with or without neuropathy and ulceration.

4.2 METHODS

4.2.1 Study Design

A cross sectional exploratory study was conducted.

4.2.2 Subjects

A priori power analysis using PASS (NCSS, 2008) was conducted based on our earlier study with an effect size of 1.38 (Chao et al., 2012). With an alpha level of 0.05, statistical power of 80% and about an estimated 10% dropout rate, 33 subjects should be recruited (i.e. 11 subjects in DM, DPN and DU groups).

Seventy-six subjects (69 people with type 2 DM but without neuropathy [DM group], 1 with diabetic peripheral neuropathy [DPN group], 1 with a history of diabetic foot ulceration [DU group], and 5 non-DM) participated in the present study. All subjects aged above 18 and had a confirmed diagnosis with type 2 diabetes were recruited from the community centers in the period of January 2014 to December 2014. Subjects with poorly controlled diabetes, renal failure requiring renal replacement therapy, history of radiotherapy to the foot, history of malignancy and having a pace maker were excluded from the present study.

Diabetic peripheral neuropathy was identified by the use of the 10-g Semmes-Weinstein monofilament (lack of feeling in at least three of the following 10 testing points: the pulp of first, third, and fifth toes; the plantar aspects of the first, third, and fifth metatarsal heads; the plantar medial and lateral sides of the midfoot; the plantar area of the heel; and the dorsal aspect of the midfoot) and a vibration perception threshold of above 25 volts at the big toe. Inability to sense 3 out of 10 measurement points with 10-g monofilament is consistent with severe neuropathy and loss of protective sensation, thus at greater risk of diabetic ulceration. Lack of vibration sense over the big toe carries similar risk.

The subject in the foot ulceration group either had a history of diabetic foot ulceration below the malleoli level or were currently suffering from that condition. Subjects in the non-DM group were recruited from the community by convenience sampling. They had no history of DM or any other form of neuropathy or arterial disease; and all of them passed the HbA1c blood test. Subjects were excluded if they had peripheral vascular disease as determined by the

absence of both posterior tibial and dorsalis pedis pulses and the presence or symptoms of intermittent claudication and with an ankle brachial index smaller than 0.9, unstable cardiac condition, or malignancy.

Sensory test was undertaken on the foot with a history or present condition of foot ulceration. For subjects who had no history of diabetic ulcers, the right foot was tested. If the ulcerated foot had been partially amputated or if any skin lesions were found on the measuring sites, the contralateral foot was tested. Ethical approval for the study was obtained from a local university. Written consent to participate in the study was obtained from each subject.

4.2.3 Outcome Measures

The temperature of the assessment room was maintained at 23 to 25° C, with humidity controlled at 45 to 60%.

4.2.3.1 Measurement of the thickness of the epidermal and subepidermal low echogenic band (SLEB)

A high-frequency ultrasound scanner with a Vevo model 708 scanhead operating at the center frequency of 55 MHz (VisualSonics Inc, Toronto, ON, Canada) was used for imaging skin morphology. This frequency gives an axial resolution of 30 μm and a lateral resolution of approximately 70 μm , producing high-resolution images to a maximum depth of 8mm. The system displays the information obtained in the form of a B-scan in a gray scale image. The ultrasound biomicroscopy scans were performed on the big toe, first metatarsal head, third metatarsal head, fifth metatarsal head, medial foot arch and the heel of the right foot. After ultrasound gel was applied over the measuring sites, the Vevo model 708 probe was placed perpendicular to the surface of the skin during the capturing of the image. The pressure of the transducer on the surface of the skin was minimized to avoid compressing the surface of the

skin. By using fractal geometry, quantitative data on the epidermal thickness were measured by analyzing the change in the echogenicity of the ultrasound image on each sonogram. The first entry echo corresponds to the interface between the coupling gel and surface of the skin, followed by a broad echo-rich band underneath corresponding to the epidermis. This is followed by a thin echolucent band, the SLEB, corresponding to the upper dermis. After boundaries of different layers were identified, the thickness of the skin at various layers, as defined as the distance between the demarcation echo lines, was then calculated by the in-house Vevo image analysis software. The mean of the measurements for the two images obtained at each testing point was used to analyze the data.

4.2.3.2 Oxyhemoglobin concentration measurements

Near infrared optical measurements were performed on six sites including the big toe, first metatarsal head, third metatarsal head, fifth metatarsal head, medial foot arch and the heel of the right foot, by a frequency-domain tissue spectrometer (Imagent®, ISS Inc., Champaign, IL). The amplitude and phase data from the four source-detector distances (ranging from 0.7 to 1.6 cm) were analyzed using the frequency-domain multi-distance method to calculate absorption and reduced scattering coefficients at two wavelengths (690 and 830 nm) at a frequency of 110 MHz. From these coefficients the absolute values of oxyhemoglobin concentration, deoxyhemoglobin concentration, total hemoglobin concentration and percentage oxygen saturation were calculated. Each site was measured twice to ensure reproducibility. The data reported reflect the average of these two measurements. The near infrared spectroscopy completed one measurement in 120 seconds, with the probe held contact with the plantar tissue.

4.2.4 Statistical Analysis

Data analysis was performed using IBM SPSS Statistics (IBM Corp. Released 2012. IBM SPSS Statistics for Windows Version 21.0. Armonk, NY: IBM Corp). The differences between the groups with regard to the baseline characteristics, oxyhemoglobin concentration and epidermal oedema were calculated by a one-way analysis of variance (ANOVA) test. As there is only one subject each in the DPN and DU group, significant findings were followed by post hoc analyses with Bonferroni correction to examine group differences between the non-DM and DM group. The relationship between the oxyhemoglobin concentration measurements and epidermal oedema was calculated using the Pearson correlation coefficient. The level of significance was set at 0.05 for all measurements.

4.3 RESULTS

4.3.1 Demographic characteristics

Details of the demographics of the subjects are shown in Table 4.1. The age ($P=0.035$) and duration of diabetes ($P=0.009$) were found significant between groups and were used as covariates in subsequent analysis.

Table 4.1 Demographic characteristics of the participants

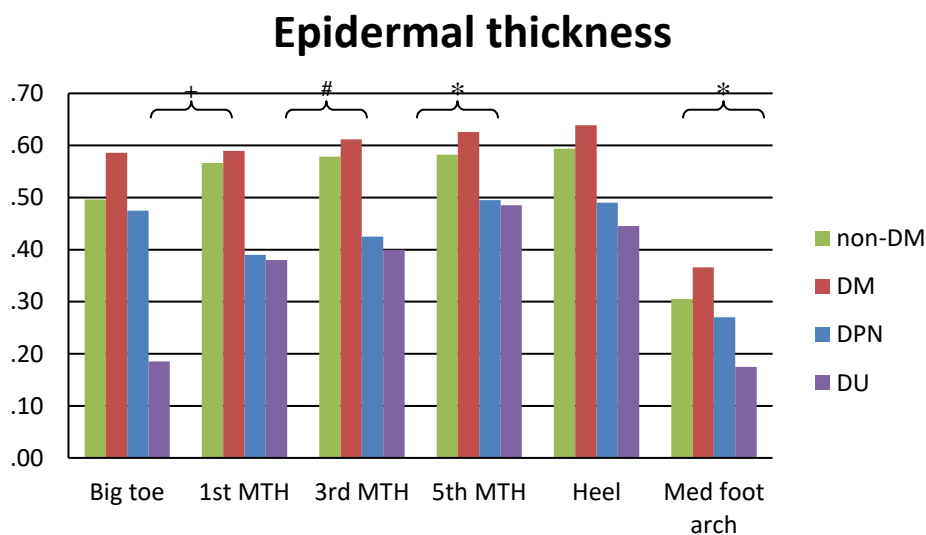
	Non-DM (n=5)	DM (n=69)	DPN (n=1)	DU (n=1)	P-value
Male / female	0 / 5	33 / 36	1 / 0	1 / 0	0.104
Age (years)	63.80±0.00	64.81±7.72	82.00±0.00	80.00±0.00	*0.035
Body mass index (kg/m ²)	22.26±4.44	25.62±4.14	24.30±0.00	28.90±0.00	0.738
Glycated hemoglobin (%)	6.30±0.41	6.96±0.84	6.90±0.00	6.10±0.00	0.345
Duration of diabetes (years)	-	12.47±8.27	14.00±0.00	3.00±0.00	#0.009
Vibration threshold (volts)	13.20±4.66	14.22±6.75	30.00±0.00	13.00±0.00	0.134
Ankle brachial index					
Left	1.15±0.05	1.18±0.09	1.31±0.00	1.17±0.00	0.444
Right	1.16±0.07	1.23±0.11	1.27±0.00	1.16±0.00	0.456

Data are mean ± SD values. DM: diabetes mellitus; DPN: diabetic polyneuropathy; DU: diabetic ulceration

* $P < 0.05$; # $P \leq 0.01$

4.3.2 Epidermal thickness in plantar skin

The epidermal thickness of plantar skin was significantly different between groups at the pulp of big toe ($P<0.001$), the first metatarsal head ($P=0.008$), the third metatarsal head ($P=0.046$), and the heel pad region ($P=0.025$). No significant different of epidermal thickness was observed between groups at the fifth metatarsal head ($P=0.189$) and the medial foot arch ($P=0.133$), but it followed a similar trend with the thickness epidermal layer found in the DM group followed by the non-DM group. Post hoc analyses with Bonferroni corrections showed that the average epidermal thickness of the pulp of big toe in the DU group was significantly thinner than that in the DM group (adjusted $P<0.001$) (Figure 4.1).



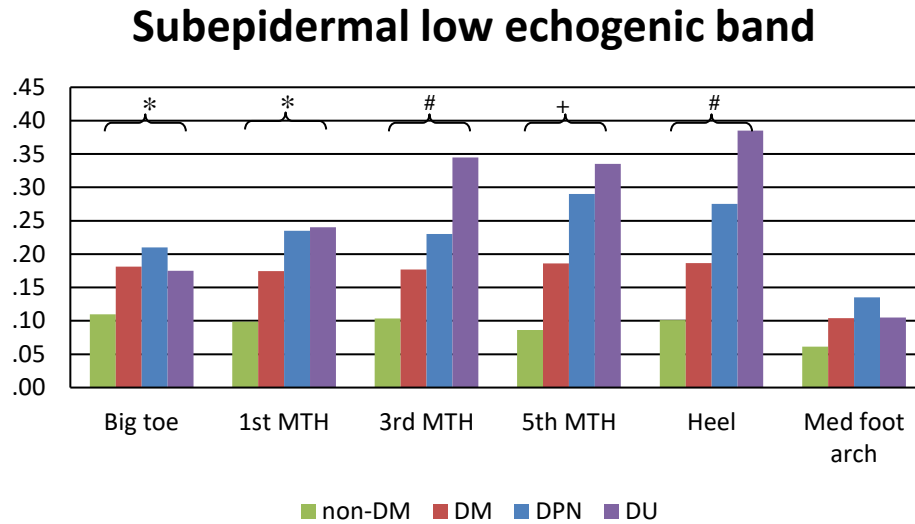
* $P < 0.05$; # $P \leq 0.01$; + $P \leq 0.001$

Figure 4.1 Comparisons of epidermal thicknesses measured at different foot regions between groups.

4.3.3 Subepidermal low echogenic band in the plantar skin

An increase in the subepidermal low echogenic band (SLEB) thickness at plantar skin represents foot oedema. We demonstrated that there was significantly different SLEB among people with DM and those without DM or DM-related complications. We found significantly thicker SLEB in DM subjects as compared to the non-DM subjects, at the first metatarsal head (0.17 vs. 0.10 mm; $P=0.029$), third metatarsal head (0.18 vs. 0.10 mm; $P=0.002$), fifth metatarsal head (0.19 vs. 0.09 mm; $P=0.001$), heel (0.19 vs. 0.10 mm; $P=0.004$) and medial arch (0.10 vs. 0.06 mm; $P=0.05$) respectively. Post hoc analyses with Bonferroni corrections showed that the average SLEB thickness of the DM group was significantly thicker than that of the non-DM group at the pulp of big toe (adjusted $P=0.042$) and the fifth metatarsal head (adjusted $P=0.018$).

The SLEB was the thickest in the DU group. The DU group had thicker third metatarsal head subepidermal oedema as compared to the DM group, as well as the non-DM group (both adjusted $P=0.03$). In addition, post hoc analysis showed that the fifth metatarsal head, heel pad region and medial foot arch were also found to be thicker in the DU group as compared to the non-DM group (adjusted $P=0.024$, 0.042, 0.024 respectively). Moreover, the DPN group had thicker fifth metatarsal head subepidermal oedema than the non-DM group (adjusted $P=0.042$).

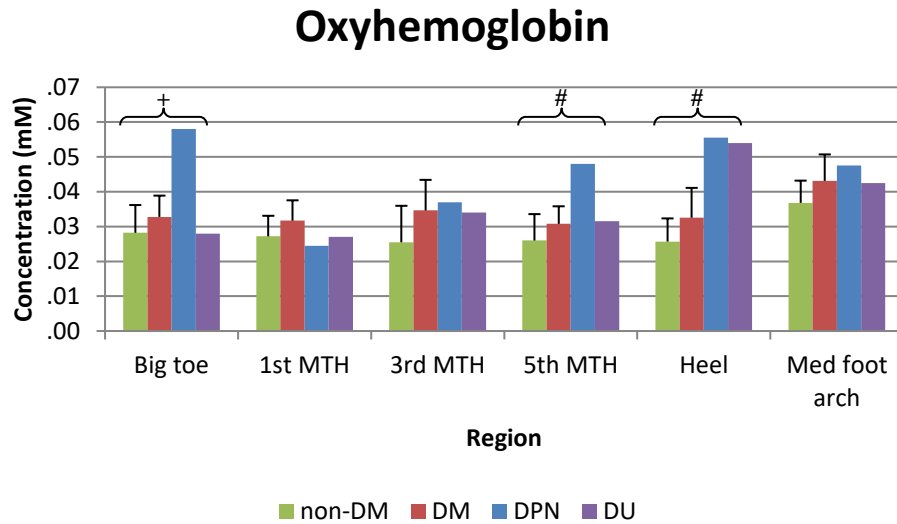


* $P < 0.05$; # $P \leq 0.01$; + $P \leq 0.001$

Figure 4.2 Subepidermal low echogenic band (SLEB) thickness measured at different foot regions were compared among groups.

4.3.4 Oxyhemoglobin concentrations of the plantar skin

The oxyhemoglobin concentrations of plantar skin were significantly different among the study groups at the big toe ($P < 0.001$), the fifth metatarsal head ($P = 0.003$) and the heel pad region ($P = 0.002$) (Figure 4.3). The DM subjects showed higher oxyhemoglobin concentrations than the non-DM subjects measured at the pulp of big toe (adjusted $P = 0.708$), the first metatarsal head (adjusted $P = 0.612$), the third metatarsal head (adjusted $P = 0.180$), the fifth metatarsal head (adjusted $P = 0.318$), the heel pad region (adjusted $P = 0.516$) and the medial foot arch (adjusted $P = 0.450$), but no between-group difference reach statistical significance after Bonferroni corrections.

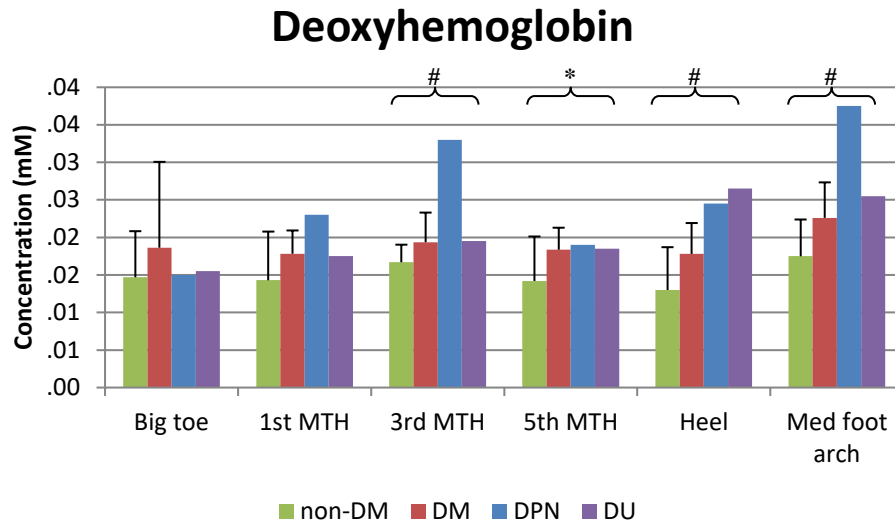


$P \leq 0.01$; + $P \leq 0.001$

Figure 4.3 Oxyhemoglobin concentrations measured at different foot regions were compared among groups.

4.3.5 Deoxyhemoglobin concentrations of the plantar skin

The deoxyhemoglobin concentrations of plantar skin were significantly different among the study groups at most measuring sites, except at the pulp of big toe ($P=0.867$) and at the first metatarsal head ($P=0.062$) (Figure 4.4).



* $P < 0.05$; # $P \leq 0.01$

Figure 4.4 Deoxyhemoglobin concentrations measured at different foot regions were compared among groups.

4.3.6 Oxygen saturation of the plantar skin

The oxygen saturation of plantar skin was not significantly different among the study groups at any measuring sites (Figure 4.5). The oxygen saturation of the DM group appeared to be lower than that of the non-DM group.

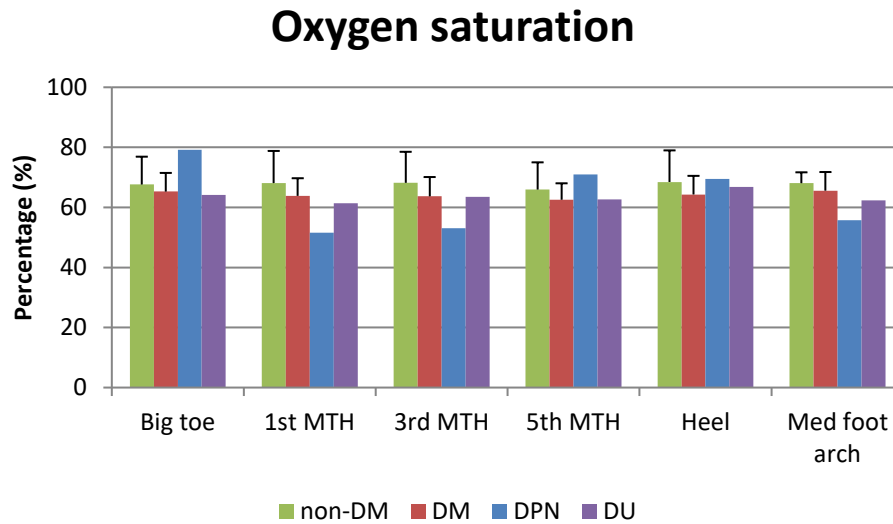
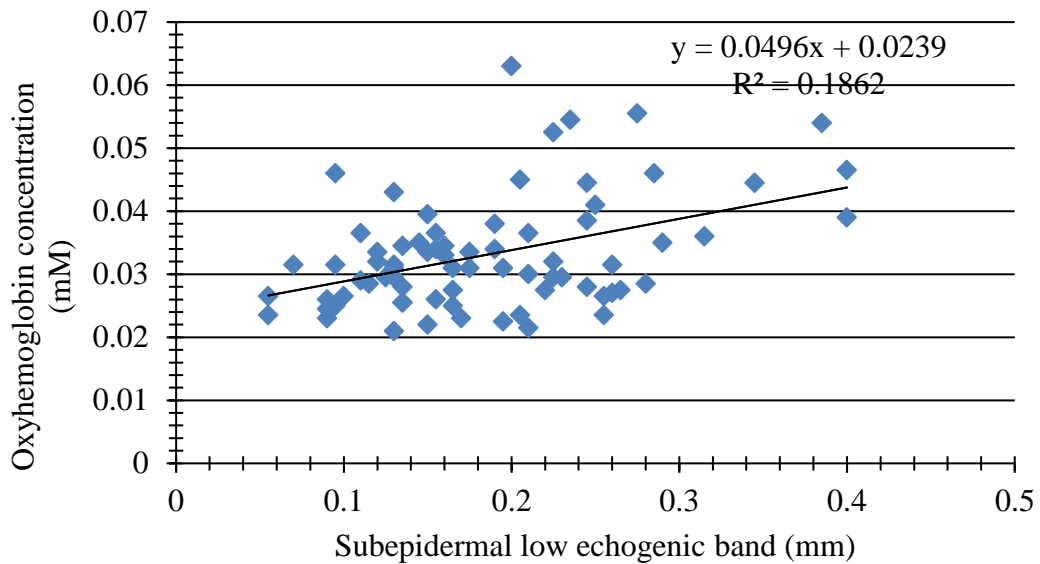


Figure 4.5 Oxygen saturation measured at different foot regions were compared among groups.

4.3.7 Relationship between the oxyhemoglobin concentration and epidermal oedema

Significant positive correlation of the oxyhemoglobin and deoxyhemoglobin concentrations with the subepidermal low echogenic band thickness was demonstrated at the heel pad region in all subjects ($r=0.432$, $P<0.001$; $r=0.480$, $P<0.001$ respectively) (Figure 4.6). Significant correlation was found at the heel region ($r=0.325$; $P<0.007$) in subjects with DM. In addition, weak positive correlation of the oxyhemoglobin and the epidermal thickness was shown at the first metatarsal head ($r=0.270$, $P=0.020$). No significant correlation between oxygen saturation and any parameters was found at any measuring sites.

(A)



(B)

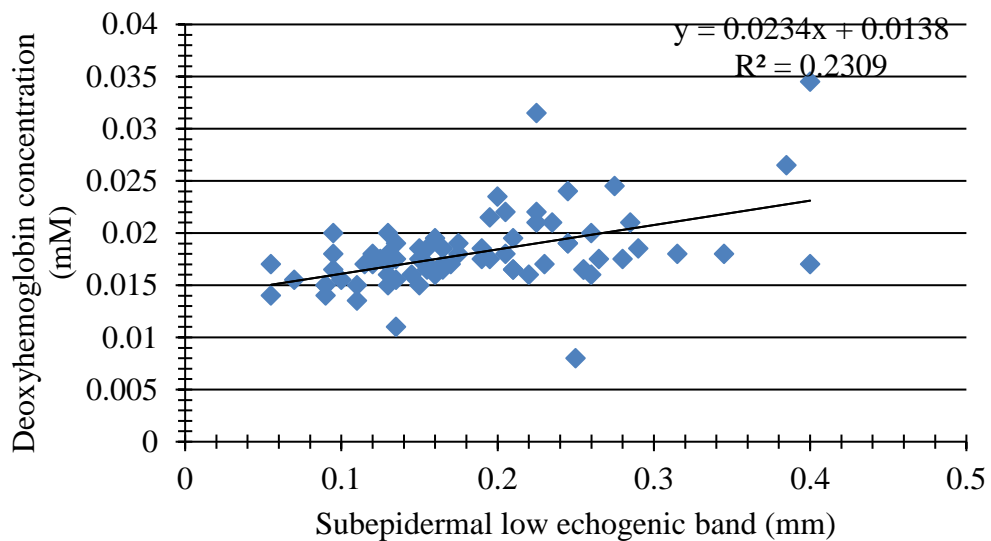


Figure 4.6 Correlation between (A) oxyhemoglobin concentrations and (B) deoxyhemoglobin concentrations, with subepidermal low echogenic band thickness.

4.4 DISCUSSION

Thickening of epidermis layer was found in DM subjects without complications as compared to the non-DM group, but thinning was found in those people with diabetic polyneuropathy or

ulceration. The epidermis is the glycolytic tissue that is affected by the level of insulin in the body that regulating the migration and proliferation of keratinocytes. Hyperglycemia in the people with diabetes might leads to an increase in cross linkage between collagen fibers, and leads to epidermal hypertrophy. The accumulated glycosylation end products may lead to angiopathy that increases epidermal thickness and decreased permeability of the capillary basement membrane. However, for those subjects with diabetic polyneuropathy, the reduction of epidermal nerves decreases the proliferation of keratinocytes that leads to epidermal atrophy (Hsieh and Lin, 1999). The thinning of the plantar skin might reduce its ability to withstand infection, thus people with diabetic polyneuropathy are more prone to complicated foot ulceration.

Our findings suggest that people with diabetes may develop subepidermal oedema, in particular for those with diabetic polyneuropathy or ulceration. The oedema is associated with an increase in the volume of interstitial tissue, which increases the distance of oxygen perfusion from the nutritive capillaries, and may impedes the oxygen delivery to the tissues. This accumulation of oedema may in turn leads to epidermal atrophy and results in foot ulceration in people with DM.

Microcirculation alternation in the diabetic foot is the main cause of foot ulcer development. For people with DM, an increase in oxyhemoglobin and deoxyhemoglobin concentration was found. Such an increase is particularly greater for those with diabetic polyneuropathy or ulceration. The skin of the plantar foot maintains a rich network of arteriovenous anastomoses that would likely maintain higher oxygenation levels. It is known that diabetic autonomic neuropathy may reduce precapillary resistance, the peripheral blood flow was shunt back from the nutritive capillaries to the arteriovenous shuts. Our findings suggests that an increase in oxyhemoglobin and deoxyhemoglobin level may lead to an increase in severity of diabetic complications.

Subepidermal oedema, low oxygen saturation and oxygen delivery might partly explain the reasons why DM limb is unstable to properly oxygenate the tissues and remove deoxyhemoglobin from the peripheral site efficiently, while the blood vessels support an increase in inflammatory mediators. The tissue oxygen saturation on the dorsal foot was also reduced in the skin of people with diabetes, and the impairment is accentuated in the presence of diabetic neuropathy (Greenman et al., 2005). An increase in glycated hemoglobin causes a shift of the oxyhemoglobin dissociation curve to the left, so that oxygen is more tightly bound to the hemoglobin. This shift cause hemoglobin to give up its sound oxygen less readily and lead to a decline in tissue oxygenation (Davidson, 2000). The present study is the first study that demonstrated a positive correlation between the subepidermal oedema and the oxyhemoglobin concentration at the heel region of people with diabetes. However, the sample size in the present study was small, larger sample size is required to confirm the present findings.

4.5 CONCLUSIONS

This chapter demonstrated that people with DM tend to have thicker epidermal skin than that of the non-DM group. However, epidermal thinning occurs for those already developed diabetic complications. Interestingly, there was significant increases in subepidermal oedema were found in people with DM, particular for those with DM complications. In addition, people with DM had higher oxyhemoglobin and deoxyhemoglobin concentrations of the plantar skin as compared to the non-DM group. In next chapter, we will examine the efficacy of pulsed electromagnetic field in restoring the oxyhemoglobin concentration in DM rats, and its related biological mechanisms in promoting diabetic wound healing in a DM rat model.

CHAPTER 5

THE EFFECTS OF PULSED ELECTROMAGNETIC FIELD ON OXYHEMOGLOBIN CONCENTRATION AND WOUND HEALING IN DIABETIC ACUTE WOUND MODEL

The changes in skin morphology and oxyhemoglobin concentration in people with DM were demonstrated in the last chapter that might be contributed to the delayed in wound healing for people with DM. Previous studies have shown that pulsed electromagnetic field (PEMF) promotes microcirculation that might assist in oedema control and restoring normal oxyhemoglobin concentration in DM foot. In this chapter, we will explore the efficacy of pulsed electromagnetic field for restoring normal oxyhemoglobin concentration and oedema control in the foot and its associated biological mechanisms for promoting acute dermal wounds healing in a streptozotocin-induced DM rat model.

5.1 INTRODUCTION

Oxygen plays a crucial role in wound healing including reepithelialization, angiogenesis and collagen synthesis (Rodriguez et al., 2008). During normal wound healing, the absorption coefficients of oxyhemoglobin were correlated with histological evidence of blood vessel regeneration observed by histological staining in diabetic rats (Weingarten et al., 2008). By using near infrared spectroscopy, the absorption and scattering coefficient was found increased immediately after diabetes induction and the coefficients continued to increase after wound induction. Moreover, the growth of blood vessels (Weingarten et al., 2010) results in an increased level of oxyhemoglobin in the wound during the inflammatory phases (Neidrauer et al., 2010). Alternatively, the oxyhemoglobin concentration would drop when angiogenesis stops and newly formed blood vessels are broken down and reabsorbed during the late proliferation phases (Weingarten et al., 2010).

However, diabetic polyneuropathy and microangiopathy that happens in people with DM may impair the wound healing process, thus the wound can get stuck in various phases of the healing and eventually become a chronic non-healing wound. The oxyhemoglobin concentrations would not decrease like the healing of normal wound (Neidrauer et al., 2010). In addition, the

vasculature in people with diabetes becomes functionally abnormal by shunting back the blood from the nutritive capillaries to the arteriovenous anastomosis (Chao and Cheing, 2009). Thus the decrease oxygen perfusion may lead to decreased oxygen concentration and impair nutrient delivery to the wound site, this may subsequently inhibit wound healing in DM foot.

Nitric oxide is an important mediator of normal wound repair (Schaffer et al., 1996). The glycosylation of the red blood cells impairs the nitric oxide vasodilator function (James et al., 2004) which inversely correlated with the oxyhemoglobin concentration (Cosby et al., 2003). The high intracellular levels of glucose and glycolysis in people with DM converts the bioavailable nitric oxide to peroxynitrite which is toxic to the endothelial cells (Bedioui et al., 2010). The damage on the arterial endothelium damage may lead to tissue hypoxia that would delay the wound healing process.

Previous studies have demonstrated that PEMF increases *in vitro* and *in vivo* angiogenesis through endothelial release of FGF-2 (Callaghan et al., 2008). In addition, PEMF significantly accelerated wound healing as compared to the control by transiently increase the myofibroblast population in streptozotocin-induced DM rats in early phase of wound healing (Cheing et al., 2014), as well as the proliferative phase in non-DM rats (Athanasidou et al., 2007). It was proposed that PEMF could accelerate calcium ions binding to calmodulin when homeostasis is interrupted (Weissman et al., 2002) that enhance the endothelium isoform of nitric oxide formation, which is important element for controlling the vascular tone.

We hypothesized that PEMF can promote wound healing by restoring the oxyhemoglobin concentration in DM rats. Therefore, the present study examined the effects of PEMF on restoring the amount of oxyhemoglobin concentrations and promoting the healing of acute dermal wounds in streptozotocin-induced diabetic rat models.

5.2 METHODS

5.2.1 Diabetic rat model

Thirty-three male Sprague-Dawley (SD) rats weighting 243 to 371 g (mean: 327.2 ± 28.7 g) were bred and supplied by the Centralized Animal Facilities of The Hong Kong Polytechnic University (Hong Kong Special Administrative Region, China). Throughout the entire study period, all animals were housed in a temperature- and humidity-controlled animal holding room with a 12h dark/light cycle. Each rat was given a single intraperitoneal injection of streptozotocin (STZ) (Sigma-Aldrich, St. Louis, MO, 50mg/kg in citrate buffer) after a 3-day acclimatization period. Those rats with a fasting blood glucose level of more than 300 mg/dl (16.7 mmol/L) 72 hours after the STZ injections were confirmed as diabetic. All procedures were performed in accordance with the Animal Subjects Ethics Subcommittee of the university. The study protocol complied with the guidelines of The Hong Kong Polytechnic University (Hong Kong Special Administrative Region, China) and all animals received humane care.

5.2.2 Wound induction

Seven days after the DM induction, seven rats died. Anesthesia was administered for twenty-six animals via an intraperitoneal injection of a mixture of ketamine and xylazine (100 mg/kg and 3.33 mg/kg body weight respectively; Alfasan International, Woerden, Holland). The hairs on the hind limbs of the rats were shaved using an electric shaver. After shaving, a 6 mm full-thickness circular shaped wound was excised aseptically by disposable biopsy punch bilaterally from the middle part of the posterior aspect of the rat's hind limbs (Figure 5.1). Sterile filter papers were inserted onto the wounds for nitrite measurement. The rats were housed individually thereafter, and were given food and sterilized water *ad libitum* throughout the study period.



Figure 5.1 The full-thickness wound excised by the 6mm biopsy punch.

5.2.3 Treatment protocol

The DM rats were randomly allocated into either the PEMF group or the sham PEMF group (Figure 5.2). The PEMF treatment was given on post-wounding day 1. The rats in the PEMF group (n=12) were fixed in the rodent restraint bags (BS4 72-6408, Harvard Apparatus, Holliston, MA) placed on top of the disc applicator of the PEMF device (BTL-4000, Magnet, BTL Industries Ltd., UK). The wound was placed at the central space area close to the wall of the applicators to ensure the delivery of a maximum uniform magnetic field was distributed. The generator produces a train of sinusoidal pulses with a width of 3 ms, giving an overall frequency of 25 Hz. The maximum field applied to the sample was 2 mT and was measured by the hand-held Gauss/Tesla meter (Model 4048, F.W. Bell, Milwaukie, OR). The wounds were exposed to active PEMF for 60 min on a daily basis until the rats were sacrificed. The rats in the sham PEMF group (n=14) were fixed in the restraint bags without exposure to PEMF.

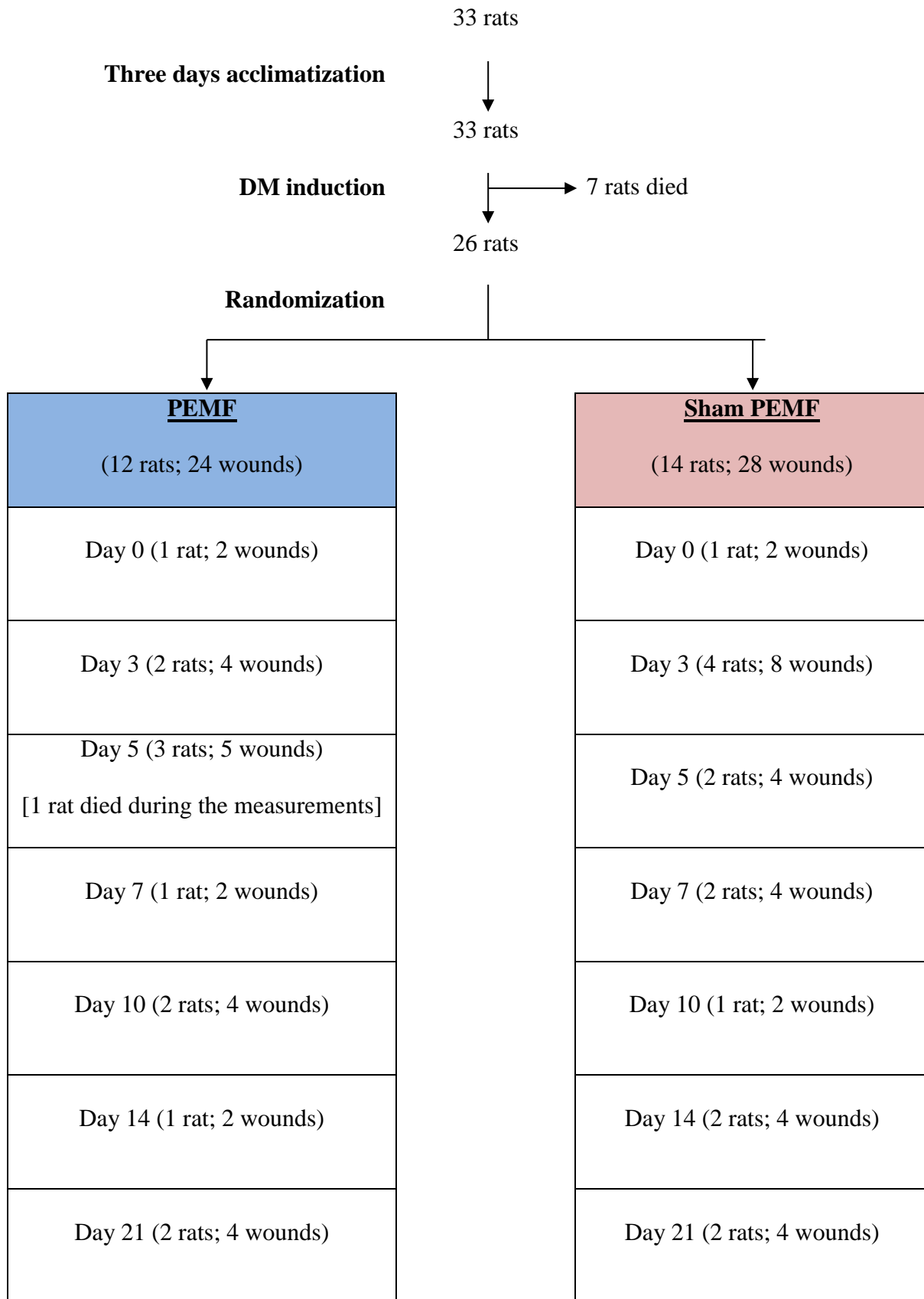


Figure 5.2 Flow chart showing the samples during the experiment

5.2.4 Outcome measures

5.2.4.1 *Oxyhemoglobin concentration of the wound*

The temperature of the assessment room was kept at 23 to 25° C, with humidity controlled at 45 to 60%. Near infrared optical measurements were performed on two locations of the wound, i.e. center of the wound and wound edges (cephalic; caudal; lateral; and medial) by a frequency-domain tissue spectrometer (Imagent®, ISS Inc., Champaign, IL). The amplitude and phase data from the four source-detector distances were analyzed using the frequency-domain multi-distance method to calculate absorption and reduced scattering coefficients at two wavelengths (690 and 830 nm) at a frequency of 110 MHz. From these coefficients, the absolute values of oxyhemoglobin concentration, and total hemoglobin concentration were calculated. Each site was measured twice to ensure reproducibility. The data reported reflect the average of these two measurements. The near infrared spectroscopy completed each cycle in 120 seconds, with the probe hand-held with firm contact to the wound tissue. Measurements were performed on pre-wounding, post-wounding on day 0, day 3, day 5, day 7, day 10, day 14 and day 21.

5.2.4.2 *Wound Assessment*

Body weight and blood glucose levels of the rats were measured on the pre-wounding, post-wounding on day 0, day 3, day 5, day 7, day 10, day 14 and day 21. Images of the wound were taken using a digital camera (Nikon Coolpix P5100, Nikon, Tokyo, Japan) and were imported to the Verge Videometer Measurement Documentation (VeV MD) system (Version 1.1.14, Vista Medical, Winnipeg, Canada) in order to calculate the area of the wound.

The percentage wound closure were defined as

$$\% \text{ Wound closure} = (\text{wound area} / \text{original wound area}) \times 100\%$$

After wound assessment, the rats from the PEMF group and sham PEMF group were sacrificed by asphyxiation with a rising concentration of CO₂ (between 0% and 100%) at different time points.

5.2.4.3 Biochemical analyses

Nitrite is a stable end products of nitric oxide biosynthesis, and were measured spectrophotometrically in filtered wound fluid. Sterile filter papers inserted from each animal were squeezed with forceps and the fluid was centrifuged at 400 g for 10 minutes and 1600 g for 20 minutes at 4 °C for cell and debris separation. Level of nitrite was determined using Griess Reagent System (Promega, WI, USA). 0.1% N-1-naphthylenediamine, 1% sulfanilamide in 5% H₃PO₄, and the wound fluid were mixed at a ratio of 1:1:2, incubated for 10 minutes (25 °C) in dimmed light, and measured at 550nm.

5.2.5 Statistical Analysis

An independent Student's t-test was conducted to compare the difference between the PEMF and the sham PEMF groups at each time point. Data analysis was performed using IBM SPSS Statistics (IBM Corp. Released 2012. IBM SPSS Statistics for Windows Version 21.0. Armonk, NY: IBM Corp). The level of significance was set at 0.05 for all measurements.

5.3 RESULTS

5.3.1 Demographic Characteristics

Throughout the entire study period, all 26 rats stayed healthy and showed no signs of infection at their wound sites until they were sacrificed. No significant group difference in blood glucose level and body weight was found at any assessment time point.

5.3.2 Wound area

In the 52 wounds measured during the 21 days period of post-wounding, wound size of the PEMF group decreased at a faster rate when compared to the sham PEMF group. By day 5 post-wounding, although wound healing appeared faster in the PEMF group than in the sham PEMF group, the difference did not reach statistical significance ($P=0.155$). All wound sizes reduced significantly in the initial few days and the wound closure were almost complete on Day 10 (Figure 5.3).

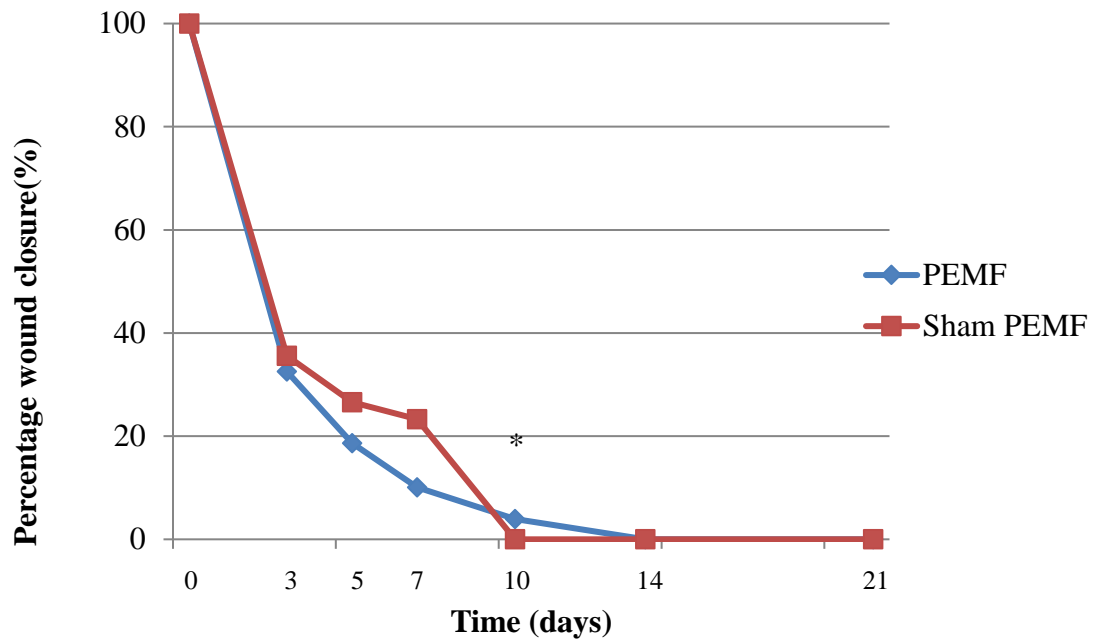
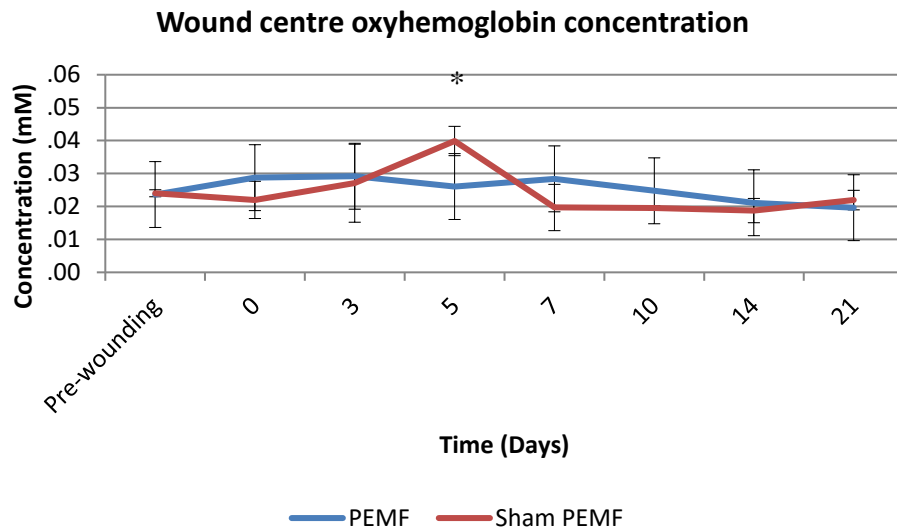


Figure 5.3 Change in percentage wound closure in the PEMF and sham PEMF groups over time. * $P < 0.05$ for between group comparison.

5.3.3 Oxyhemoglobin at the wound sites

On day 5, the oxyhemoglobin in the central wound area were significantly higher in the sham PEMF group as compared to PEMF group ($P=0.015$) (Figure 5.4).

(A)



(B)

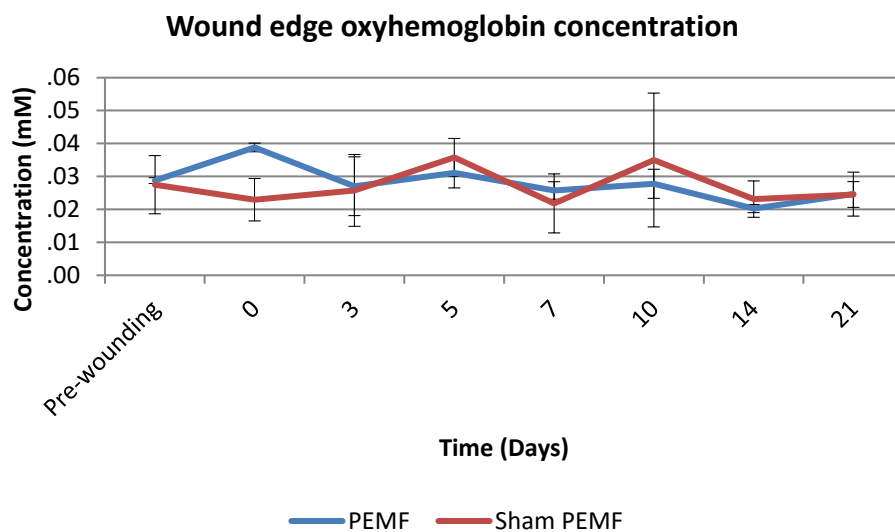
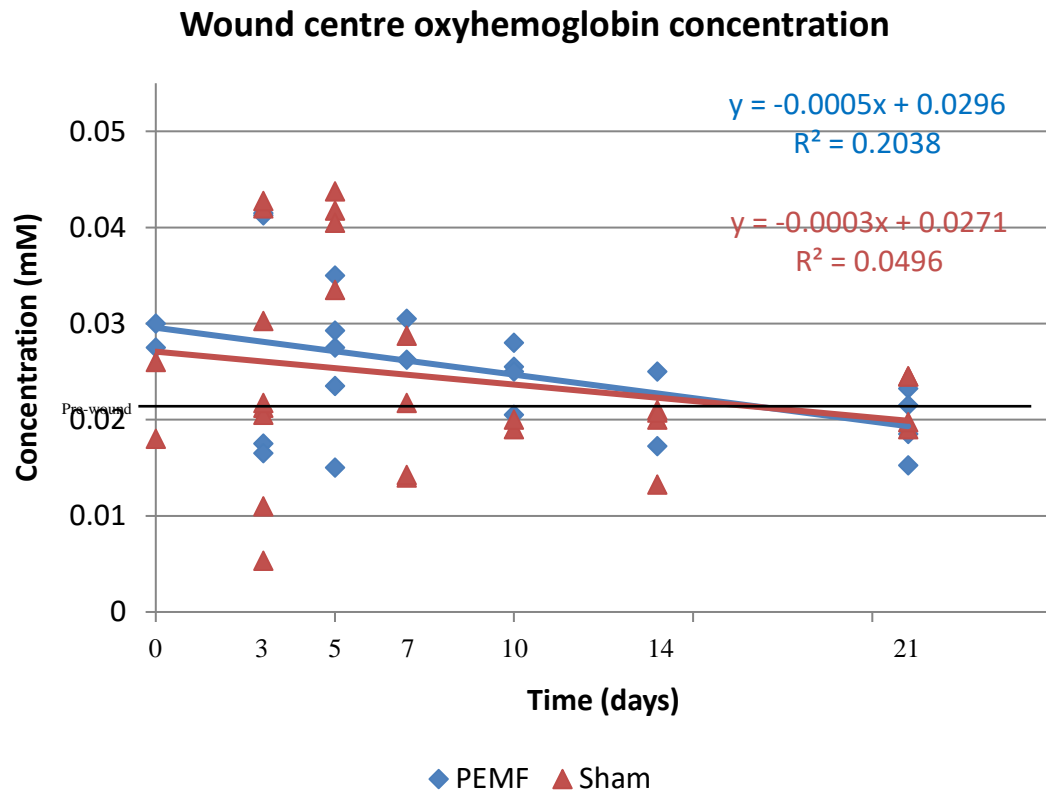
* $P < 0.05$

Figure 5.4 The mean oxyhemoglobin concentration of the PEMF and sham PEMF group, as measured by the near-infrared spectroscopy at the (A) wound center and (B) wound edge over time.

The scatter plot shows that the oxyhemoglobin level at wound central and edges rose upon post-wounding in both the PEMF and sham PEMF groups. Then the level of oxyhemoglobin decreased and converged with pre-wounding value as the wound healed. The PEMF group

showed a faster reduction of oxyhemoglobin in the wound sites (both central and edges) as compared to the sham PEMF group over time (Figure 5.5A). Alternately, the oxyhemoglobin level of the sham PEMF group remained elevated at the wound edges (Figure 5.5B).

(A)



(B)

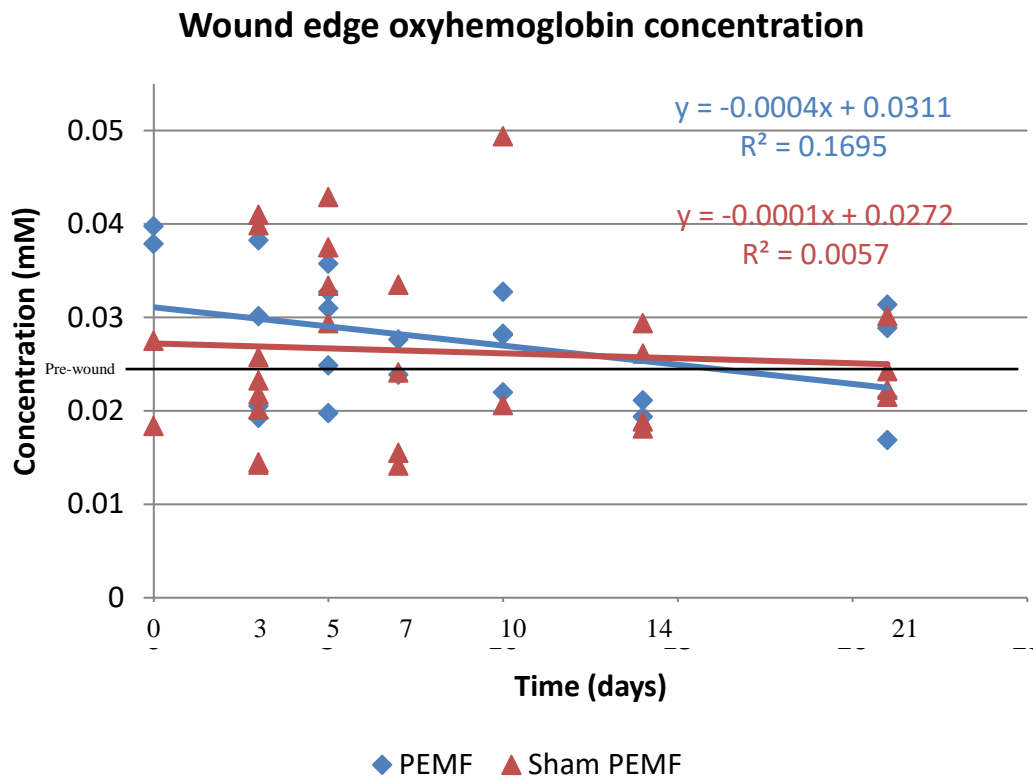
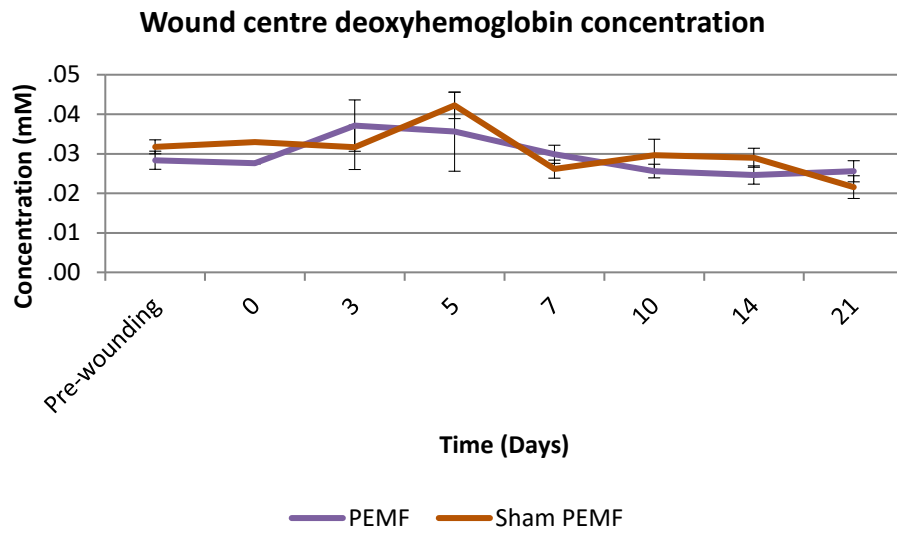


Figure 5.5 Scatter plot on oxyhemoglobin concentration of the PEMF and sham PEMF group, as measured by the near-infrared spectroscopy at the (A) wound center and (B) wound edge over time.

5.3.4 Deoxyhemoglobin of at the wound sites

There were no significant between-group difference in the deoxyhemoglobin concentration at wound centre and edges at any time point measured (Figure 5.6).

(A)



(B)

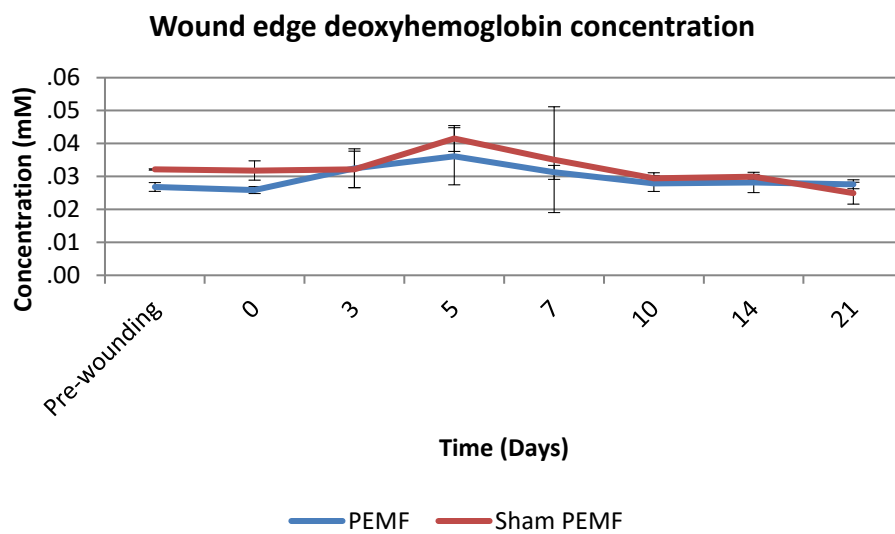
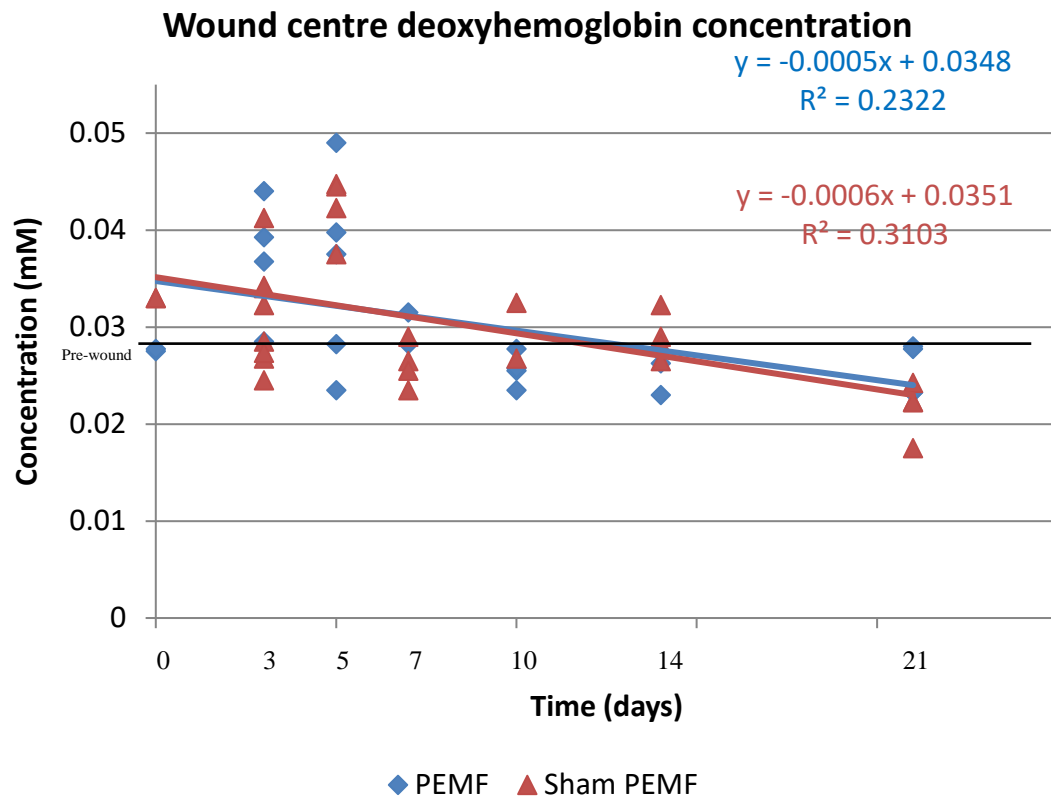


Figure 5.6 The mean deoxyhemoglobin concentration of the PEMF and sham PEMF group, as measured by the near-infrared spectroscopy at the (A) wound center and (B) wound edge over time.

From the scatter plot, the deoxyhemoglobin level at wound central and edges rose upon post-wounding in both the PEMF and sham PEMF groups. In addition, the deoxyhemoglobin

concentration decreased at similar speed and converged with pre-wounding value as the wound healed (Figure 5.7).

(A)



(B)

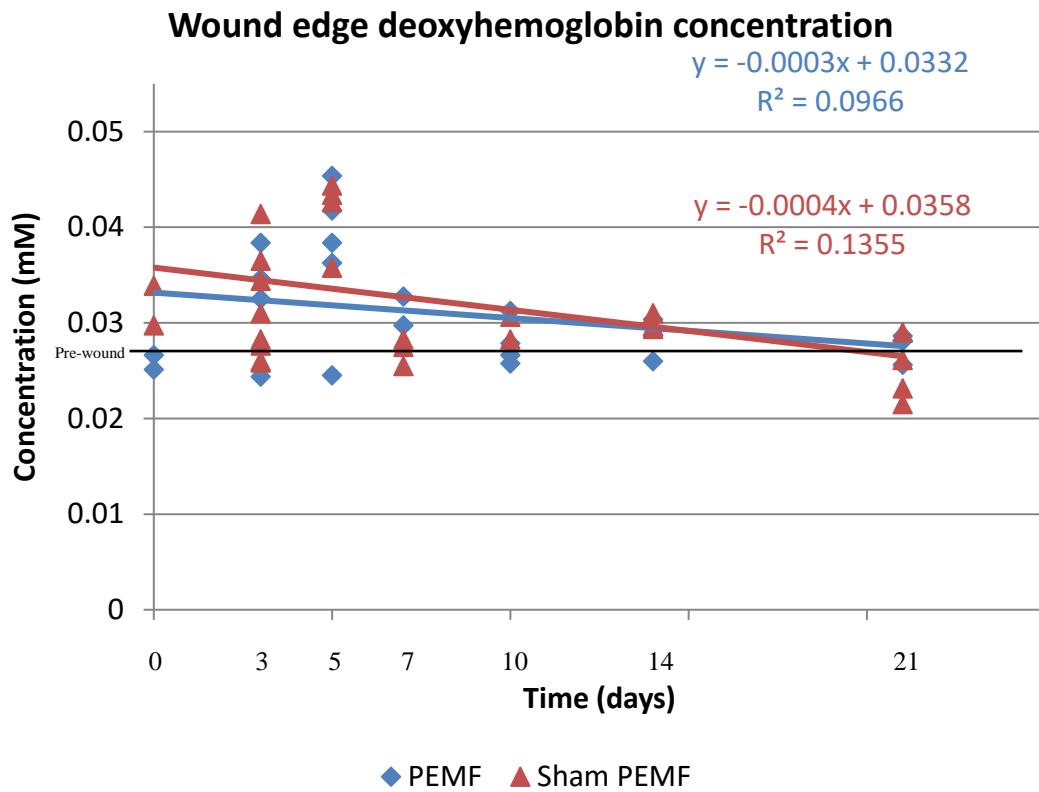
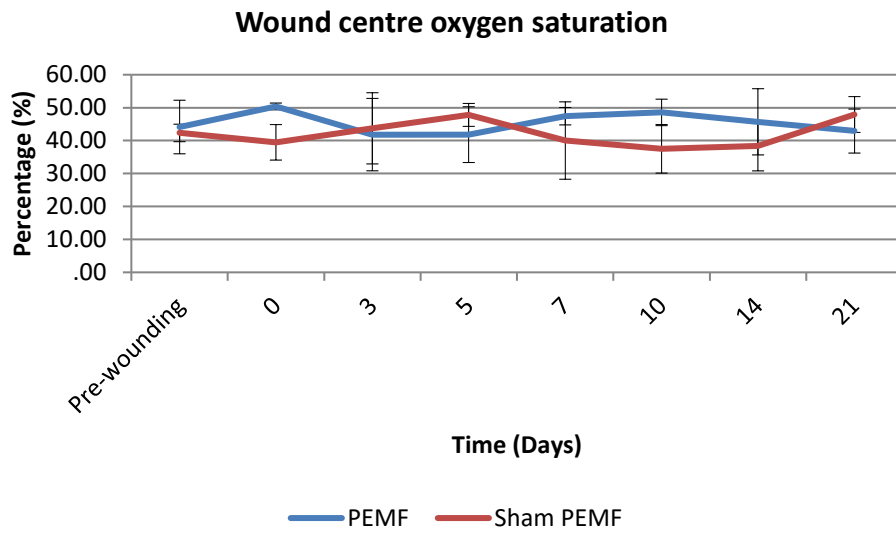
* $P < 0.05$

Figure 5.7 Scatter plot on deoxyhemoglobin concentration of the PEMF and sham PEMF group, as measured by the near-infrared spectroscopy at the (A) wound center and (B) wound edge over time.

5.3.5 Oxygen saturation of at the wound sites

Significant between-group difference was found in oxygen saturation on Day 10 at wound edges ($P=0.037$), but marginally non-significant difference was found at the wound central ($P=0.066$) (Figure 5.8).

(A)



(B)

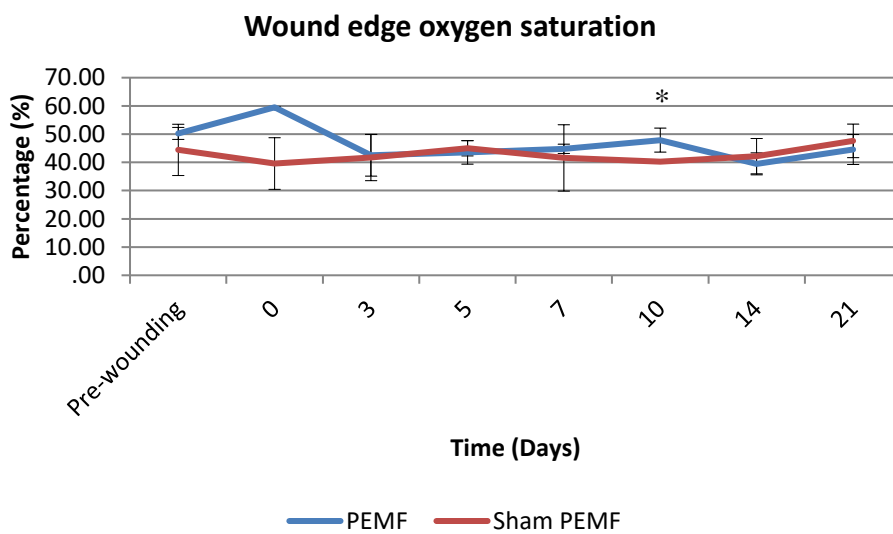
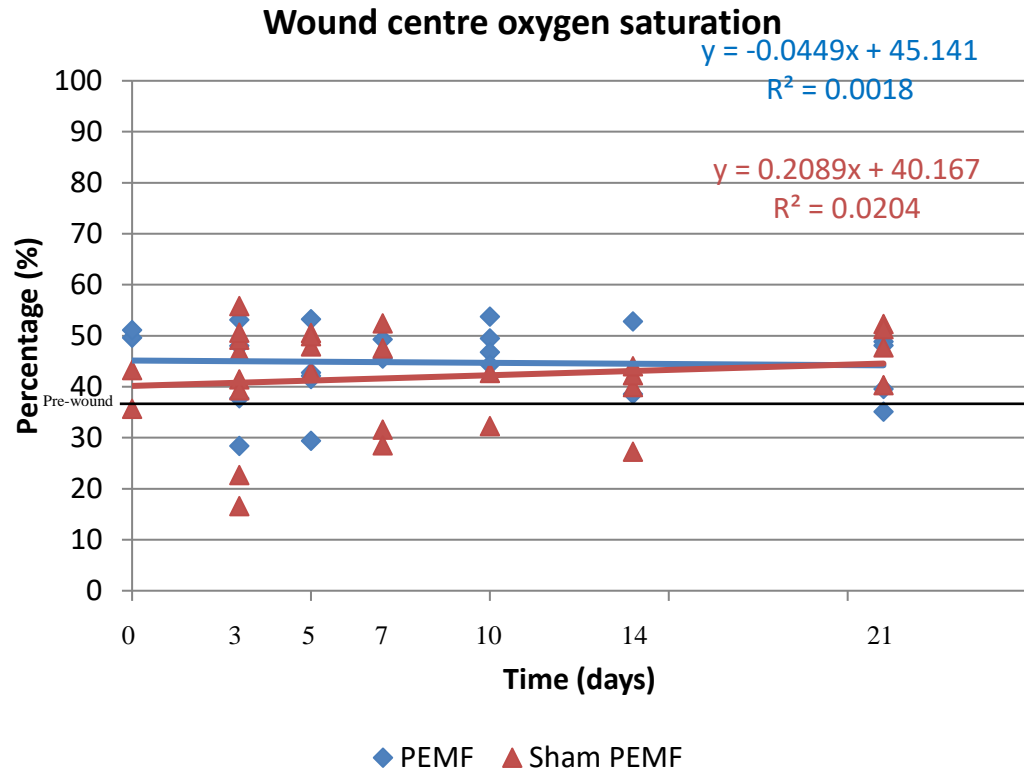
* $P < 0.05$

Figure 5.8 The mean oxygen saturation of the PEMF and sham PEMF group, as measured by the near-infrared spectroscopy at the (A) wound center and (B) wound edge over time.

The oxygen saturation in both groups converged with pre-wounding value as the wound healed (Figure 5.9).

(A)

)



(B)

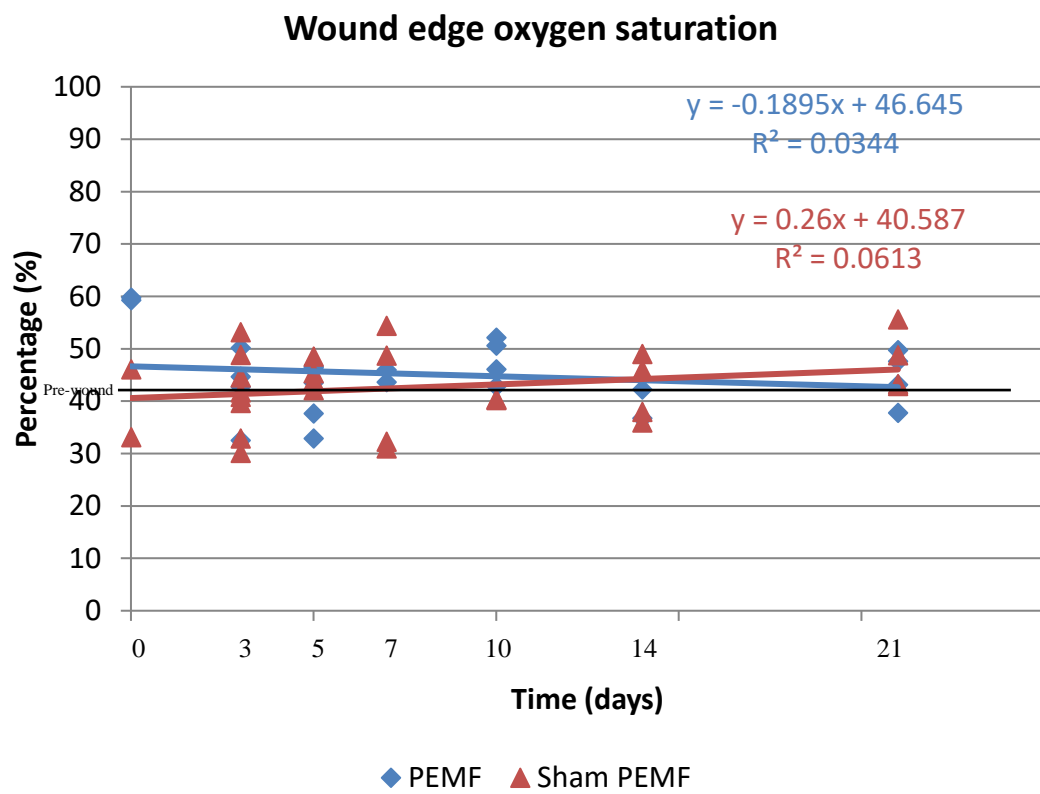
* $P < 0.05$

Figure 5.9 Scatter plot on oxygen saturation percentage of the PEMF and sham PEMF group, as measured by the near-infrared spectroscopy at the (A) wound center and (B) wound edge over time.

5.3.6 Biochemical analysis

Nitrite concentration reached the peak at 47.6 μM in PEMF group, while the nitrite concentration was still increasing to 24.9 μM in the sham group on Day 5. Yet, there was no statistical significance found in any time points.

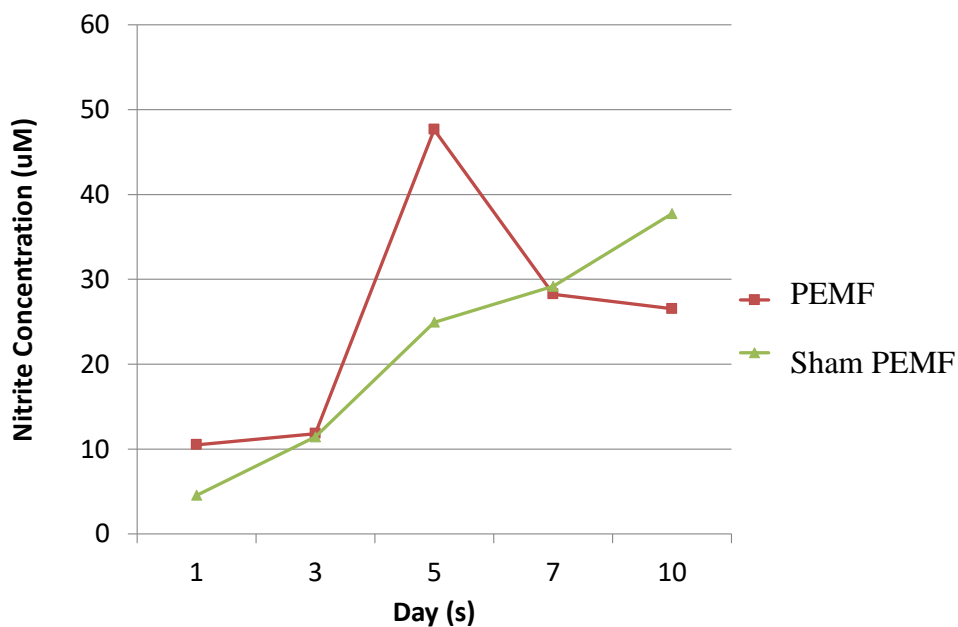


Figure 5.10 Nitrite concentration of the rats in PEMF and sham PEMF group over time.

5.4 DISCUSSION

The use of NIRS allows the clinician to assess wound healing process in a non-invasive manner, and the rate of change of oxyhemoglobin can be used to predict whether the wound would heal

or not (Neidrauer et al., 2010). Wound healing consisted of three interrelated and overlapping phases including the inflammatory phases, proliferative phases and remodeling phases. An increase of oxygen supply leading to neovascularization is necessary for newly formed granulated tissue at the inflammatory phase. The higher value of oxyhemoglobin upon wound incision in the two groups suggested that the vessel in-growth (Weingarten et al., 2008) for the supply of oxygenated blood to the wound. In the later stage, blood vessels would stop taking oxygen because of apoptosis, and there is a decrease in the supply of oxygen to the wound. During wound healings, the levels of oxyhemoglobin would decrease when angiogenesis stops and newly formed blood vessels broken down.

The rates of change in hemoglobin concentration over time were quantified by calculating a linear trendline. Using the slopes of oxyhemoglobin acquired from the wound center in this study, the oxyhemoglobin concentrations decreased faster in the PEMF group as compared with the sham PEMF group. Thus, our findings support PEMF to be a potential treatment modality that could speed up the early stage of healing process of DM wound. In contrast, the concentrations of deoxyhemoglobin over the wound would be expected to remain relatively constant (Neidrauer et al., 2010), this may explain why our findings show that the change of deoxyhemoglobin level in the two groups were comparable during wound healing process.

Diminished wound nitric oxide synthesis in wound fluid and ex vivo nitric oxide production by wound cells were found in a diabetic wound model (Schaffer et al., 1997). In diabetic mice, cutaneous eNOS activity and nitrite levels were lower when compared to non-DM mice, paralleled by increased levels of superoxide anion level (Tie et al., 2016). The endogenous deficiency in NOS enzyme leads to decreased wound nitric oxide production and impaired cutaneous vasodilation. Our results showed that PEMF might be able to speed up the nitrite production in early phase of acute diabetic wound.

Diabetes influence many phases of the normal wound healing process. We adopt an acute wound model in the present study. Therefore, the changes in oxyhemoglobin concentration might be only attributing to acute local inflammation. A chronic wound model can be developed in future study to evaluate if PEMF also produced similar beneficial effects in chronic wounds. In addition, a larger sample size and histological examination can be performed to explore the underlying mechanisms of PEMF on promoting the healing of diabetic wound.

5.5 CONCLUSIONS

Pulsed electromagnetic field may promote dermal wounds healing in a streptozotocin-induced diabetic rat model by restoring the oxyhemoglobin concentration. Yet, PEMF might potentially speed up the nitrite production in early phase of acute wound healing. In the next chapter, we will report the efficacy of using pulsed electromagnetic field to promote healing of chronic non-diabetic wound model.

CHAPTER 6

**EFFICACY OF PULSED ELECTROMAGNETIC FIELD IN PROMOTING NON-
DIABETIC DERMAL WOUND HEALING WITH OR WITHOUT PSEUDOMONAS**

AERUGINOSA

Pulsed electromagnetic field therapy (PEMF) have been demonstrated in the last chapter that IT could enhance the healing of diabetic acute wound in the rat model. However, the effectiveness of PEMF in chronic diabetic wound model is still unknown. In this chapter, we will explore the efficacy of pulsed electromagnetic field in promoting wound healing of non-diabetic dermal wounds with or without *Pseudomonas aeruginosa* in mice.

6.1 INTRODUCTION

The management of chronic wounds is an important health problem worldwide. *Pseudomonas aeruginosa* is a common gram-negative and rod-shaped bacterium that grows well at 25 to 37°C. An estimated 51,000 healthcare-associated *Pseudomonas aeruginosa* infections occur in US per annum (Centers for Disease Control and Prevention, 2018). It can cause serious life-threatening infections in plants, animals and even in healthy people, in particular for those with wounds from surgery or from burns (Centers for Disease Control and Prevention, 2018).

Pseudomonas infections are widely known to cause chronic biofilm-based infections in their hosts (Fazli et al., 2009) and are generally treated with antibiotics. However, the wounds with *Pseudomonas aeruginosa* has been difficult to treat because of increasing antibiotic resistance, with more than 13% of them are multidrug-resistant and 400 deaths per year (Centers for Disease Control and Prevention, 2018). Pulsed electric field has been used to prevent *Pseudomonas aeruginosa* development that reduced the area of biofilm coverage by 50% (Tompkins et al., 2006). PEMF significantly influenced the growth rate but not on antibiotic susceptibility (Segatore et al., 2012).

Various studies have been conducted to examine the effects of biophysical energies including PEMF to promote wound healing, however, all previous studies were carried out in acute wound rather than chronic wound models (Kwan et al., 2019). Therefore, the present study

would examine the efficacy of PEMF in promoting wound healing of non-diabetic dermal wounds with or without *Pseudomonas aeruginosa* in mice.

6.2 METHODS

6.2.1 Animal model

Twenty female C57BL/6 mice (18 weeks) of age were used for the study. Throughout the entire study period, all mice were housed individually in a temperature- and humidity-controlled biosafety level 2 laboratory in The Hong Kong Polytechnic University with a 12h dark/light cycle. Mice were fed with *ad libitum* rodent chow and water, supported by the Centralised Animal Facilities of The Hong Kong Polytechnic University (Hong Kong Special Administrative Region, China). The study protocol complied with the guidelines of The Hong Kong Polytechnic University (Hong Kong Special Administrative Region, China) and all animals received humane care.

6.2.2 Wound induction

The mice were anesthetized with an intraperitoneal injection of ketamine and xylazine (100 mg/kg and 3.33 mg/kg body weight respectively; Alfasan International, Woerden, Holland). The dorsal skin was shaved, and treated with depilatory cream to remove hair. One circular, full-thickness wound was excised on the back of each mouse using a 6 mm biopsy punch. A warm pad was used to keep the mice body temperature at 37°C immediately after the surgery for 30 minutes and then caged individually thereafter. All procedures were performed in accordance with the Animal Subjects Ethics Subcommittee of the university.

6.2.3 *P.aeuginosa* biofilm

Biofilms were prepared by adopting the procedures developed at the Center for Biofilm Engineering at Montana State University with minimal modification (Zhao et al., 2012). *P.aeuginosa* (PAO1) biofilms were prepared by using 6-mm diameter polycarbonate membrane filters cut by biopsy punch, sterilized with 5-minutes ultraviolet C light exposure on both sides. PAO1 obtained from the frozen stock was grown overnight in lysogeny broth (LB) medium at 37°C. The PAO1 culture was diluted 1:1000 in sterile phosphate buffer solution; 2µl of the diluted solution was placed on each of the 6-mm filters, which were plated on LB agar plates cultured at 37°C for 72 hours.

6.2.4 Biofilm application and animal care

Five mice died after the wounding surgery. Application of biofilm on mice was performed 48 hours after the initial wounding procedure (Zhao et al., 2010). The bacteria-inoculated filters were removed from the agar plate after 72 hours incubation. A single filter was placed on each wound so the surface with bacterial biofilm was in direct contact with the wound. The filter was then removed from the wound, leaving behind the PAO1 biofilm. Seven mice were inoculated with biofilm and eight control mice did not receive biofilm (Figure 6.1). Mastisol® liquid adhesive was applied to the skin surrounding the wound and allowed to dry for 2 minutes. Wounds were then covered with a 2cm diameter transparent and semi-occlusive dressing (Tegaderm®, 3M, St.Paul, MN). To evaluate general health of the mice, body weight of each mouse was monitored throughout the study period. Mice losing more than 30% weight, represented in distress, were euthanized.

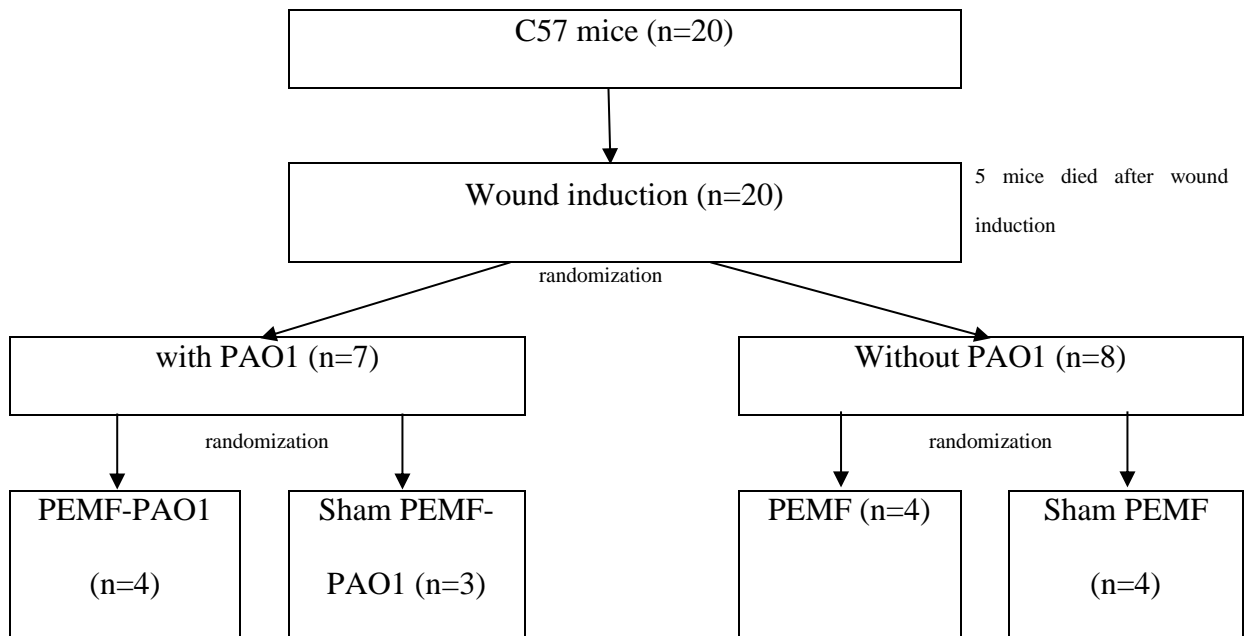


Figure 6.1 Flow chart showing the samples obtained during the study period.

6.2.5 Treatment protocols

The magnetic field output was calibrated with a hand-held magnetometer (Model 4048, F.W. Bell, Milwaukie, OR, USA) before the study. The mice were randomly allocated into either the PEMF group or the sham PEMF group (Figure 6.1). The PEMF treatment was given on post-biofilm inoculation day 1. The dermal wound was exposed to PEMF applicators (BTL-4000, Magnet, BTL Industries Ltd., UK) that delivering a train of sinusoidal pulses with a width of 3 ms, giving an overall frequency of 20 Hz. The maximum field applied to the sample was 5 mT for 60 minutes on a daily basis until Day 7.

6.2.6 Outcome measures

Mice were sacrificed by cervical dislocation under anesthesia. A One Touch® Blood Glucose Meter (LifeScan Inc., Milpitas, CA) was used to measure blood glucose levels.

6.2.6.1 Macrophotography and image analysis

Macrophotographs of the mouse wounds and a square of 2x2 cm were photographed using a Nikon digital camera (Nikon Coolpix P5100, Nikon, Tokyo, Japan). Wound size was measured by image calibration using the 2x2 square and subsequent calculation of wound area using ImageJ. Wound closure was calculated as Percentage Closed = [(Area on Day 0 – Open Area on Day of Assessment)/Area on Day 0] x 100.

6.2.6.2 Tissue Oxygenation

Near infrared optical measurements were performed on the center of the wound by a frequency-domain tissue spectrometer (Imagent®, ISS Inc., Champaign, IL). The amplitude and phase data from the four source-detector distances were analyzed using the frequency-domain multi-distance method to calculate absorption and reduced scattering coefficients at two wavelengths (690 and 830 nm) at a frequency of 110 MHz. From these coefficients the absolute values of oxyhemoglobin concentration, and total hemoglobin concentration were calculated. Two measurements at each site were conducted to ensure reproducibility. The data reported reflect the average of these two measurements. The near infrared spectroscopy completed one measurement in 120 seconds, with the probe was held by hand with firm contact to the wound surface in a parallel manner.

6.2.7 Statistical Analysis

Two-way ANOVA was conducted to compare the difference of wound percentage change between the PEMF and sham PEMF groups in acute or chronic wounds. Data analysis was performed using IBM SPSS Statistics (IBM Corp. Released 2012. IBM SPSS Statistics for

Windows Version 21.0. Armonk, NY: IBM Corp). The level of significance was set at 0.05 for all measurements.

6.3 RESULTS

Both groups in the acute wound models without PAO1 (both PEMF and sham PEMF group) were almost healed after 7 days of treatment, with the PEMF group appear to heal faster than did the sham PEMF group ($P=0.253$) (Figure 6.2). For the chronic wound models, PEMF-PAO1 group had 80% decrease in wound size as compared to the baseline, alternatively the sham-PAO1 group had an increase in wound size after 7 days (between group $P=0.001$) (Figure 6.3).

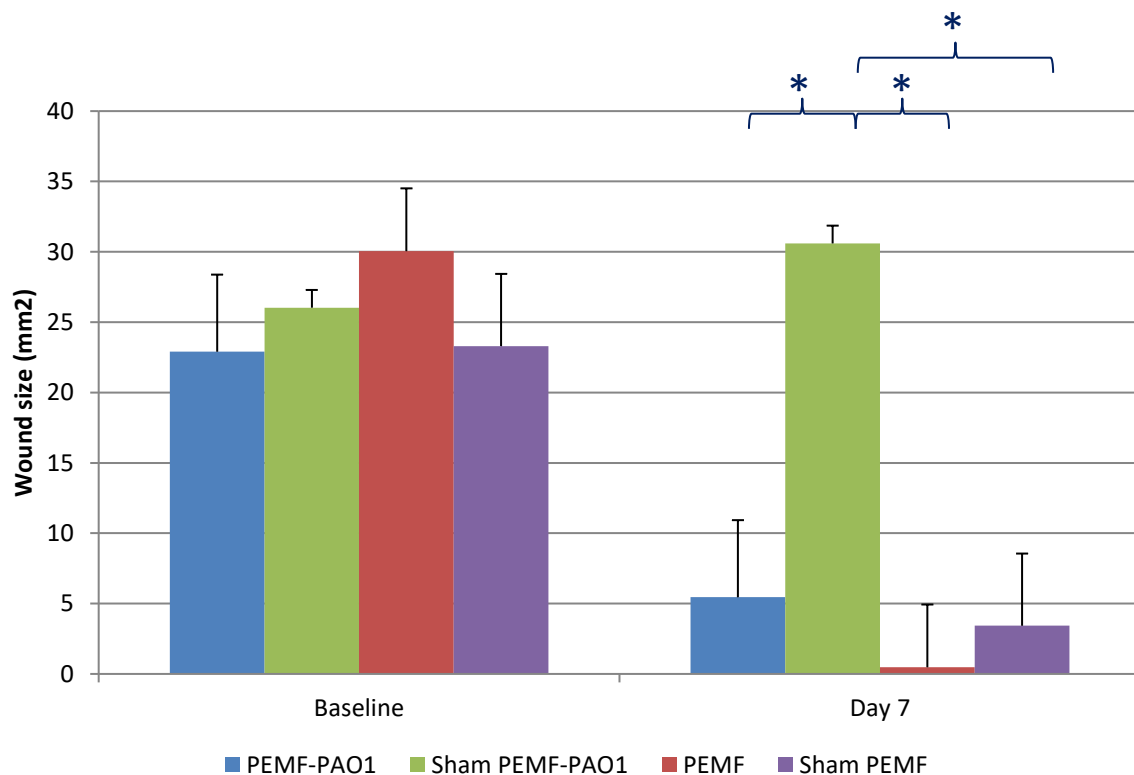


Figure 6.2 Wound size recorded in various treatment groups on Day 7. * $P<0.05$

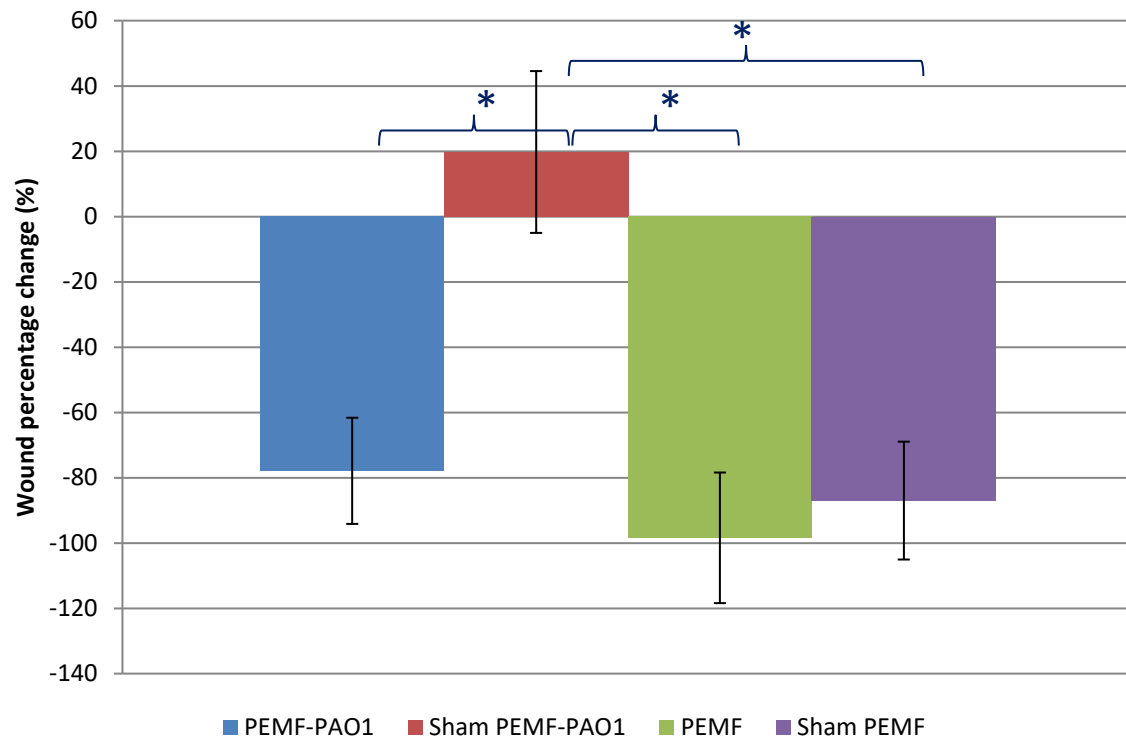


Figure 6.3 Wound percentage change recorded in various treatment groups on Day 7.

* $P < 0.05$

Near infrared spectroscopy was used to measure the optical properties including oxyhemoglobin, deoxyhaemoglobin (Figure 6.4) and oxygen saturation (Figure 6.5) at the baseline and post-wounding before inoculation. All oxyhemoglobin, deoxyhemogloin and oxygen saturation measurements were significantly higher at post-wounding than that in the baseline (all $P<0.05$).

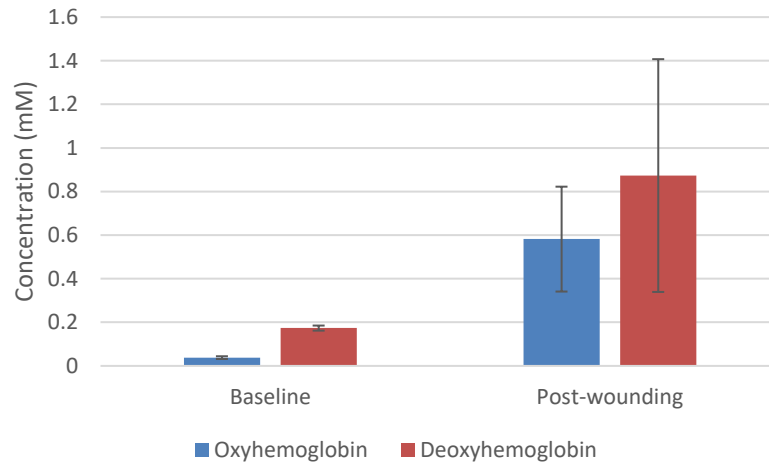


Figure 6.4 Oxyhemoglobin and deoxyhemoglobin as measured by near infrared spectroscopy at baseline and post-wounding in C57 mice.

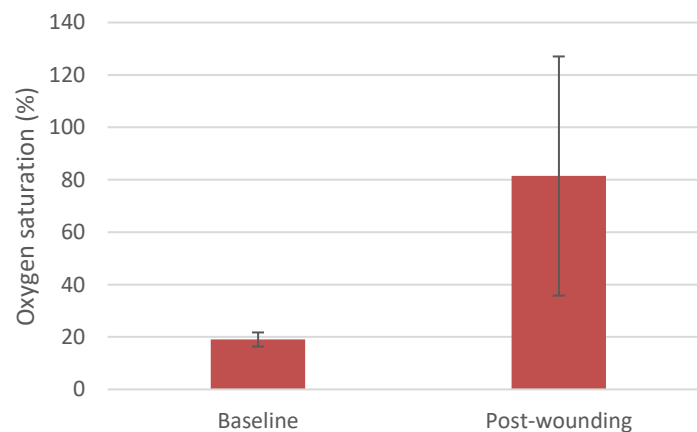


Figure 6.5 Oxygen saturation as measured by near infrared spectroscopy at baseline and post-wounding in C57 mice.

6.4 DISCUSSION

Chronic wounds are a major clinical problem that leads to considerable morbidity and mortality. One of the important factors contributing unhealed chronic wound is the presence of biofilm. Previously, there was no suitable chronic wound models available for wound studies. Zhao and colleagues successfully developed a chronic wound model with *Pseudomonas aeruginosa* in diabetic mice (Zhao et al., 2010, Zhao et al., 2012). This chapter serves as a pilot study in evaluating the efficacy of pulsed electromagnetic field in promoting non-diabetic wound healing with or without *Pseudomonas aeruginosa* in mice.

Compared to most of the control wounds without biofilm that healed within 7 days, none of the wounds challenged with *Pseudomonas aeruginosa* biofilm healed within 7 days post-wounding. Importantly, the wound size enlarged for those inoculated with *Pseudomonas aeruginosa* but did not expose to PEMF treatment. Ulcers infected with *Pseudomonas aeruginosa* infection are usually significantly larger than that infection in human study (Gjodsbol et al., 2006). Therefore, our present findings support the use of *Pseudomonas aeruginosa* for establishing chronic wound models in mice.

Near infrared spectroscopy (NIRS) can provide essential information about blood perfusion with oxyhemoglobin and deoxyhemoglobin, as well as oxygen saturation. This has been used to monitor rats wound (Papazoglou et al., 2006, Papazoglou et al., 2005) and human nonhealing diabetic foot ulcers (Weingarten et al., 2012). The oxyhemoglobin concentration was significantly higher post wounding than that in intact skin. Neidrauer and co-workers (2010) suggested that unhealing wounds tend to have higher oxyhemoglobin than healed wound, probably because the wound healing process are kept in the inflammatory stage (Neidrauer et al., 2010). The present findings demonstrated that NIRS can also be used in monitoring oxyhemoglobin and deoxyhemoglobin concentration during various wound healing stages in mice.

Pulsed electromagnetic field has been used to promote healing and microcirculation in human diabetic ulcers (Kwan et al., 2015). Our research team also demonstrated that PEMF can promote myofibroblast proliferation and improve tensile biomechanical properties in streptozotocin-induced diabetic Sprague-Dawley rats (Cheing et al., 2014, Choi et al., 2018, Choi et al., 2016). Yet, due to a lack of an appropriate chronic wound model, there was no animal study done on investigating the efficacy of PEMF on healing of chronic wound. The present pilot study demonstrated that PEMF can significantly promote chronic wound healing in non-diabetic mice. In the next chapter, we will report the efficacy of using PEMF in promoting chronic wound healing in transgenic diabetic (db/db) mice.

CHAPTER 7**EFFICACY OF PULSED ELECTROMAGNETIC FIELD IN PROMOTING
DIABETIC WOUND HEALING WITH OR WITHOUT PSEUDOMONAS
AERUGINOSA IN TRANSGENIC MICE**

Transgenic mouse studies have been exceedingly useful as a disease model for providing insights in the potential mechanisms involved in treatments for the human diseases. The effectiveness of pulsed electromagnetic field in promoting chronic wound healing in non-diabetic mice was demonstrated in the last chapter. Pulsed electromagnetic field (PEMF) has shown promising results in an acute wound in diabetic model, yet, its effectiveness in managing chronic wound model in diabetic animal is still unknown. In this chapter, we will explore the efficacy of PEMF in the healing promotion of dermal wounds with or without *Pseudomonas aeruginosa* in a transgenic diabetic mice model.

7.1 INTRODUCTION

Chronic wounds accounts for 48% of all wounds managed (Guest et al., 2017) and represent a significant burden to people with diabetes and the healthcare system (Posnett and Franks, 2008). One of the primary impediments to the healing of chronic diabetic wounds is biofilm phenotype infections. Eighty-five percent of lower-limb amputations in people with diabetes are preceded by biofilm infected foot ulceration (Mavrogenis et al., 2018). Bacteria that reside within mature biofilms are highly resistant to conventional therapies. Most common strategies for management of biofilm-related diabetic foot ulcers in clinical practice are frequent debridement and antibiotics prescriptions.

Pseudomonas aeruginosa is one of the most prevalent populations of bacteria identified in people with diabetes, and is capable of performing all essential roles required for pathogenesis (Dowd et al., 2008). A major difficulty in studying chronic wounds is the absence of appropriate animal models. Zhao and colleagues successfully established a chronic wound model by *Pseudomonas aeruginosa* for research study (Zhao et al., 2010, Zhao et al., 2012). Using db/db mice, a 6mm-wound was induced by the use of biopsy punch, then the wound was

inoculated with *Pseudomonas aeruginosa*, which led to an unhealed wound by day 28 (Zhao et al., 2010). Moreover, both histology and genetic analyses showed proliferative epidermis, deficient vascularization and increased inflammatory cytokines (Zhao et al., 2012), which indicated that this model can mimic chronic wound in clinical setting thus can be used to evaluate the anti-biofilm strategies for treating chronic wound.

Our earlier study demonstrated that pulsed electromagnetic fields (PEMF) produced beneficial effects on enhancing healing of acute wound (Cheing et al., 2014, Choi et al., 2018, Choi et al., 2016). In our previous human study, PEMF has shown positive effects on managing chronic diabetic ulcers (Kwan et al., 2015). Moreover, our recent systematic review indicated that PEMF can promote diabetic wound healing in animal models (Kwan et al., 2019). However, only acute wound models have been used in all published animal studies that evaluated the efficacy of biophysical energies on enhancing diabetic wound healing (Kwan et al., 2019). Therefore, this chapter focus on evaluating the efficacy of PEMF on healing promotion of dermal wounds with or without *Pseudomonas aeruginosa* in transgenic diabetic mice.

7.2 METHODS

7.2.1 Animal model

Seventy-six genetically diabetic female mice (db/db) 9 weeks of age weighting 47.7 to 64.8 g (mean 54.4 ± 4.4 g) were purchased for the study in early 2018. Throughout the entire study period, all mice were housed individually in a temperature- and humidity-controlled biosafety level 2 laboratory in The Hong Kong Polytechnic University with a 12h dark/light cycle. Mice were fed with *ad libitum* rodent chow and water, supported by the Centralised Animal Facilities of The Hong Kong Polytechnic University (Hong Kong Special Administrative Region, China).

The study protocol complied with the guidelines adopted by the university and all animals received humane care during the study.

7.2.2 Wound induction

The mice were anesthetized with an intraperitoneal injection of ketamine and xylazine (100 mg/kg and 3.33 mg/kg body weight respectively; Alfasan International, Woerden, Holland). The dorsal skin was shaved, and treated with depilatory cream to remove hair. One circular, full-thickness wound was excised on the back of each mouse using a 6 mm biopsy punch. A warm pad was used to keep the mice body at 37°C immediately after the wound induction surgery for 30 minutes and the mice were caged individually thereafter. All procedures were performed in accordance with the Animal Subjects Ethics Subcommittee of the university.

7.2.3 *P.aeuginosa* biofilm

Biofilms were prepared by adopting the procedures developed at the Center for Biofilm Engineering at Montana State University with minimal modification (Zhao et al., 2012). *P.aeuginosa* (PAO1) biofilms were prepared by using 6-mm diameter polycarbonate membrane filters cut by biopsy punch, sterilized with 5-minutes ultraviolet C light exposure on both sides. PAO1 obtained from the frozen stock was grown overnight in lysogeny broth (LB) medium at 37°C. The PAO1 culture was diluted 1:1000 in sterile phosphate buffer solution; 2µl of the diluted solution was placed on each of the 6-mm filters, which were plated on LB agar plates cultured at 37°C for 72 hours.

7.2.4 Biofilm application and animal care

Application of biofilm on mice was performed 48 hours after the initial wounding procedure (Zhao et al., 2010). The bacteria-inoculated filters were removed from the agar plate after 72 hours incubation. A single filter was placed on each wound so the surface with bacterial biofilm was in direct contact with the wound. The filter was then removed from the wound, leaving behind the PAO1 biofilm. Fifty-one mice were inoculated with biofilm and twenty-five control mice did not receive biofilm. Mastisol ® liquid adhesive was applied to the skin surrounding the wound and allowed to dry for 2 minutes. Wounds were then covered with a 2cm diameter transparent and semi-occlusive dressing (Tegaderm®, 3M, St.Paul, MN). All the wound dressings were removed on day 14 post-inoculation. Mice were observed until day 32 post-wounding. To evaluate general health of the mice, body weight of each mouse was monitored throughout the study period. Mice losing more than 30% weight, represented in distress, were euthanized.

7.2.5 Treatment protocols

The output of magnetic field output was calibrated with a hand-held magnetometer (Model 4048, F.W. Bell, Milwaukie, OR, USA) before the study. The mice were randomly allocated into either the PEMF group or the sham PEMF group (Figure 7.1). The PEMF treatment was given on post-biofilm inoculation day 1. The dermal wound was exposed to PEMF applicators (BTL-4000, Magnet, BTL Industries Ltd., UK) that delivering a train of sinusoidal pulses with a width of 3 ms, giving an overall frequency of 20 Hz. The magnetic field strength applied to the wound was 5 mT for 60 minutes on a daily basis until the mice were sacrificed.

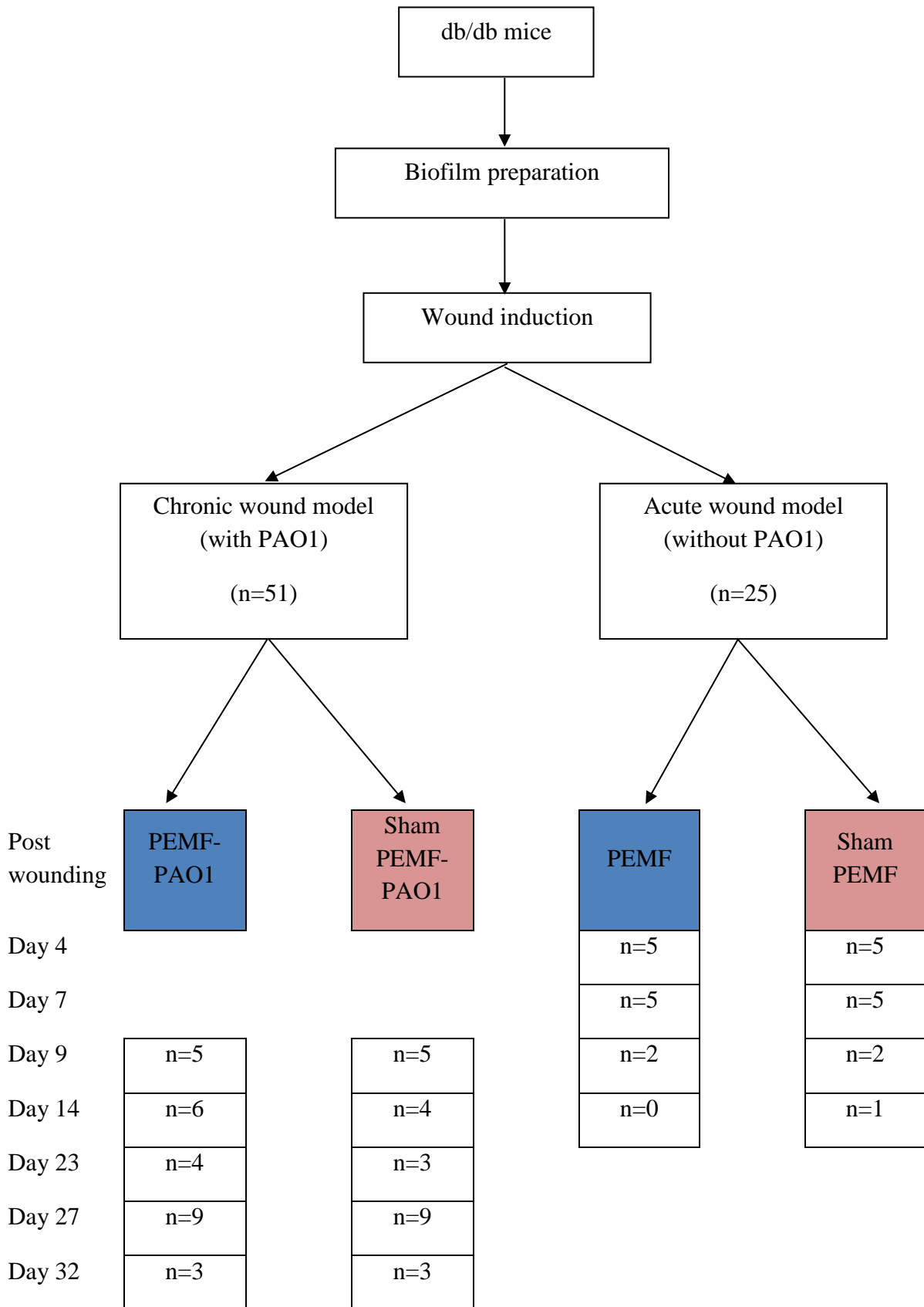


Figure 7.1 Flow chart showing the number of samples obtained during the study period.

7.2.6 Outcome measures

Mice were sacrificed by cervical dislocation under anesthesia. A One Touch ® Blood Glucose Meter (LifeScan Inc., Milpitas, CA) was used to measure blood glucose levels. For histological analysis, wounds including a 1 cm margin of surrounding skin were removed by 8 mm biopsy punch.

7.2.6.1 Macrophotography and image analysis

Macrophotographs of the mouse wounds and a square of 2x2 cm were photographed using a Nikon digital camera (Nikon Coolpix P5100, Nikon, Tokyo, Japan). Wound size was measured by image calibration using the 2x2 square and subsequent calculation of wound area using ImageJ. Wound closure was calculated as Percentage Closed = [(Area on Day 0 – Open Area on Day of Assessment)/Area on Day 0] x 100.

7.2.6.2 Histology

Full thickness of the wound tissues was excised. At least 5 mm of the apparently normal skin away from the wound edges was excised together with the wound samples. The wound samples were immediately fixed with 4% paraformaldehyde in phosphate-buffered saline (PBS, pH 7.4) and were kept in 70% ethanol until the tissue was processed. Each fixed wound tissue sample was cut into half before undergoing tissue processing and paraffin embedding. Sections of 5 µm were prepared for hematoxylin and eosin (H&E) staining. The sections on slides were first deparaffinized and hydrated, and stained with picro-sirius red stain according to the standard procedures (Kiernan, 2002). The picro-sirius red staining was observed through circularly polarized light under a Leica DMRB microscope. Images were captured using a Leica DFC 490 digital camera (Leica Microsystems, Wetzlar, Germany). Collagen fibre deposition, collagen fibril alignment, anisotropy and collagen fibre orientation were measured

quantitatively. The captured images were imported and analyzed using NIS Elements Advanced Research image analysis software (Nikon Instruments, Melville, NY, USA).

7.2.6.3 Immunohistochemistry

Three key factors related to angiogenesis, vascular endothelial growth factor (VEGF), CD31 and alpha smooth muscle actin (α -SMA) were investigated using immunohistochemical staining. Tissue sections were deparaffinized and rehydrated through graded alcohol in water. After blocking with a 5% normal horse serum (NHS) in PBS, the tissue sections were incubated with mouse monoclonal primary antibody against α -SMA (1:500; Sigma-Aldrich, Darmstadt, Germany), rabbit anti-VEFG primary antibody (1:400; Milipore, Darmstadt, Germany) and mouse anti-CD31 primary antibody (1:200; BioLegend, San Diego, CA). The sections were subsequently incubated with Alexa Fluor 555-conjugated donkey secondary antibodies (Molecular Probes, Carlsbad, CA) at 1:300 dilutions for 1 hour at room temperature. Image taken under 200 and 400 magnifications at the representative area of the slides were captured using an epifluorescent microscope (Eclipse 80i, Nikon Instruments, Melville, NY) and a SPOT Flex Digital Camera (Diagnostic Instruments, Sterling Heights, MI).

7.2.6.4 Tissue Oxygenation

Near infrared optical measurements were performed on the center of the wound by a frequency-domain tissue spectrometer (Imagent®, ISS Inc., Champaign, IL). The amplitude and phase data from the four source-detector distances were analyzed using the frequency-domain multi-distance method to calculate absorption and reduced scattering coefficients at two wavelengths (690 and 830 nm) at a frequency of 110 MHz. From these coefficients the absolute values of oxyhemoglobin concentration, and total hemoglobin concentration were calculated. Each site was measured twice to ensure reproducibility. The data reported reflect the average of these

two measurements. The near infrared spectroscopy completed one measurement in 120 seconds, with the probe was held contact with the wound surface in a parallel manner.

7.2.6.5 Biomechanical properties

The biomechanical properties of healing skin wound tissues in terms of maximum load, maximum stress, Young's modulus and energy absorption capacity were collected via Bluehill 3 Systems (Instron Corporation, Norwood, MA, USA) ex vivo using a material testing system (Instron ElectroPuls E1000 manufactured by Instron Corporation, Norwood, MA, USA). Seven mice were randomly selected and sacrificed by cervical dislocation under anesthesia on day 24 and day 32 post-wounding, and the animal bodies were stored in a -80 °C freezer until use. At least 6 h prior to biomechanical testing, the bodies were thawed at room temperature and the skin wound specimens on back were carefully dissected from the wound site to remove all surrounding soft tissues. The remaining skin layer was cut into strips with the dimension of 6.0 mm x 25.0 mm. The specimen geometry, including the length, width, and thickness, was measured using Vernier digital calipers before biomechanical testing. The skin strips were then mounted on the clamps of the material testing system. The room temperature was controlled at around 25 °C and the wound specimen was kept moist by wrapping with plastic film until the experiment started. The specimens were tested with the same protocols adopted in our previous study (Choi et al., 2018). The tissue specimen was elongated to a 2.5% strain position at 0.167 mm/s for 10 preconditioning oscillation cycles to minimize the deep freeze effect on the wound tissue. After preconditioning, the specimen was elongated to 2.5% strain for 5 min and viscoelasticity testing was conducted accordingly (Ng et al., 2004). Unloading then took place for another 5 min to allow the specimen to return to its original length. Tensile biomechanical properties were measured by elongating the specimen at a speed of 8.33 mm/s until failure. Load and deformation were recorded at 100 Hz. The load relaxation property was measured by

subtracting the final load by the initial load, then dividing by the initial load times 100%. The failure test was conducted according to the protocol of a previous study (Ng et al., 2011). A load-deformation curve was plotted to examine the structural properties of the specimen and the curve was transformed into a stress-strain curve by dividing the load with the cross-sectional area (stress) and the elongation with the original length (strain) to examine the biomechanical properties.

7.2.7 Statistical Analysis

Two-way ANOVA with post-hoc LSD tests were used to examine the group x time interactions and the overall group (PEMF versus sham) effects. An independent Student's t-test was conducted to compare the difference between the PEMF and sham PEMF groups in acute or chronic wounds at each time point. Data analysis was performed using IBM SPSS Statistics (IBM Corp. Released 2012. IBM SPSS Statistics for Windows Version 21.0. Armonk, NY: IBM Corp). The level of significance was set at 0.05 for all measurements.

7.3 RESULTS

7.3.1 Demographic Characteristics

The db/db mice in both PEMF-PAO1 and sham PEMF-PAO1 groups showed a decrease in body weight after PAO1 inoculation. Yet, there were no significant between-group difference observed in body weight throughout the study period (Figure 7.2).

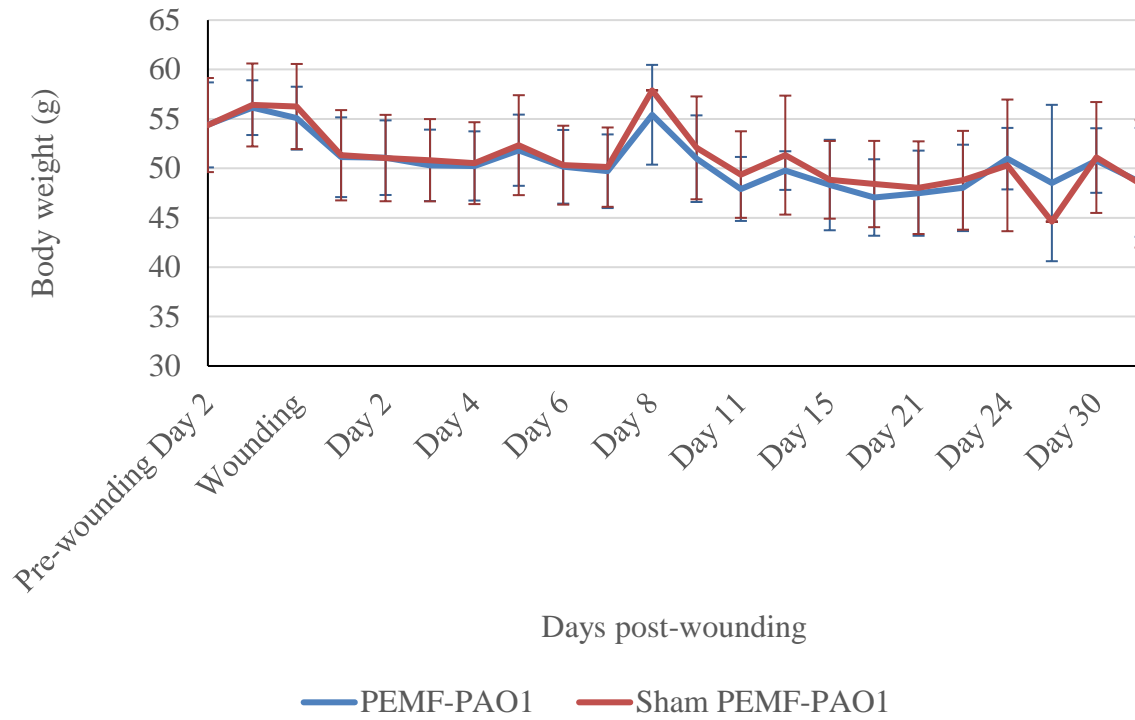


Figure 7.2 Body weight (mean \pm SD) measurement in the PEMF-PAO1 and sham PEMF-PAO1 groups throughout the study period.

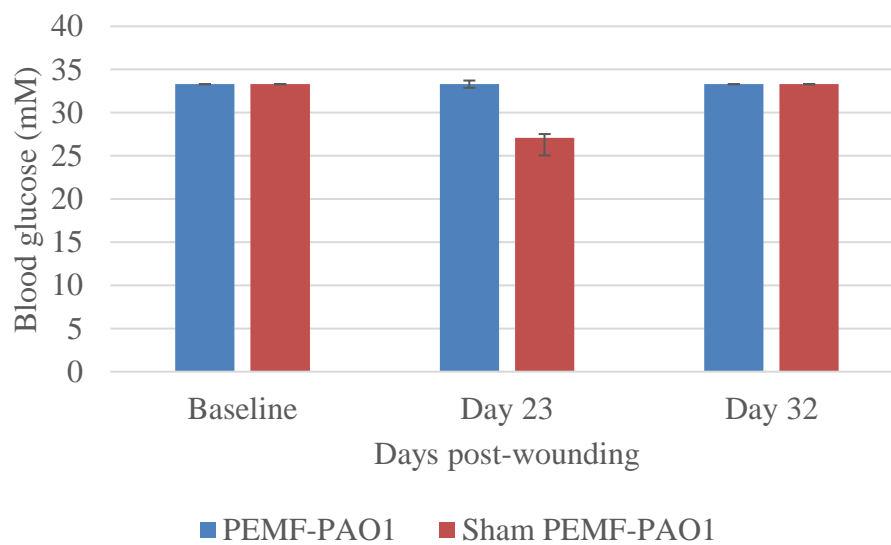


Figure 7.3 Blood glucose level (mean \pm SD) measurement in the PEMF-PAO1 and sham PEMF-PAO1 groups on post-wounding Day 23 and 32.

Blood glucose level in both PEMF-PAO1 and sham PEMF-PAO1 groups remain stable throughout the study period (Figure 7.3).

7.3.2 Gross morphology

7.3.2.1. *Wound area*

The experimental wounds created by the 6mm biopsy punch were consistent in size and shape without bleeding. Representative photographs of the morphological changes in wounds over time are shown in Figure 7.4. New hair grew around the chronic wounds from Day 23 onward.

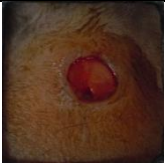

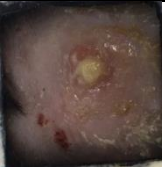

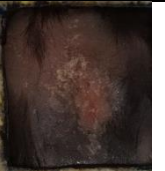


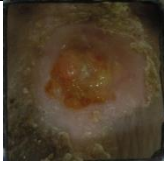
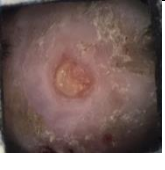






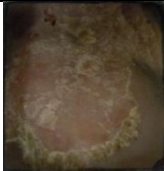

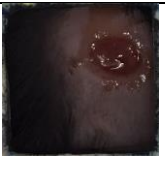


	Postwounding	Baseline	Day 4	Day 7	Day 9	Day 14	Day 23	Day 27	Day 32
Chronic wound	PEMF-PAOI		/	/					
	Sham PEMF-PAOI		/	/					
Acute wound	PEMF					/	/	/	
	Sham PEMF					/	/	/	

Figure 7.4 Representative macro photographs of acute and chronic wounds taken from 0 to 32 days post-wounding of db/db mice in PEMF and sham groups.

Figure 7.5 demonstrates the percentage of chronic wounds that had completely healed in db/db mice based on visual inspection. No chronic wounds from any of the subgroups had completely healed on day 14. By day 17, 25% of all wounds in PEMF-PAO1 group and sham PEMF-PAO1 group were completely healed. By day 23, 83.3% of the wounds in the PEMF group were completely healed, as compared with 70% in the control subgroup. Seventy-five percent of the wounds in PEMF and 50% of the wounds in the sham PEMF-PAO1 were completely healed at day 32. Overall, PEMF-PAO1 group showed a higher percentage of individuals with complete healing than the sham PEMF-PAO1 group at all measurement time-points.

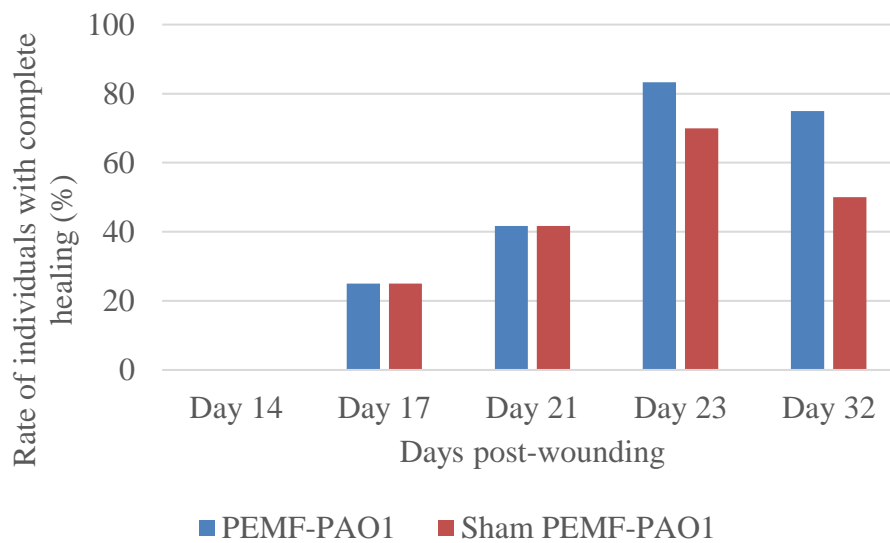


Figure 7.5 Percentage of mice achieving 100% wound closure in the PEMF-PAO1 and Sham PEMF-PAO1 groups.

For the wound closure percentage in chronic model, there are significant group x time interaction ($P=0.029$). The wound size in PEMF group decreased significantly on Day 21 as compared to baseline (within group $P=0.003$), whereas no difference was found in change of wound size in sham group on Day 21 ($P=0.66$). PEMF could significantly accelerate wound healing in chronic wound model (Figure 7.6).

In the acute wound model, there is an increase in wound size with or without PEMF on Day 2 and Day 4. However, both groups completely healed on Day 7.

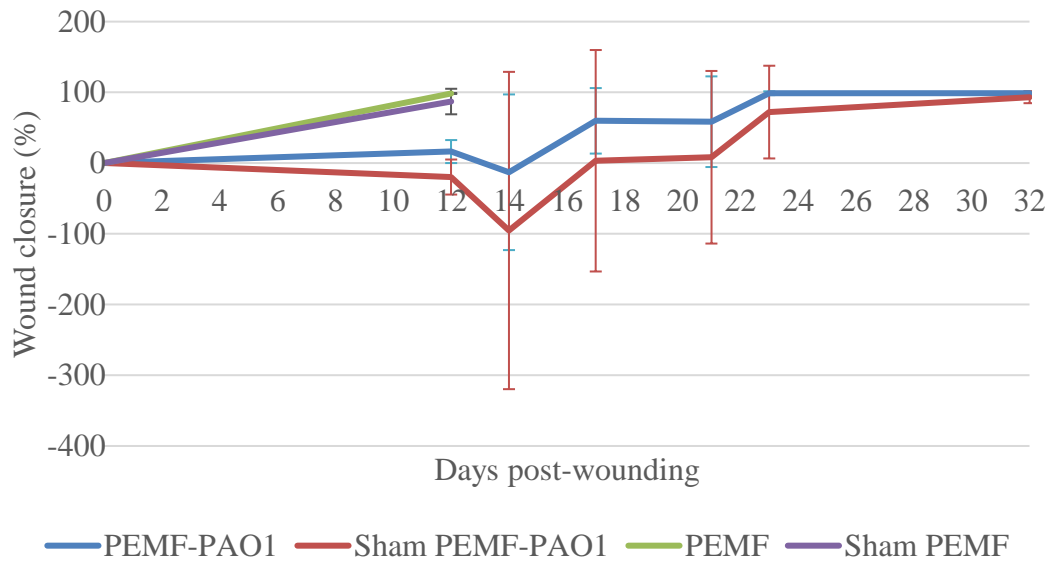


Figure 7.6 Percentage of wound closure (mean±SD) of the 6 mm diameter circular wound was monitored throughout the study period until day 32.

7.3.2.2. *Re-epithelization*

Sham PEMF-PAO1 wound presented with a gap in the epidermis filled with a loose crust of inflammatory tissue on day 14 (Figure 7.7). Morphometric analysis of PEMF-PAO1 mice on day 23 postwounding showed a complete re-epithelization, whereas sham PEMF-PAO1 had an increase in the epithelial migration and a decrease in the wound gap but incomplete re-epithelialization, suggesting that PEMF might enhance wound closure in diabetic chronic wound models although it did not reach statistical significance ($P=0.19$) (Figure 7.8). On day 32, even though the dermis was still under the process of remodeling stage, the organization of the granulation tissue of the PEMF-PAO1 group demonstrated a more advanced healing stage with greater degree of collagen deposition than that in the sham group.

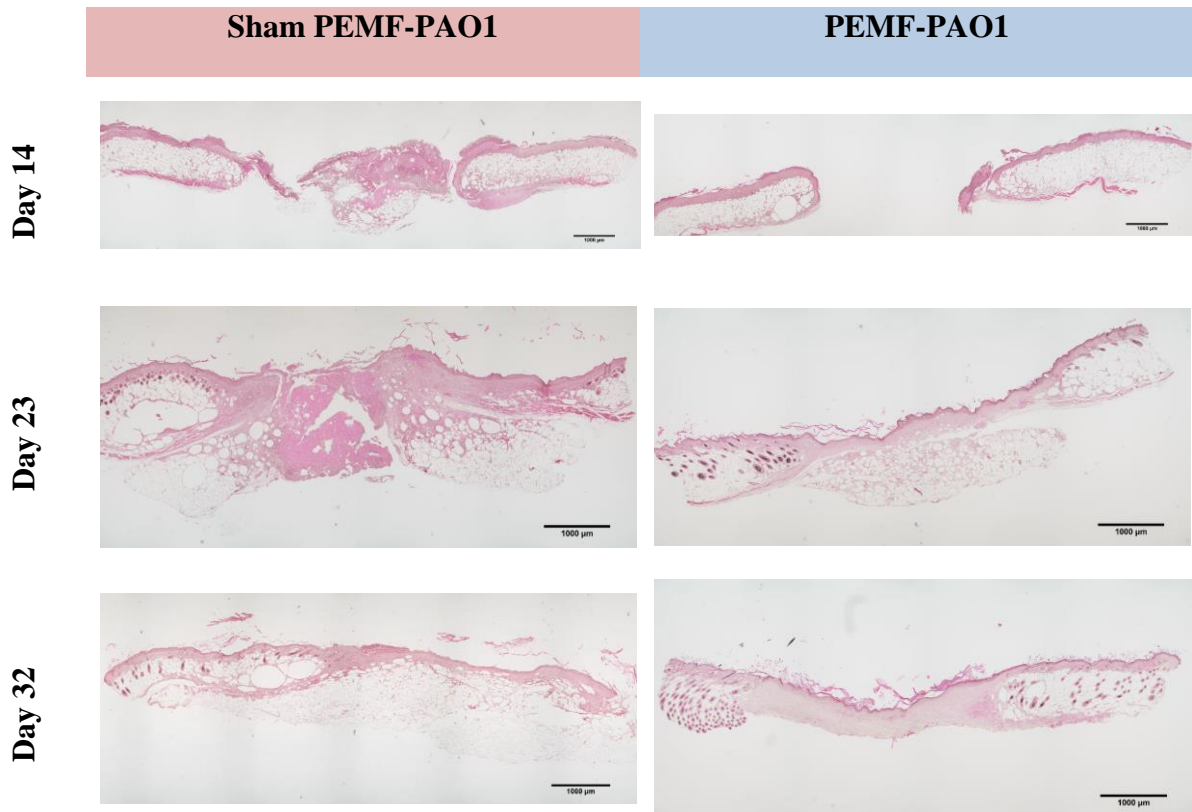


Figure 7.7 H&E stained sections of wound tissue obtained on day 14, 23 and 32 in PEMF-PAO1 and sham PEMF-PAO1 group.

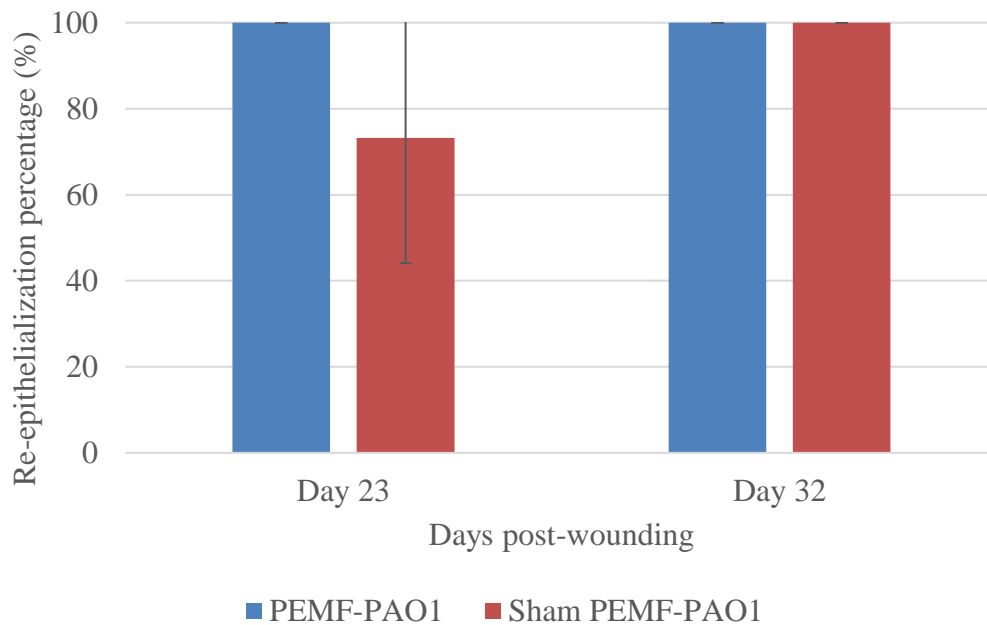


Figure 7.8 Re-epithelialization percentage of chronic wound in PEMF-PAO1 and sham PEMF-PAO1 group on day 23 and 32.

7.3.2.3. Granulation thickness

By evaluating hematoxylin and eosin-stained cryosections, our findings indicated that granulation tissue formation obtained in chronic wounds treated with PEMF on day 23 and 32 (291.4 ± 92.2 and 331.8 ± 138.7) was not statistically different from that of the sham PEMF-PAO1 group (325.2 ± 53.1 and 358.7 ± 199.3) (between group $P=0.61$ and 0.86 respectively) (Figure 7.9).

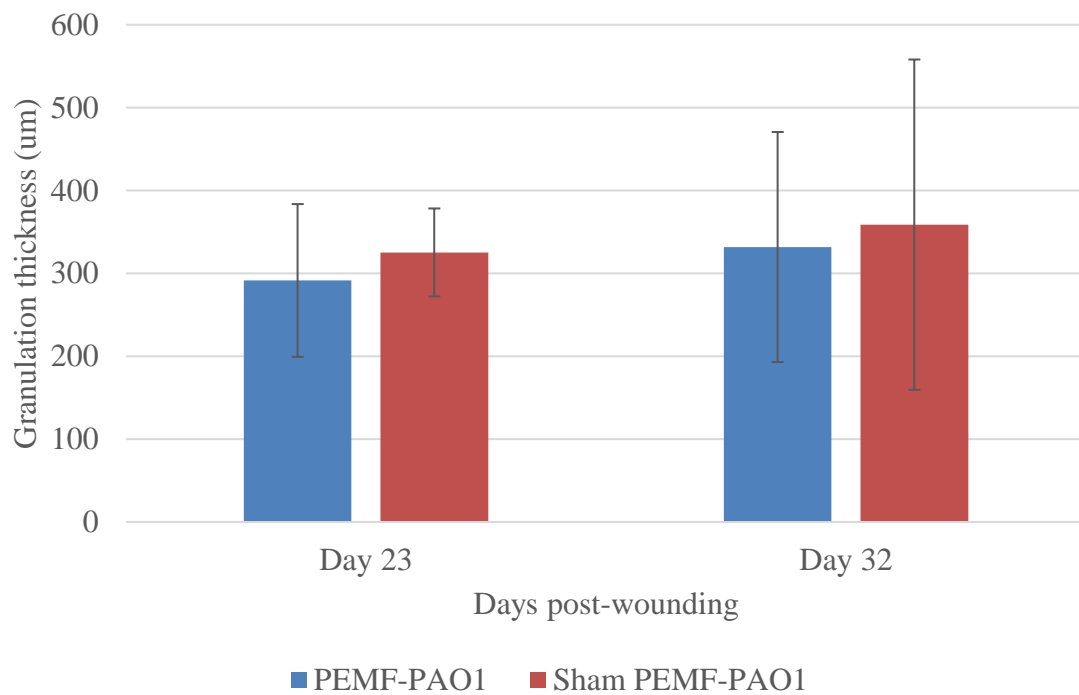


Figure 7.9 Granulation tissue thickness of PEMF-PAO1 and sham PEMF-PAO1 group measured in hematoxylin and eosin-stained cryosections on day 23 and 32.

On day 23 and 32 post-wounding, the vessel counts in PEMF-PAO1 wounds (763.2 ± 143.4 and 919.5 ± 131.5 count/mm²) appeared to be higher as compared to sham PEMF-PAO1 groups (580.5 ± 61.8 and 791.6 ± 157.3 count/mm²), however, the between group difference did not reach significance level ($P=0.11$ and 0.34 respectively) (Figure 7.11).

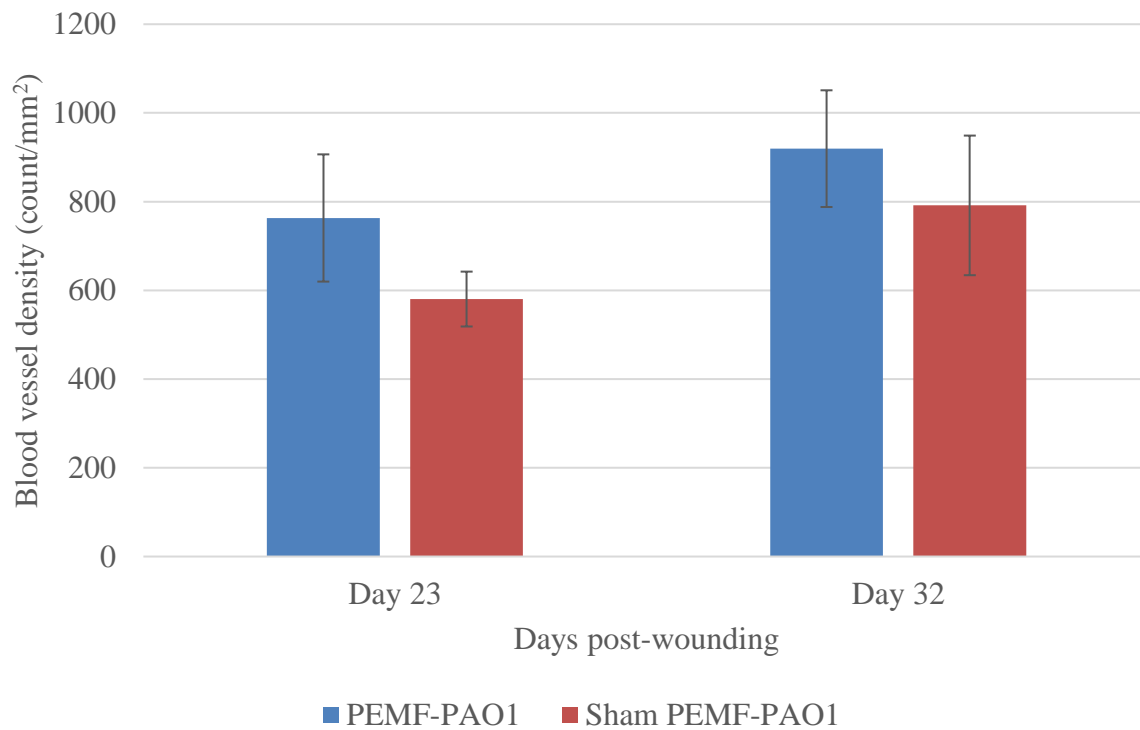


Figure 7.11 Density of vessels in the chronic wound bed in diabetic mice in PEMF-PAO1 and sham PEMF-PAO1 group on day 23 and 32.

7.3.3.2. *Vascular endothelial growth factor (VEGF)*

Immunochemical staining of the wound skin for the expression of VEGF was performed on day 23 and 32 (Figure 7.12). PEMF-PAO1 group presented more blood vessels as well as the high expression of VEGF than did sham PEMF-PAO1 group on day 23 (87.0 ± 11.0 vs. 77.03 ± 9.3 ; $P=0.30$) and 32 (81.5 ± 30.6 vs. 51.1 ± 14.5 ; $P=0.29$) (Figure 7.13); however, the group difference did not reach significance.

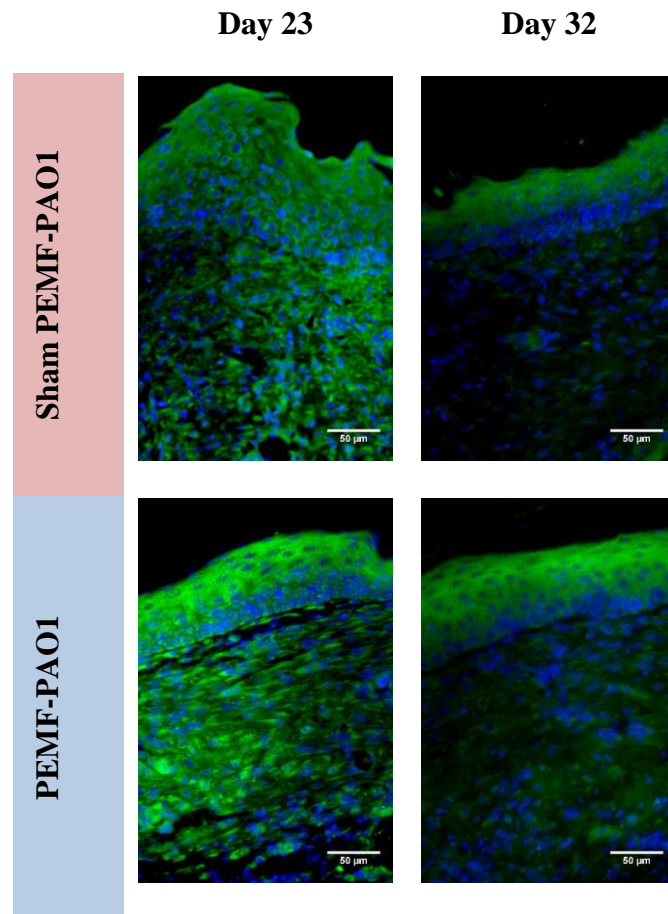


Figure 7.12 Immunohistochemical staining for VEGF expressions in PEMF-PAO1 and sham PEMF-PAO1 groups on day 23 and 32 post-wounding.

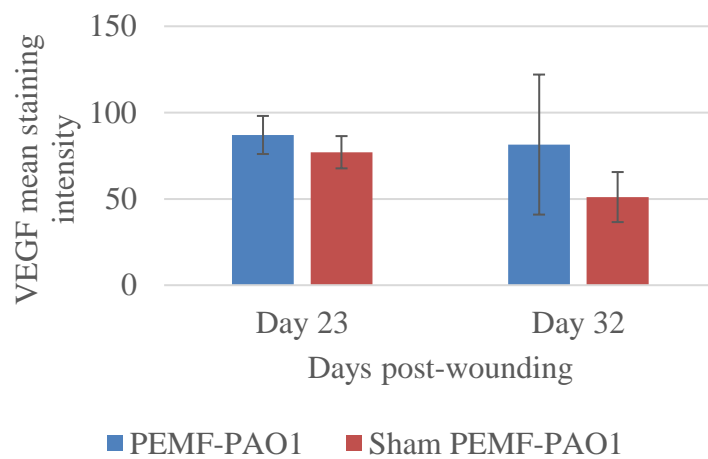


Figure 7.13 VEGF mean staining intensity of PEMF-PAO1 and sham PEMF-PAO1 groups on day 23 and 32.

7.3.3.4. Oxygenation

Figure 7.14 shows that the oxyhemoglobin level at wound remained stable from prewounding to day 14 in both PEMF-PAO1 and sham PEMF-PAO1 groups. In general, the oxyhemoglobin level in the PEMF-PAO1 group was lower than that of the sham PEMF-PAO1 group. On day 32, there was a drastic increase in the level of oxyhemoglobin in both PEMF-PAO1 (0.08 ± 0.04 mM) and sham PEMF-PAO1 group (0.10 ± 0.08 mM) on day 32 (between group $P=0.71$). There were no between group difference throughout the study.

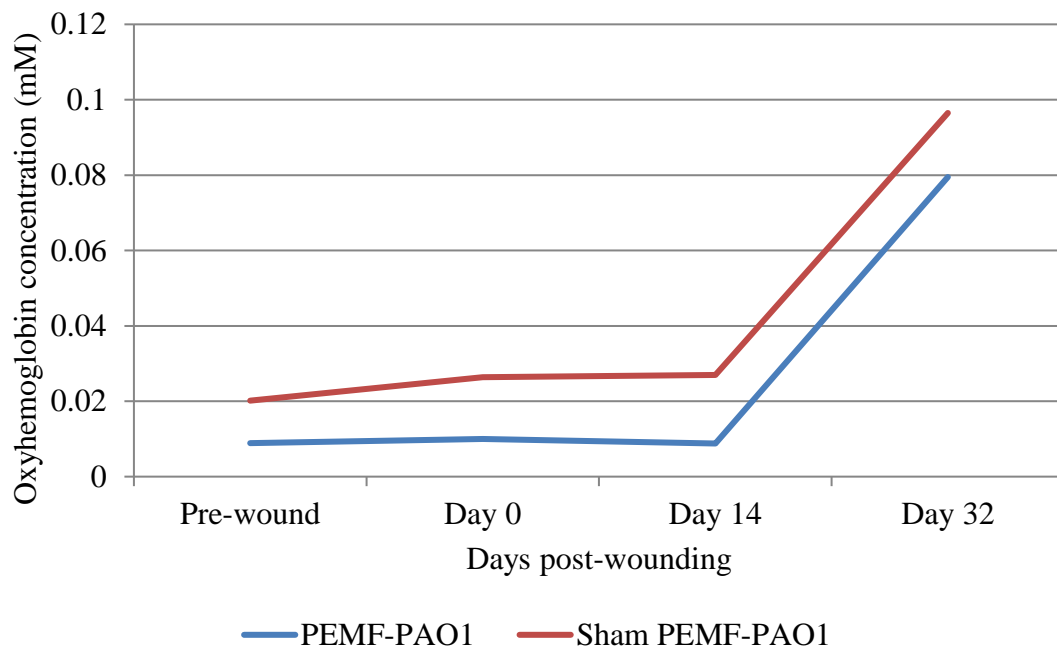


Figure 7.14 The mean oxyhemoglobin concentration of the PEMF-PAO1 and sham PEMF-PAO1 group, as measured by the near-infrared spectroscopy on different days of wound healing.

The deoxyhemoglobin level increased from pre-wounding to day 32 in both PEMF-PAO1 and sham PEMF-PAO1 groups in a parallel manner. There were no significant between-group difference throughout the study period.

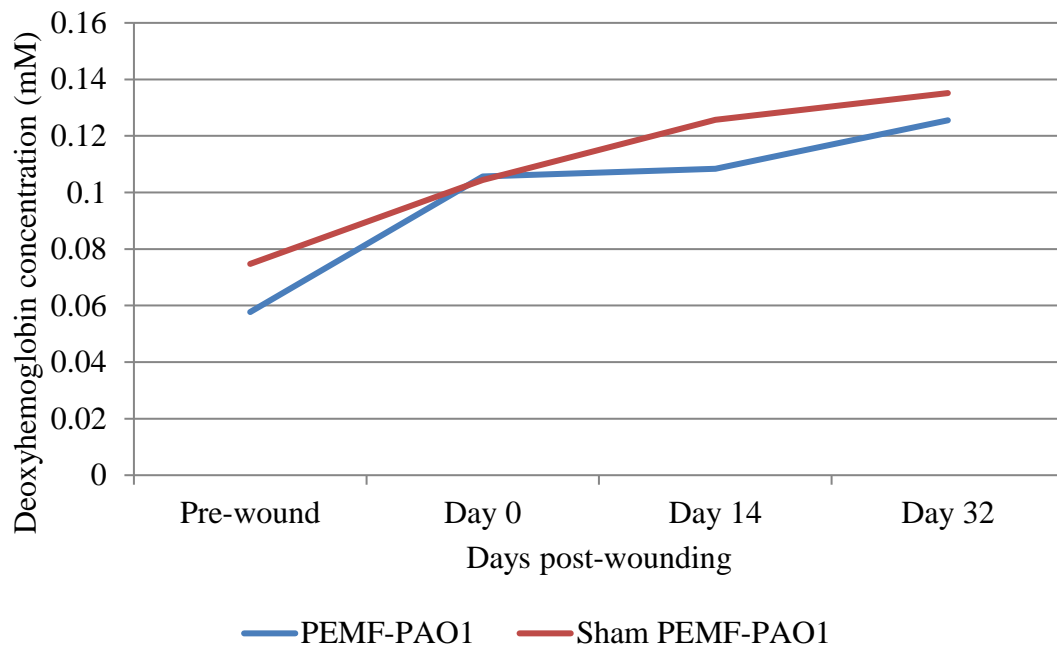


Figure 7.15 The mean deoxyhemoglobin concentration of the PEMF-PAO1 and sham PEMF-PAO1 group, as measured by the near-infrared spectroscopy on different days of wound healing.

The oxygen saturation level at wound had a gradual decrease from pre-wounding to day 14 in both PEMF-PAO1 and sham PEMF-PAO1 groups. In general, the oxygen saturation level in the PEMF-PAO1 group was lower than that in the sham PEMF-PAO1 group. Then the level of oxygen saturation in both PEMF-PAO1 and sham PEMF-PAO1 groups increased drastically from day 14 to day 32 (38.10 ± 10.98 vs. 42.35 ± 27.01 ; between group $P=0.78$), however, the between-group difference did not reach significance level throughout the study.

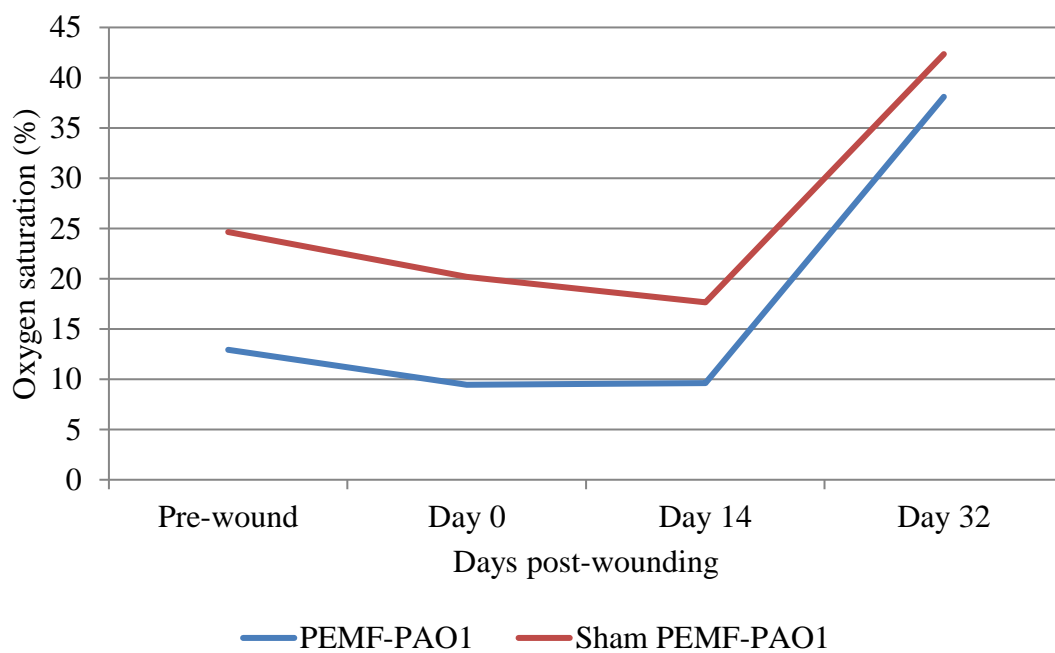


Figure 7.16 The mean oxygen saturation of the PEMF-PAO1 and sham PEMF-PAO1 group, as measured by the near-infrared spectroscopy on different days of wound healing.

7.3.4 Tissue repair

7.3.4.1. Growth factor

The representative photographs of the α -SMA in the PEMF-PAO1 and sham PEMF-PAO1 group measured on day 23 and 32 are shown in Figure 7.17.

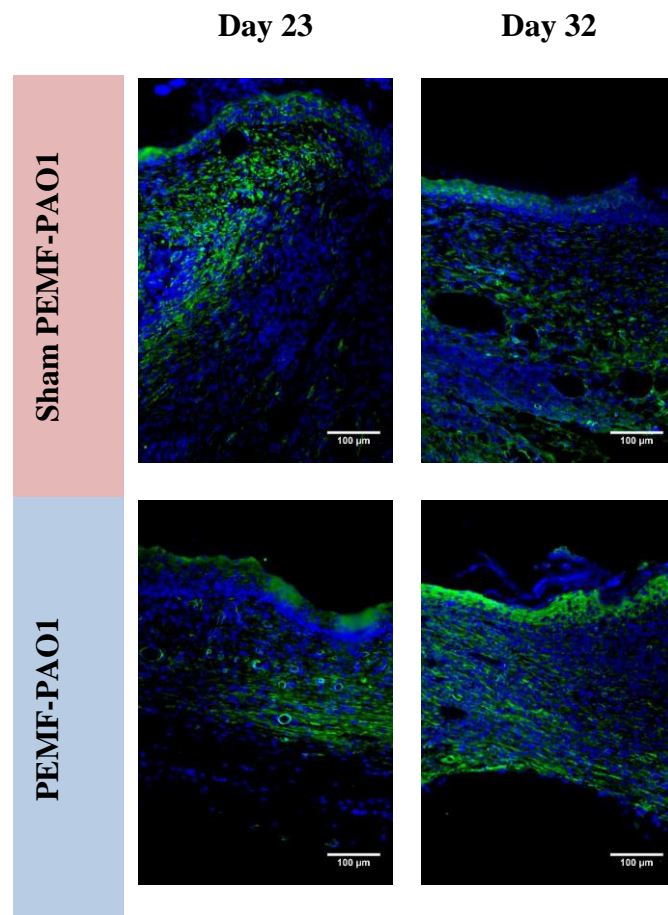


Figure 7.17 The population of α -SMA measured in PEMF-PAO1 and sham PEMF-PAO1 groups on day 23 and 32.

There was higher α -SMA staining area fraction in PEMF-PAO1 group (0.73 ± 0.02) than the sham PEMF-PAO1 group (0.60 ± 0.13) ($P=0.15$) on day 23 (Figure 7.18). Both PEMF-PAO1 (0.79 ± 0.46) and sham PEMF-PAO1 (0.85 ± 0.19) groups illustrated an increase in α -SMA staining area fraction by day 32, however, the between-group difference did not reach significance at any time point.

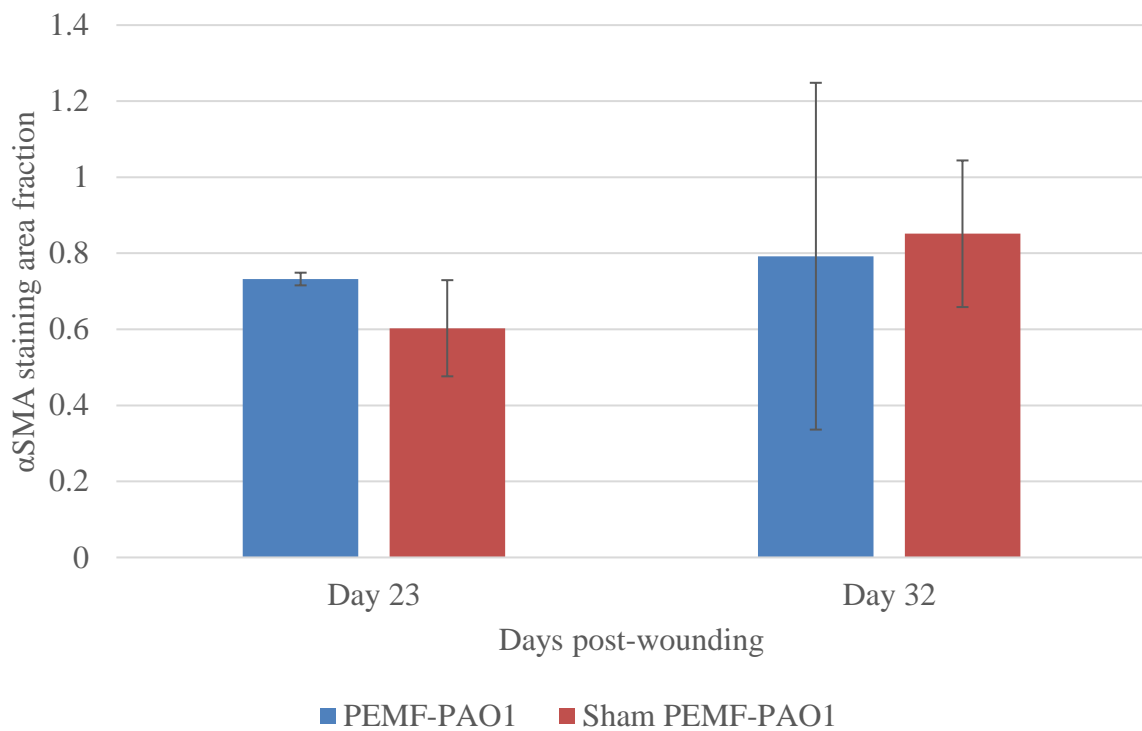


Figure 7.18 The α -SMA staining area fraction of the PEMF-PAO1 and sham PEMF-PAO1 wounds recorded on post-wounding day 23 and 32.

On day 23, the mean α -SMA staining intensity in the PEMF-PAO1 group (135.50 ± 11.99) was higher than did the sham PEMF-PAO1 group (125.29 ± 3.48) (between-group $P=0.22$) (Figure 7.19). On day 32, both PEMF-PAO1 (176.26 ± 56.48) and sham PEMF-PAO1 (212.05 ± 47.98) groups demonstrated an increase in α -SMA staining area fraction, however, the between-group difference did not reach significance level throughout the study period.

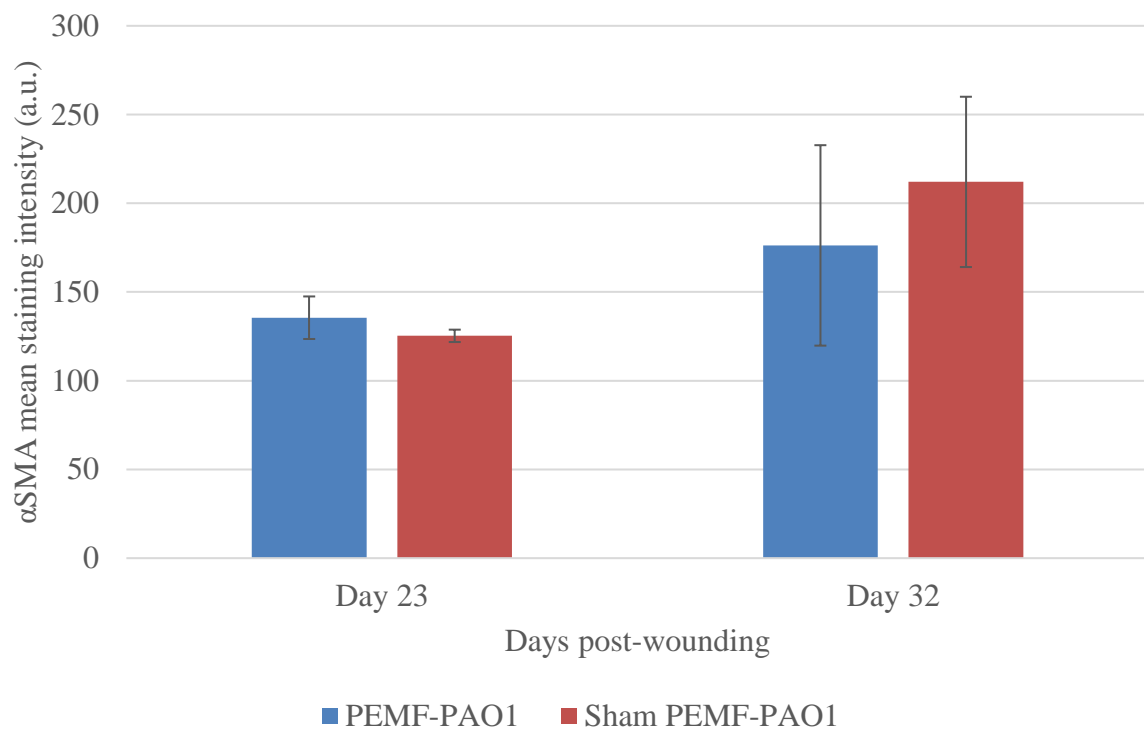


Figure 7.19 The α -SMA mean staining intensity (arbitrary unit) of the PEMF-PAO1 and sham PEMF-PAO1 wounds.

7.3.4.2. *Collagen deposition*

With picro-sirius red polarization microscopy, type I collagen fibres appeared red with high intensity. All these fibres were observed only in the dermal layer (Figure 7.20)

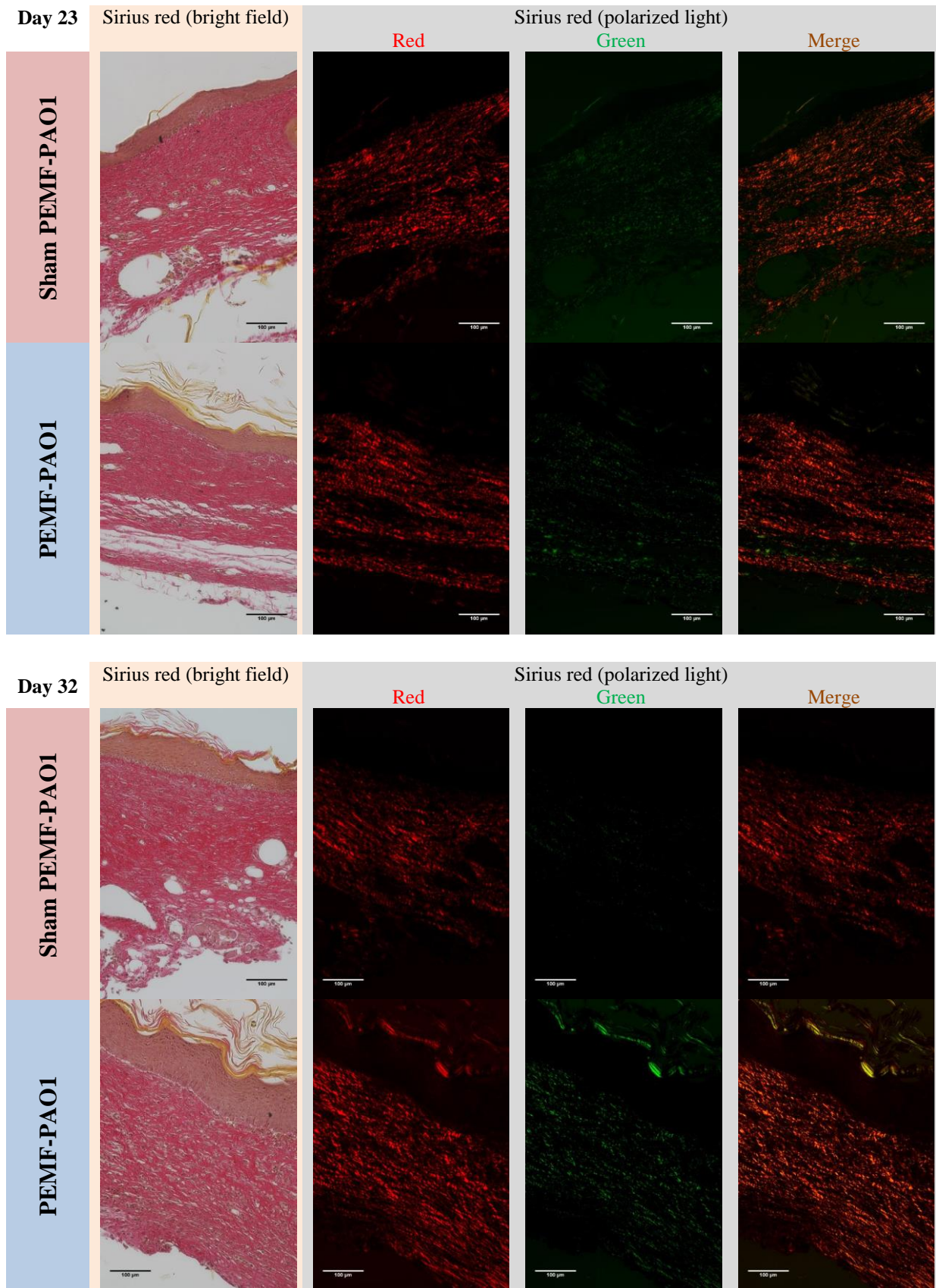


Figure 7.20 Representative picro-sirius red stained sections from PEMF-PAO1 and sham PEMF-PAO1 groups on days 23 and 32.

On day 32, PEMF-PAO1 exhibited an increase in collagen ratio, indicating a decrease of the proportion of immature collagen fibres. The results obtained from the stained sections revealed no statistical difference in thick mature (red) to thin immature (green) collagen ratio in wound tissues between PEMF-PAO1 and sham PEMF-PAO1 groups on day 23 ($P=0.74$) and day 32 ($P=0.68$) (Figure 7.21).

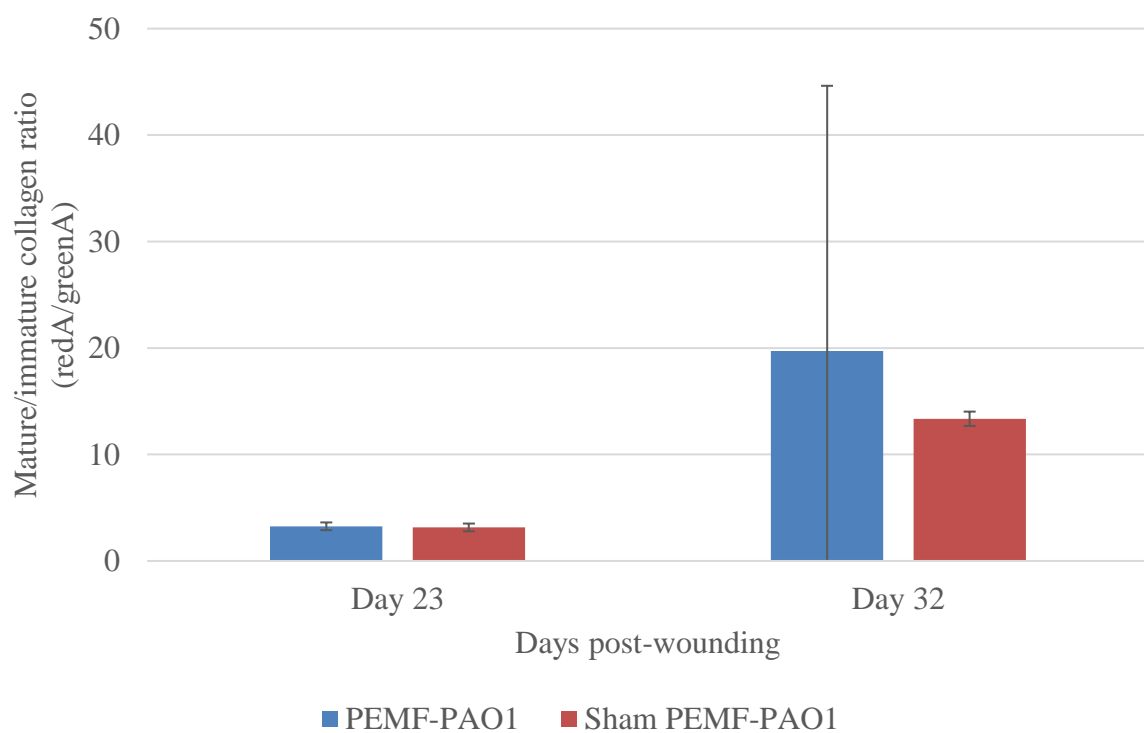


Figure 7.21 Thick mature (red) to thin immature (green) collagen ratio of chronic wound tissues in PEMF-PAO1 and sham PEMF-PAO1 groups on day 23 and 32.

The type I collagen fibre deposition represented by redA/ROIA decreased from day 23 to day 32. The type I collagen fibre deposition in the wound tissues of PEMF-PAO1 group was greater than that of sham at each time point measured. However, there was no statistical significance between PEMF-PAO1 and sham groups at any time points (Figure 7.22).

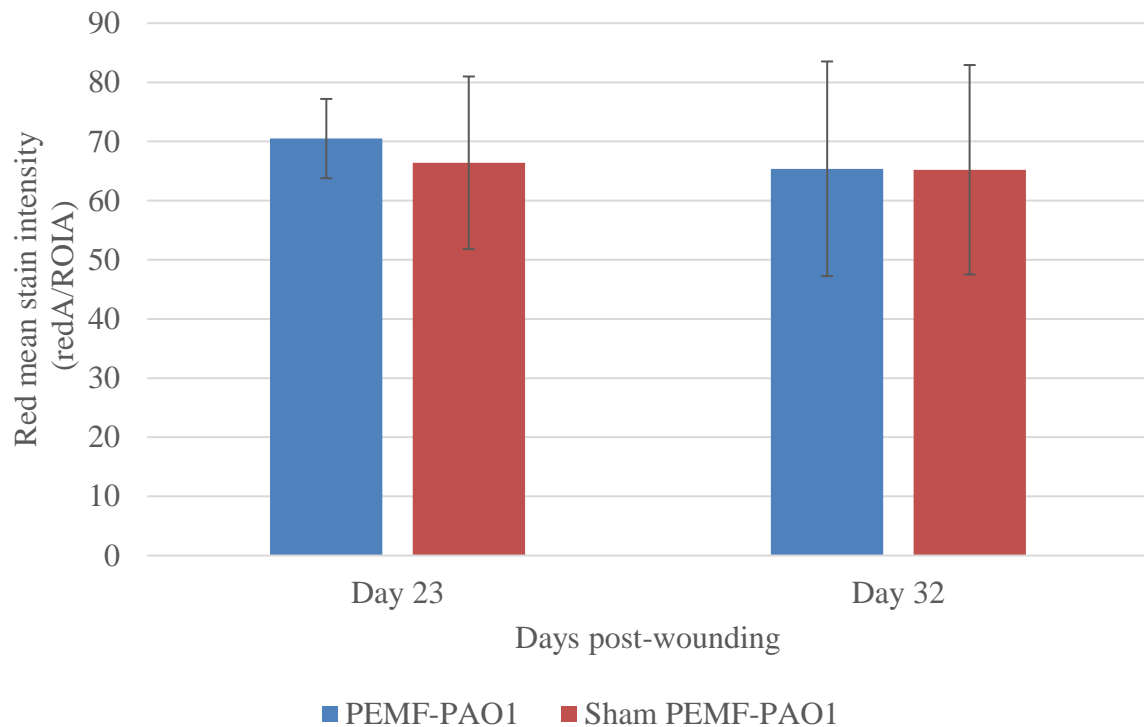


Figure 7.22 Type I collagen fibril deposition of samples from PEMF-PAO1 and Sham PEMF-PAO1 groups on days 23 and 32.

Collagen fibril alignment, represented by the intensity of birefringence, was similar between groups with no significant differences between days or groups detected (Figure 7.23).

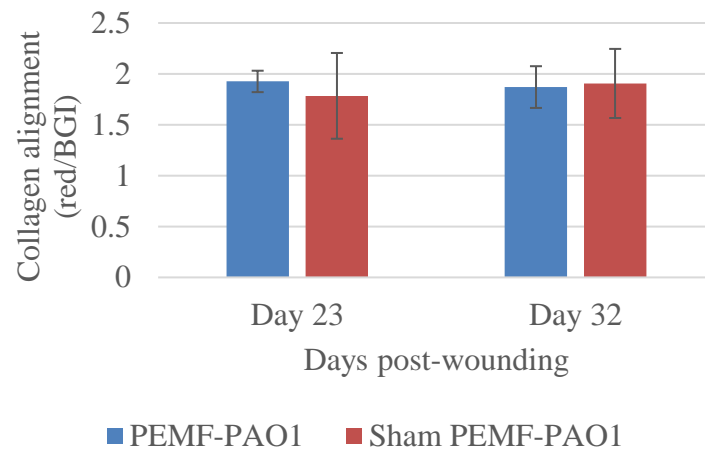


Figure 7.23 Type I collagen fibril alignment of samples from PEMF-PAO1 and Sham PEMF-PAO1 groups on days 23 and 32.

The collagen fibre anisotropy index significantly increased from day 23 to day 32 (Figure 7.24). During the study period (either day 23 or day 32), the collagen fibre anisotropy index in the two groups are were similar and no significant between-group difference was recorded.

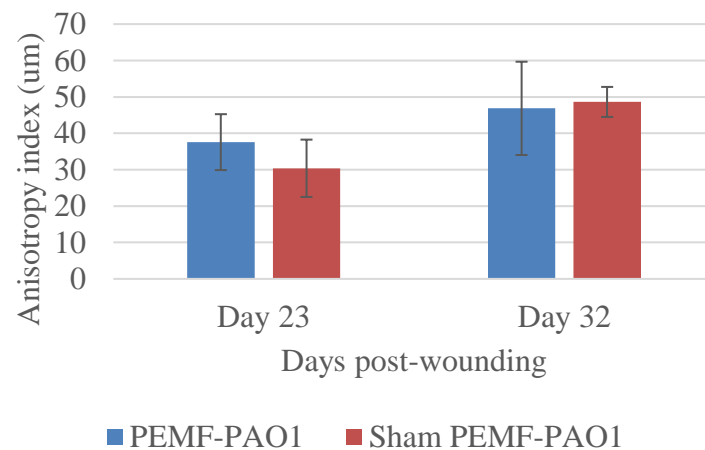


Figure 7.24 Type I collagen fibre anisotropy of samples from PEMF-PAO1 and sham PEMF-PAO1 on days 23 and 32.

In the plane of sections, no qualitative between-group difference was found in the orientation of collagen fibres in terms of parallelism to the epidermis (Figure 7.20). The orientation of the individual collagen fibres was more or less parallel to the epidermis. No significant between-group difference of the collagen fibre orientation angle was found at any time points (Figure 7.25).

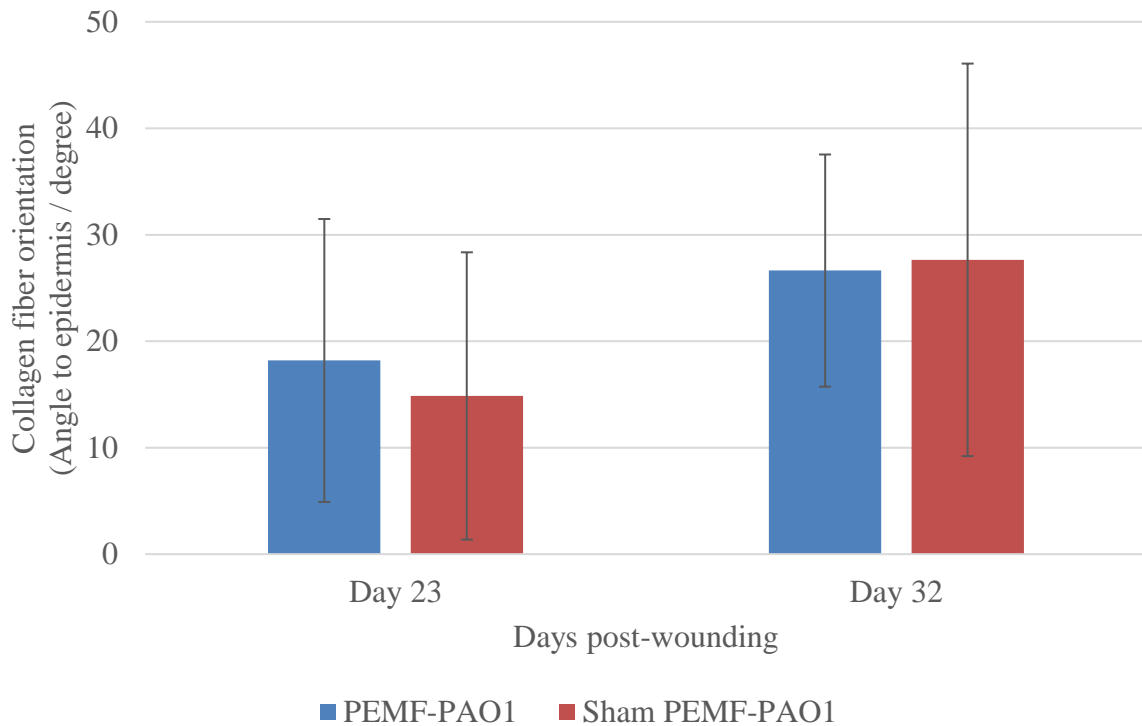


Figure 7.25 Type I collagen fibre orientation angle measured from the epidermis between PEMF-PAO1 and sham PEMF-PAO1 groups on day 23 and 32.

7.3.5 Biomechanical parameters for the wound specimen

There was no statistical difference on the wound thickness between PEMF-PAO1 and sham PEMF-PAO1 on day 23 and 32. The maximum load of the PEMF-PAO1 group was greater than that of the sham PEMF-PAO1 group on day 23, but lower on day 32. Maximum stress of PEMF-PAO1 group was smaller on day 23 but greater on day 32 than the sham PEMF-PAO1

group. Young's Modulus of PEMF-PAO1 was also smaller than the sham PEMF-PAO1 on day 23, but PEMF-PAO1 showed a greater Young's Modulus on day 32 than the sham PEMF-PAO1 group. The energy absorption capacity of PEMF-PAO1 group was greater than that of sham on day 23 and day 32. Despite differences in various biomechanical parameters were found between PEMF-PAO1 and the sham PEMF-PAO1 groups, none of these parameters reach statistical significance at any time points measured (Table 7.1).

Table 7.1 Biomechanical parameters to the healing mice skin wounds of db/db mice as measured by the material testing system ex vivo.

Days post-wounding	PEMF-PAO1		Sham PEMF-PAO1	
	Day 23 (n=2)	Day 32 (n=1)	Day 23 (n=3)	Day 32 (n=1)
Maximum load (N)	3.24±0.26	3.05	3.68±0.73	2.76
Maximum stress (MPa)	0.35±0.09	0.40	0.36±0.13	0.25
Young's modulus (MPa)	1.37±0.42	1.27	1.61±0.67	0.98
Energy absorption capacity (mJ)	15.11±4.50	19.94	12.28±1.34	10.32

7.4 DISCUSSION

The PAO1 biofilm chronic wound model was adopted in a previous study (Zhao et al., 2010). It is characterized with a reproducibly delayed wound healing in db/db mice by an average of

2 weeks that remained unhealed at 4 weeks post-inoculation (Zhao et al., 2012). Earlier work published by our research team have shown that PEMF can improve diabetic wound healing in acute wound models (Cheing et al., 2014, Choi et al., 2018, Choi et al., 2016, Kwan et al., 2015). Moreover, studies from other research group have reported that PEMF inhibited PAO1 growth rate, disintegrated the cell wall and resulted in cell material leakage (Inhan-Garip et al., 2011). By day 32, our present findings illustrated that only 50% of sham PEMF-PAO1 wound healed completely, compared to 75% in the PEMF-PAO1 group. Despite the PEMF-PAO1 group tend to present with greater re-epithelization percentage, however, the between-group difference did not reach statistically significance.

Our earlier study proved that PEMF can significantly increase collagen fibre in early phase of acute diabetic wound healing that associated with myofibroblast population enhancement (Cheing et al., 2014, Choi et al., 2016). However, PEMF did not produce significant changes in collagen orientation in acute wound of streptozotocin-induced DM rats (Choi et al., 2016). On day 23, fibrils alignment was laid down in a more parallel manner in PEMF treated chronic wounds by anisotropy. Our results also demonstrated that type I collagen deposition in PEMF-PAO1 group appeared to be greater on Day 23 and 32. Our present findings suggested that PEMF could promote collagen synthesis and disposition in diabetic wound.

Previous studies demonstrated that PEMF promotes angiogenesis by stimulating endothelial proliferation and releasing soluble proangiogenic protein FGF-2 in an acute diabetic wound model (Callaghan et al., 2008, Goudarzi et al., 2010). Choi et al. and coworkers (2016) postulated that the FGF-2 may act on the fibroblast to promote proliferation and collagen deposition possibly through alpha-smooth muscle actin (α -SMA) and vascular endothelial growth factor (VEGF). VEGF regulates epithelialization, connective tissue formation and angiogenesis, its level usually increased in acute wounds and decreased in chronic wounds (Bao et al., 2009). In our study, both α -SMA and VEGF level appeared to increase on day 23

suggesting PEMF might potentially be able to shorten the chronicity duration in this PAO1 biofilm chronic wound model in DM mice.

Tissue oxygenation is also a crucial factor for wound healing, and low oxygen pressure is associated with delayed wound healing. In particular, microvascular dysfunction is a common and one of the main causes of chronic DM foot ulcer. The presence of biofilm may aggravate the underlying tissue hypoxia. In the present study, the oxyhemoglobin concentration in the sham PEMF-PAO1 group maintained at a higher level than the PEMF-PAO1 group throughout the study period, whereas both groups presented with increasing trends. It has been hypothesized that chronic non-healing DM wounds may get ‘stuck’ in various phases of the healing process, resulting in oxyhemoglobin concentrations remained high in non-healing wounds (Neidrauer et al., 2010). The increase in oxyhemoglobin concentration might be associated with an increase in VEGF and blood vessel density showed in the present study, as in the healing process in the late inflammatory and proliferative stages.

Our present study showed that PEMF treatment potentially promotes healing of chronic wound in transgenic DM mice, in terms of accelerating wound closure and re-epithelization, enhance angiogenesis and improve tissue repairing. One of the limitations in the present study is that we did not investigate the bacteria growth rate and morphological change under PEMF treatment. Future studies are warranted to optimize the treatment protocols of PEMF and determine the underlying mechanisms on bacteria morphological changes of PAO1.

CHAPTER 8

CONCLUSIONS AND SUGGESTIONS FOR FUTURE RESEARCH

Foot ulcer is a major complication of diabetes mellitus that may lead to amputation. Oedema of the foot and oxygenation dysfunction caused by microvascular disturbance might contribute to failure in the wound healing process. Our earlier published systematic reviews showed that biophysical modalities is effective in promoting wound healing of *in vivo* and *in vitro* diabetic wound models (Kwan et al., 2019); and in people with diabetes (Kwan et al., 2013).

Therefore, this thesis consists of four inter-related studies. In Study I, we first investigated the skin morphology and oxyhemoglobin concentration of plantar soft tissue in people with type 2 diabetes mellitus (DM) with or without neuropathy and ulceration. Study II examined the efficacy of pulsed electromagnetic field on restoring oxyhemoglobin concentration and promoting acute dermal wounds healing; and the underlying biological mechanisms of pulsed electromagnetic field in streptozotocin-induced DM rat models. In Study III, we examined the efficacy of pulsed electromagnetic field in promoting dermal wounds healing with or without *Pseudomonas aeruginosa* (PAO1) in a chronic wound model. In Study IV, we further examined the efficacy of pulsed electromagnetic field (PEMF) in promoting wounds healing in acute and chronic dermal wounds with or without PAO1 in transgenic diabetic mice.

Study I entitled ‘The association between oxyhemoglobin concentration with epidermal oedema in the diabetic foot.’ In Study I, the skin morphology and oxyhemoglobin concentration of plantar soft tissue was examined in seventy-six human subjects (69 people with diabetes but without neuropathy [DM], 1 with diabetic neuropathy [DPN], 1 with a history of diabetic foot ulcer [DU] and 5 without diabetes [non-DM]). Assessment including the measurement of: (1) High frequency ultrasonography with a Vevo model 708 scanhead operating at the center frequency of 55 MHz for imaging skin morphology on the big toe, first metatarsal head, third metatarsal head, fifth metatarsal head, medial foot arch and the heel of the right foot; (2) The concentration of oxy- and deoxy-hemoglobin by the use of near infrared spectroscopy at the pulp of big toe. The average epidermal thickness of the pulp of big toe in

the DU group was significantly thinner than that of the DM group. The increase in subepidermal low echogenic band thickness of foot representing the oedema at plantar skin, and there was significant between-group difference in thickness among people with or without diabetes or diabetic-related complications at the pulp of big toe, the first metatarsal head, the third metatarsal head, the fifth metatarsal head and the heel pad region. The subepidermal low echogenic band was the thickest in the DU group. The DM subjects showed higher oxyhemoglobin and deoxyhemoglobin concentrations than that in the non-DM subjects. Significant positive correlation of the oxyhemoglobin and deoxyhemoglobin concentrations with the subepidermal low echogenic band thickness was demonstrated at the heel pad region. In addition, weak positive correlation of the oxyhemoglobin and the epidermal thickness was shown at the first metatarsal head. No significant correlation between oxygen saturation and any parameters was found at any measuring sites.

Study II entitled ‘The effects of pulsed electromagnetic field on oxyhemoglobin concentration and wound healing in diabetic acute wound model.’ We then examined the efficacy of pulsed electromagnetic field in an acute wound model in rat. In Study II, twenty-six male Sprague-Dawley (SD) rats weighting 243 to 371 g (mean: 327.2 ± 28.7 g) were used in this study. After DM induction by the use of streptozotocin, wounds were induced with 6mm biopsy punch on the lateral side of lower hind limbs (3mm distal to fibula head). For the PEMF group, the wounds of the rats were exposed to active pulsed electromagnetic fields (2 mT, 25 Hz) for one hour daily. Rats in the sham group were restrained in the bag (same as the PEMF group) for an hour but did not expose to any PEMF. The assessment procedures included: (1) taking a photo by the use of a digital camera and a Verge Videometer Measurement Documentation software were used for calculating the area of the wound; (2) The concentration of oxy- and deoxy-hemoglobin were measured by the use of near infrared spectroscopy at the wound center and wound edges. The wound size of the PEMF group decreased at a faster rate

than that of the sham PEMF group over time. All wound sizes reduced significantly in the initial few days and almost completely closed at Day 10. The oxyhemoglobin concentrations in central wound area of PEMF group were significantly lower than that in sham PEMF group on day 5. Moreover, the oxyhemoglobin concentration decreased faster in PEMF group than did the sham PEMF group over time. Further to the change in wound size and oxyhemoglobin, nitrite concentration of the wounds in PEMF and sham groups was examined throughout the study period. Nitrite is a stable end product of nitric oxide. The Nitrite concentration in the PEMF group (47.6 μM) tended to be higher than did the sham group (24.9 μM), but the between-group difference did not reach significance level in any time point.

Study III entitled ‘Efficacy of pulsed electromagnetic field in promoting non-diabetic dermal wound healing with or without *Pseudomonas aeruginosa*.’ Since diabetic wound healing is a complex process that might be contributed by the underlying pathology or exogenous bacteria, we set off to examine whether pulsed electromagnetic field would promote healing in wound infected with *Pseudomonas aeruginosa* (PAO1) without diabetes. In Study III, fifteen C57 mice aged 18 weeks were used. Wounds were induced with 6 mm biopsy punch at the back of mice. *Pseudomonas aeruginosa* were inoculated covered with Tegaderm in 7 mice, whereas only Tegaderm (without PAO1) were applied to the other 8 mice as control group. For the PEMF group, the wounds of the mice were exposed to active electromagnetic fields (5 mT, 20 Hz) for one hour daily. For the sham group, mice were restrained in the bag for an hour without exposing to any PEMF. After 7 days of PEMF treatment, the wound area in sham group with PAO1 was significantly enlarged; in contrast, the wound area was reduced by 80% in the PEMF group with PAO1 as compared to the baseline.

Study IV entitled ‘Efficacy of pulsed electromagnetic field in promoting dermal wounds healing with or without *Pseudomonas aeruginosa* in diabetic wound model.’ In the last part of this thesis, we investigated the effectiveness of pulsed electromagnetic field to promote

healing of chronic wound infected with *Pseudomonas aeruginosa* (PAO1) in transgenic DM mice. In Study IV, seventy-three db/db mice (aged 9 weeks) were used in a two by two model. Wounds were induced with 6 mm biopsy punch at the back of the mice. Chronic wound model was adopted by inoculating *Pseudomonas aeruginosa* (PAO1) to the wound then covered the wound with Tegaderm in 48 mice; whereas an acute wound model without PAO1 was adopted in the other 25 mice in which only Tegaderm were applied to cover the wound. The mice in each group were further randomly allocated into the PEMF group or control group. For the PEMF group, the wounds of the mice were exposed to active PEMF (5mT, 20 Hz) for one hour daily. For the control group, mice were not exposed to any PEMF. After 9 and 14 days of post wounding, the wound area in the sham group with PAO1 was significantly enlarged, whereas the wound size of the PEMF group reduced significantly. In contrast, the mice that had acute wound with or without PEMF completely healed after 9 days of post wounding. Further histological analysis were done on the chronic wound model for wound closure, angiogenesis and tissue repair in wound healing progression day from 26 and 35 days post wounding. On day 26 post wounding, a trend of greater re-epithelialization percentage was observed in the PEMF group as compared to the control group. On day 26 and 35 post wounding, there was a trend of greater blood vessel density and VEGF mean staining intensity shown in the PEMF group than that of the sham PEMF group. For tissue repairing, α -SMA increased in PEMF group on Day 26 and decreased on Day 35. A similar trend was found in collagen orientation and alignment. PEMF group shower a higher energy absorption capacity, maximum load, maximum stress and Young's modulus than the sham PEMF group on day 35 post.

Diabetic foot ulceration is preventable by early detection of risk factors. Our findings suggest that evaluation of plantar skin morphology and oxyhemoglobin concentration is an important predictor for foot ulceration in people with diabetes, therefore, these assessment procedure should be added in routine clinical screening. For examining the plantar skin morphology and

oxygenation concentration in people with DM (Study I), there were limited number of subjects with diabetic peripheral neuropathy or ulceration because of difficulty in subject recruitment. Therefore, our sample size was relatively small. A large scale of study is warranted to assess DM subjects who have different severity of peripheral neuropathy, with or without ulceration. In Study II, we used a SD rats to examine the efficacy of PEMF in promoting diabetic acute wound healing. In Study III, we also used C57 mice to examine the effects of PEMF in promoting non-diabetic chronic wound healing. In Study IV, we used transgenic diabetic mice to examine the effects of PEMF in promoting chronic diabetic wound healing. There were positive findings observed in difference animal species, however the results may not be able to translate directly to clinical practice due to the differences in actual skin structures between human and animals. Randomized controlled clinical trials remain the golden standard for investigating if pulsed electromagnetic field could promote chronic wound healing in patients with diabetes. Different species of rodents have been used in the present thesis including streptozotocin-induced diabetic SD rats, C57 mice or transgenic db/db mice. SD rats are characterized with defective early inflammatory response to wounding, therefore a commonly used ideal type 1 diabetic model for acute wound healing research. Yet, majority of people with chronic wound have type 2 diabetes, complicated with multiple risk factors that lead to wound infection. Transgenic db/db mice have persistent hyperglycemia and develop robust neuropathy (O'Brien et al., 2014), while C57 mice is their littlemate. Moreover, a chronic diabetic animal model was successfully established with db/db mice (Zhao et al., 2010, Zhao et al., 2012). Therefore, different animal models were adopted in the present thesis.

It would also be interesting to investigate whether PEMF can reduce the oedema and restore oxyhemoglobin concentration in people with diabetic ulceration with or without bacterial infection. Incidence rate of diabetic foot ulcer recurrence is very high, 40% of patients have a recurrence within 1 year after ulcer healing and 65% within 5 years (Armstrong et al., 2017).

Pulsed electromagnetic field may play a leading role in maximizing ulcer-free days by improving the crucial factors including minimize inflammation, improve circulation and normalize cellular function. Future randomized controlled trial is warranted to determine whether our observations can be translated to clinical practice.

APPENDICES

APPENDIX I

Research Project Informed Consent Form

Project title: Examination on foot oedema in people with diabetes and its potential influence on skin oxygenation

Investigator(s):

Prof. Gladys CHEING, PhD, Department of Rehabilitation Sciences, The Hong Kong Polytechnic University

Ms. Rachel KWAN, MPhil, PT, Department of Rehabilitation Sciences, The Hong Kong Polytechnic University

Project information:

The purpose of this study is to examine the extent of foot oedema and its potential influence on skin oxygenation for people with diabetes.

People aged above eighteen diagnosed with Type 2 diabetes with or without peripheral neuropathy will be recruited. Exclusion criteria are uncontrolled heart diseases, history of stroke, malignancy radiotherapy, or renal diseases. Subjects who are taking medications that might affect their circulation, sensation and motor functioning; any history of alcoholism or surgery done in either of the lower limbs will also be excluded. Subepidermal oedema of the foot will be measured by high frequency ultrasonography. Skin oxygenation over the foot will be conducted by using near infrared spectroscopy. Blood doping will be performed for HbA1c investigation. Foot examination included monofilaments and biothesiometry will be performed on each patients for sensation. A written consent will be obtained from the subjects.

All the measurements methods are absolutely safe with no known side-effects. Subjects will not be exposed to any painful stimulation during assessment. Subjects are under no obligation to take part in this study and free to withdraw from the study at any time. Subject's personal information and data acquired from this study is strictly confidential and will not be disclosed to people who are not related to this study. Fifty dollars of travelling allowance will be given to each participant upon completion of assessment. Written report on the investigation will be send to each participant by mail around 2 weeks post assessment. The findings in this research study may help us to have better understand of diabetic foot complications, which would be important for management of diabetes.

If you would like more information about this study, please contact Prof. Gladys Cheing at telephone 2766 6738 and you will be given a signed copy of consent form. If you have any complaint about the conduct of this research study, please do not hesitate to contact Ms Gloria Man, secretary of Departmental Research Committee of The Hong Kong Polytechnic University at tel. no. 2766 4394.

Thank you for your interest in participating in this study.

Consent:

I, _____, have been explained the details of this study. I voluntarily consent to participate in this study. I understand that I can withdraw from this study at any time without giving reasons, and my withdrawal will not lead to any punishment or prejudice against me. I am aware of any potential risk in joining this study. I also understand that my personal information will not be disclosed to people who are not related to this study and I agree to provide details about my condition to the investigators of this study. My name or photograph will not appear on any publications resulted from this study.

I can contact the chief investigator, Prof. Gladys Lai-Ying Cheing at telephone 27666738 for any questions about this study. If I have complaints related to the investigator(s), I can contact Ms Gloria Man, secretary of Departmental Research Committee, at 27664394. I know I will be given a signed copy of this consent form.

Signature (subject):

Date:

Signature (witness):

Date:

APPENDIX II

香港理工大學康復治療科學系科研同意書

科研題目：糖尿病患者足部水腫及血氧之檢測

科研人員： 鄭荔英教授（香港理工大學康復治療科學系）

關麗珠小姐（註冊物理治療師）

科研內容：

本研究之目的為透過早期檢測糖尿病患者足部水腫及血氧預防糖尿病足的形成。

此科研的研究對象為年滿十八歲，被醫生確診為二型糖尿病，沒有中風、腎病、嚴重心臟病等病歷，及未曾接受過放射治療或下肢手術。參加者將接受高頻超聲波量度足底部的皮下水腫，及以近紅外線光譜儀能量度氧合血紅蛋白、還原血紅蛋白濃度及血氧飽和度。參加者亦會接受足部觸感覺測試，及抽血檢驗糖化血色素。研究對象將被邀請到香港理工大學進行所有測試。

對項目參與人仕和社會的益處：

此研究費用全免，能為糖尿病患者足部水腫提供更有效的檢測，研究結果將對今後糖尿病足部治療提供寶貴資料。參加者可於完成整項測試後收取港幣五十元交通津貼，亦可於測試後約兩星期收到書面檢測報告。

潛在危險性：

此研究的所有測試測試都十分安全，沒有潛在危險性，測試過程中不會引起疼痛。參與者有權在任何時候、無任何原因放棄參與此次研究，不會導致任何懲罰或不公平對待。個人資料將不會洩露給與此研究無關的人員。研究對象如有關於此項研究的疑問，可在辦公時間內致電鄭荔英教授(2766 6738)查詢。若研究對象對此研究有任何投訴，可聯繫文女士（部門科研委員會秘書），電話：2766 4394。

多謝閣下的積極參與。

同意書：

本人_____已瞭解此次研究的具體情況。本人願意參加此次研究，本人有權在任何時候、無任何原因放棄參與此次研究，而此舉不會導致我受到任何懲罰或不公平對待。本人明白參加此研究課題的潛在危險性以及本人的資料將不會洩露給與此研究無關的人員，我的名字或相片不會出現在任何出版物上。

本人可以用電話 2766 6738 來聯繫此次研究課題負責人，鄭荔英博士。若本人對此研究人員有任何投訴，可以聯繫文女士（部門科研委員會秘書），電話：2766 4394。本人亦明白，參與此研究課題需要本人簽署一份同意書。

簽名（參與者）：_____ 日期：

簽名（證人）：_____ 日期：

APPENDIX III

檢查須知

參加者年齡必須十八歲或以上被醫生確診為二型糖尿病患者，沒有中風、腎病、糖尿病、嚴重心臟病等病歷，及未曾接受過下肢手術並自願參加。參加者於報名後將會收到香港理工大學的註冊物理治療師電話聯絡，確認參加者身體狀況適合參加此項研究，並預約時間親臨香港理工大學進行檢查。完成整項研究後，參加者可即時獲得港幣五十元交通津貼。

此項研究所使用的檢查方法，已通過香港理工大學的安全評審。高頻超聲波及近紅外線光譜儀均是非入侵性的檢測儀，測試沒有潛在危險性，測試過程中不會引起疼痛。參與者有權在任何時候、無需任何原因放棄參與此次研究，而此舉不會影響其正接受的醫治。

參加者的個人資料將受到保密。參與者的資料將不會洩露給與此研究無關的人員。參加者的名字不會出現在任何出版物上。

閣下如有任何查詢
預約檢查
可在辦公時間內致電

香港理工大學
康復治療科學系
物理治療部關姑娘
(香港註冊物理治療師)

電話：6056 7822

檢查地點
紅磡香港理工大學
ST010

主辦：



協辦：



糖尿病足

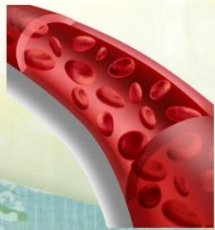
對血液微循環的影響

足部水腫

足部水腫是糖尿病患者常見的問題，嚴重者會引起足部血液微循環改變，以致氧氣及養份未能順利傳送，而導致各種糖尿病足併發症。

根據科學研究指出，糖尿病患者的血管經常會出現結構上及功能上的變異，¹大概一半患者的足部潰瘍由血管病變而產生，嚴重患者可能須要接受截趾或截肢手術。

及早檢查足部水腫及血液微循環的情況能有效預防及減低糖尿病併發症例如足部潰瘍的發生。

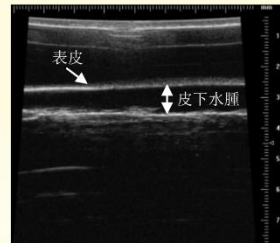


¹ Chao CYI, Cheing GLY. Microvascular dysfunction in diabetic foot disease and ulceration. Diabetes/metabolism research and reviews 2009;25:604-14.

預防勝於治療

本研究採用最新的科技檢查足部。高頻超聲波透過影像用於量度足底部的皮下水腫（圖一）。

²最新科學文獻指出糖尿病足部潰瘍患者的皮下水腫比糖尿病患者及健康人士嚴重。



圖一、利用高頻超聲波影像量度糖尿病足的皮下水腫

近紅外線光譜儀能量度氧合血紅蛋白、還原血紅蛋白濃度及血氧飽和度。優良的微血液微循環能把氧氣及營養順利傳送，保持皮膚健康，促進傷口癒合。

² Chao CYI, Zheng YP, Cheing GLY. The association between skin blood flow and edema on epidermal thickness in the diabetic foot. Diabetes technology & therapeutics 2012; 14(7):602-9.

免費測試

檢查範圍

- 糖化血色素，需抽血檢驗
- 足部觸覺感，測試神經病變
- 足部血液微循環
- 足部皮下水腫

參加者可在香港理工大學接受物理治療師進行大概 1 小時的足部檢查。此足部檢查在一般診所均未有提供，仍採用最新高頻超聲波及近紅外線光譜儀等先進儀器來測試第二型型糖尿病患者足部變化。此測試能更深入檢測足部水腫及血液循環的情況，有效及早偵測糖尿病足部病變。

所有檢查費用全免，參加者可即時獲知檢查結果。參加者亦可於測試後約兩星期收到書面報告。



Review

Efficacy of Biophysical Energies on Healing of Diabetic Skin Wounds in Cell Studies and Animal Experimental Models: A Systematic Review

Rachel Lai-Chu Kwan ¹, Song Lu ¹, Harry Ming-Chun Choi ¹, Luther C. Kloth ² and Gladys Lai-Ying Cheing ^{1,*}

¹ Department of Rehabilitation Sciences, The Hong Kong Polytechnic University, Hong Kong, China;

rachel.lc.kwan@ (R.L.-C.K.); songlu.u.washington@ (S.L.);

harry.choi@ (H.M.-C.C.)

² Department of Physical Therapy, College of Health Sciences, Marquette University, Milwaukee,

WI 53201-1881, USA; luther.kloth@

* Correspondence: Gladys.Cheing@ ; Tel.: +852-2766-

Received: 18 December 2018; Accepted: 14 January 2019; Published: 16 January 2019



Abstract: We have systematically assessed published cell studies and animal experimental reports on the efficacy of selected biophysical energies (BPEs) in the treatment of diabetic foot ulcers. These BPEs include electrical stimulation (ES), pulsed electromagnetic field (PEMF), extracorporeal shockwave (ECSW), photo energies and ultrasound (US). Databases searched included CINAHL, MEDLINE and PubMed from 1966 to 2018. Studies reviewed include animal and cell studies on treatment with BPEs compared with sham, control or other BPEs. Information regarding the objective measures of tissue healing and data was extracted. Eighty-two studies were eventually selected for the critical appraisal: five on PEMF, four each on ES and ECSW, sixty-six for photo energies, and three about US. Based on the percentage of original wound size affected by the BPEs, both PEMF and low-level laser therapy (LLL) demonstrated a significant clinical benefit compared to the control or sham treatment, whereas the effect of US did not reveal a significance. Our results indicate potential benefits of selected BPEs in diabetic wound management. However, due to the heterogeneity of the current clinical trials, comprehensive studies using well-designed trials are warranted to confirm the results.

Keywords: biophysical energies; skin wounds; diabetes mellitus; cell; experimental models; systematic review

1. Introduction

Thirty million children and adults in the United States have diabetes [1]. The incidence rate of diabetic foot ulcer is 6% [2], and 45% of diabetic patients die during the first year after the initial amputation [3]. Neuropathy, peripheral vascular disease and infection are the major risk factors for non-healing foot ulceration in patients with diabetes [4]. Increased inflammation and expression of matrix metalloprotease-9, protein tyrosine phosphatase-1B in wound tissue and elevated level of serum growth factors were also found as the main factors associated with failure to heal diabetic foot ulcers [5]. Thus, treatments that manage neuropathy, ameliorate microcirculation and promote growth factor release may be helpful in treating chronic wounds or reducing their recurrence.

Biophysical energies (BPEs) are commonly used in physiotherapy daily practice [6]. BPE options for treating diabetic foot ulcers have included electrical stimulation (ES), MHz or kHz ultrasound (US), extracorporeal shockwave (ECSW), photo energies and pulsed electromagnetic field (PEMF). A systematic review reports positive findings on the use of the BPEs (ES, photo energies, and US) in managing foot ulcers [7] and peripheral neuropathy [8] in patients with diabetes. BPEs have been used

to accelerate healing of chronic diabetic foot ulcers [9] and venous ulcers [10]. Moreover, BPEs may restore diabetes-associated microvascular [9] and neurological changes [11] that are important risk factors for delayed wound healing in patients with diabetes.

Despite the positive findings reported in some clinical studies, it is almost impossible to recruit homogeneous groups of patients in practice. Patients may respond differently to the same intervention due to variations in the severity of wound, location or chronicity. In contrast, the homogeneity in both experimental and control groups can be achieved in studies utilizing cell or animal models, and they also provide more insights into the mechanisms by which BPEs promote wound healing. Previous animal studies have shown that BPEs enhance macrophage migration [12] and antibacterial effects on ulcers [13]. In addition, BPEs have been shown to accelerate collagen deposition and enhance wound contraction in healthy Sprague-Dawley rats [14]. These animal model-based pre-clinical studies have brought some insights into the mechanisms of BPEs. However, it is important to note that rodent models cannot fully recapitulate human responses to BPEs due to mechanistic differences in wound healing, so findings from such studies may not be directly translated into clinical practice.

Thus far, there is a lack of updated review in the literature that evaluates the efficacy of BPEs for wound healing in cellular or animal models. The purpose of this review is to survey the current literature for studies that use cell culture and animal models to evaluate the efficacy of BPEs on diabetic wound healing, and to infer the underlying mechanisms of how BPEs promote wound healing.

2. Methods

This study followed the guidelines suggested by de Vries and co-worker [15] for reporting systematic reviews of animal studies.

2.1. Data Sources and Searches

The literature search for this review was restricted to published results of cellular studies and animal experiments. Databases including MEDLINE, CINAHL and PubMed were searched, covering the period from their inception to December 2018. This review was also restricted to articles published in English. Published review articles were also excluded. Keywords and Medical Subject Headings (MeSH) including PEMF, US, ECSW, ES, and LLL were combined with wound healing (limited to “cell” and “animal”) (Appendix A). A manual search of bibliographic references of relevant articles and existing reviews was also conducted to identify studies not captured by the electronic database search.

2.2. Study Selection

Published studies that reported the efficacy of BPEs in treating diabetic wounds were eligible for inclusion. The inclusion criteria were as follows:

- Biophysical energies
- Diabetic wound
- Cell or animal experiments

The exclusion criteria were as follows:

- Co-interventions (e.g., co-medication)
- No diabetic wounds
- Human studies
- Systematic review or meta-analysis

2.3. Data Extraction and Quality Assessment

Literature search was conducted independently by two reviewers (RK and MC). Articles were screened according to the title, the abstract, followed by the full paper if necessary. Duplicates were checked and removed after excluding the publications that were clearly unrelated to the purpose

of this study. The full text of publications satisfying the inclusion criteria was obtained for review. At all stages, whenever there were disagreements between the two reviewers, they were resolved by discussing between themselves, sometimes with a senior and experienced reviewer (GC) or the corresponding author when necessary.

Each included experimental animal study was assessed for methodological quality by the same two reviewers independently, using SYRCLE's risk of bias tool [16]. The checklist consists of: (1) sequence generation; (2) baseline characteristics; (3) allocation concealment; (4) random housing; (5) investigator blinding; (6) random outcome assessment; (7) assessor blinding; (8) incomplete outcome data addressed; (9) selective outcome reporting; and (10) other source of bias.

Details of the studies were extracted and summarized using a data extraction sheet. Attempts were made to obtain any missing data by contacting the authors of the studies. Data from studies published in duplicate were included only once. The data collection form consisted of demographic data (author and year published), study design characteristics (experimental groups and number of animals), animal model characteristics (species, gender, and disease etiology), intervention characteristics (dosage, timing, and duration), outcomes measures and other (dropouts).

2.4. Primary Outcomes

Objective measures of healing were investigated, including the healing rate of diabetic wounds, the time for complete closure, and the proportion of subjects with wound closure within the trial period.

3. Results

3.1. Search Results

Using the pre-defined keywords and MeSH, we identified 1731 publications pertaining to the use of BPEs for diabetic wound treatment in animal and cellular models. By screening the title and abstract, we obtained 135 relevant articles and retrieved the full text for 103 publications after removing 32 duplicated articles. Of the 103 articles, 21 were excluded for reasons related to the study design ($n = 4$), not diabetic wounds ($n = 8$), with co-interventions ($n = 6$) or human study ($n = 1$). Two articles were also not included due to the lack of English version [17,18]. Finally, 82 studies that specifically examined the effects of BPEs on diabetic wound healing were critically appraised. Figure 1 illustrates the trial selection process.

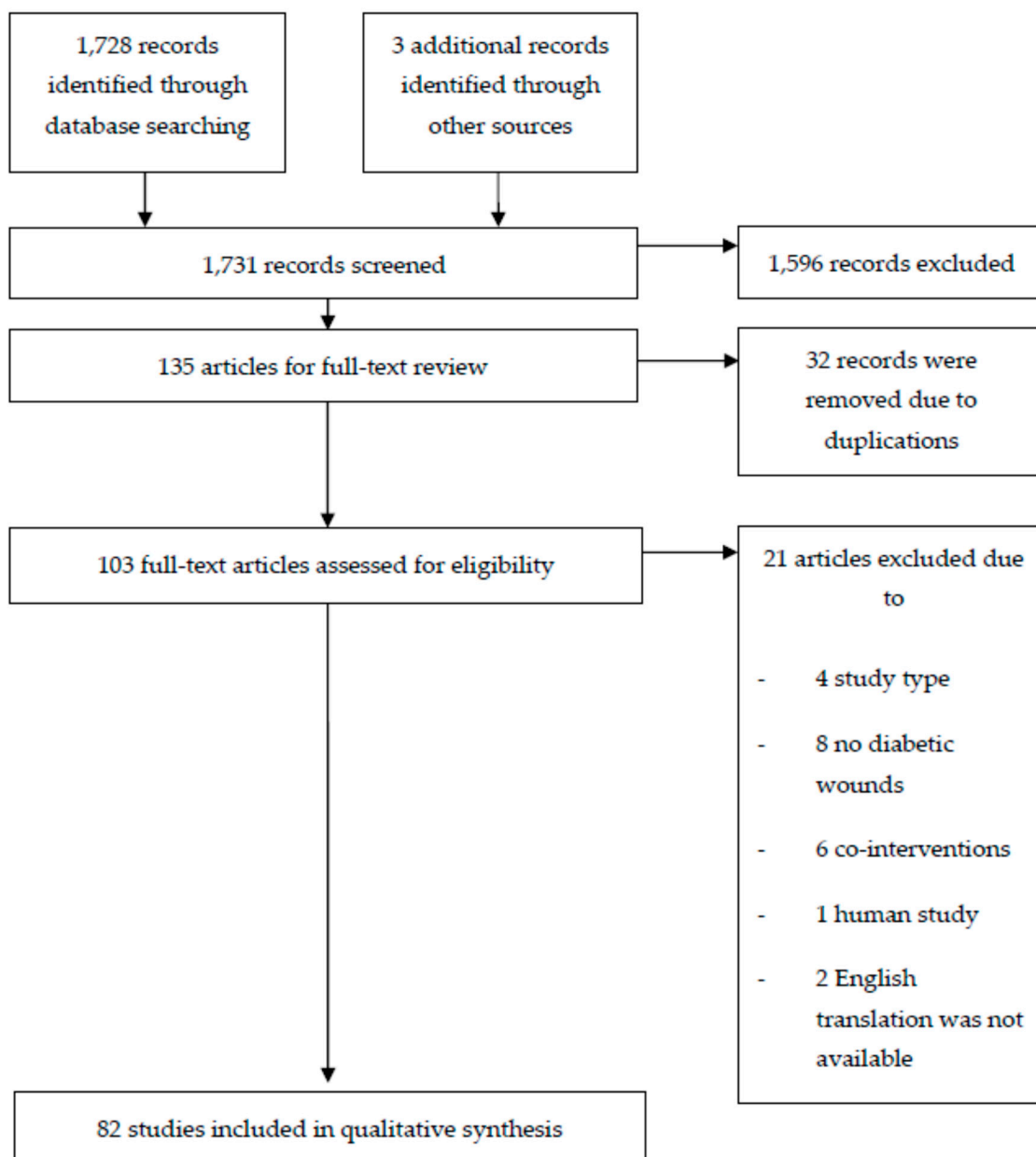


Figure 1. Systematic reviews flow diagram of the selected BPEs literature search.

3.2. Characteristics of Studies

Tables 1–6 present the descriptive information on each of the studies reviewed. The trials were conducted between 1984 and 2018. Overall, there were five trials on PEMF [19–23], three trials on US [24–26], four trials on ECSW [27–30], four trials on ES [31–34] and sixty-six trials on LLL [35–100]. The majority of them (60/82; 73%) were published after 2008.

Table 1. Outcomes of PEMF energy for treating diabetic ulcers.

Reference	Study Type	Sample Type	Parameters	Outcome Measure	Main Results
Callaghan et al., 2008 [19]	In vivo	db/db mice (<i>n</i> = 6 in each group) C57BL6 mice (<i>n</i> = 6 in each group) FGF-2 knockout mice (<i>n</i> = 6)	E: Asymmetric; 4.5 ms pulses; 15 Hz; magnetic flux density increased from 0 to 12 G in 200 μ s and return to 0 in 24 μ s; custom designed cage; 8 hrs daily C: Identical cages with inactive generators	1. Gross wound closure 2. Overall wound closure time 3. Cell proliferation 4. Vascularity	1. Accelerated closure by Day 7 (E: 60 \pm 5% vs C: 78 \pm 6%) in db/db mice. No significant improvement in wound closure rate observed in FGF-2 knockout mice. 2. Time to closure (E: 16 \pm 4 vs C: 24 \pm 5 days) in db/db mice. 3. Higher proliferation (E: 31.5 \pm 5 vs C: 7.52 \pm 8 cells per high-power field) in db/db mice. 4. Day 7 (E: 28 \pm 4 vs C: 17 \pm 4 cells per high power field); Day 14 (E: 32 \pm 6 vs C: 21 \pm 5 cells per high power field).
	In vitro	Human umbilical vein endothelial cells	(No of plates = 6) 50 Hz inside the incubators measured less than 2 mG; harvested at each time point (0 to 12 h)	1. Murine endothelial cells culture 2. FGF-2 secretion	1. Increased proliferation over 24 h (E: 237,876.6 \pm 488 vs C: 153,386.6 \pm 391 cpm). 2. Increased after 8 h of incubation (E: 20.5 \pm 6.75 vs C: 6.25 \pm 0.75 cpm).
Goudarzi et al., 2010 [20]	In vivo	Male Wistar rats	E (<i>n</i> = 7): 20 Hz, 4 ms, 8 mT, 1 h/day for 10 days, with restrainer in energized coil C (<i>n</i> = 7): caged for same time without exposure to electromagnetic fields	On Days 0, 4, 8, 12, and 16 1. Wound healing percentage 2. Wound healing duration 3. Wound tensile strength	1. Wound healing percentage increased in treatment group more than control (<i>p</i> < 0.01). 2. Healing time decreased in treatment group more than sham. 3. Increased stress value in treatment group (<i>p</i> < 0.001).
Cheing et al., 2014 [21]	In vivo	Male Sprague-Dawley rats	E (<i>n</i> = 28): 5 mT, 25 Hz, 1 h daily, sinusoidal pulses, 40 ms, in plastic cylindrical container C (<i>n</i> = 28): in plastic cylindrical container without exposure to electromagnetic fields	1. Wound closure 2. Myofibroblast	1. Increased in wound closure on Day 10 and Day 14 (E: 96.73 \pm 0.4 vs C: 92.93 \pm 0.57%) in treatment group (<i>p</i> < 0.05). 2. Increased in myofibroblast on Day 7 and Day 10 in treatment group (<i>p</i> < 0.05).

Table 1. Cont.

Reference	Study Type	Sample Type	Parameters	Outcome Measure	Main Results
Choi et al., 2016 [22]	In vivo	Male Sprague-Dawley rats	E ($n = 20$): 5 mT, 25 Hz, 1 h daily, sinusoidal pulses, 40 ms, in plastic cylindrical container C ($n = 20$): in plastic cylindrical container without exposure to electromagnetic fields	<ol style="list-style-type: none"> 1. Type 1 collagen fiber deposition 2. Collagen fibril alignment 3. Collagen fiber anisotropy and orientation 4. Correlation between type 1 collagen fiber abundance and myofibroblast population 	<ol style="list-style-type: none"> 1. Significantly greater in treatment group than control group on Day 7 (E: 0.0100 ± 0.00578 vs C: 0.00181 ± 0.000902; $p = 0.013$). 2. No significant difference between groups 3. No significant difference between groups 4. Significantly more myofibroblast population on Day 7 (E: 2 ± 2 vs C: 1 ± 1; $p = 0.042$) and Day 10 (E: 4 ± 2 vs C: 2 ± 2; $p = 0.024$) in treatment group than control.
Choi et al., 2018 [23]	In vivo	Male Sprague-Dawley rats	E1: 2 mT, 25 Hz, 1 h daily E2: 10 mT, 25 Hz, 1 h daily C: in plastic restrainer bag without exposure to electromagnetic fields	<ol style="list-style-type: none"> 1. Wound area 2. Tensile biomechanical properties 3. Wound thickness 	<ol style="list-style-type: none"> 1. All wounds closed by Day 14. The percent wound area of E1 was significantly smaller than C on Day 3 ($p = 0.024$). 2. Maximum load of E2 was significantly greater than E1 ($p = 0.012$). Energy absorption capacity of E2 was significantly greater than C and E1 on Day 5 ($p = 0.036$ and 0.008 respectively). On Day 14, the Young's modulus of E2 was significantly smaller than C ($p = 0.023$). 3. Wound thickness of E2 was significantly greater than E1 (Day 3: $p = 0.002$) and C (Day 5: $p = 0.014$, Day 21: $p = 0.022$).

E, Experimental group; C, Control group.

Table 2. Outcomes of US energy for treating diabetic ulcers.

Reference	Study Type	Sample Type	Parameters	Outcome Measure	Main Results
Thawer et al., 2004 [24]	In vivo	Male CD-1 mice	E (<i>n</i> = 27): alternate days, via vapor of 15 mL prewarmed saline, perpendicular for no more than 1 cm from wound bed, 1.5 min, 5 treatments over 10 days, 45 kHz, 0.1 Watt/cm ² C (<i>n</i> = 23): via intravenous drip of 15 mL prewarmed saline, perpendicular for no more than 1 cm from wound bed, 1.5 min, 5 treatments over 10 days,	1. Wound size 2. Granulation tissue 3. Collagen deposition 4. Blood vessels	1. Wound size in both groups decreased with no significant difference (E: 0.30 ± 0.26 vs C: 0.30 ± 0.17 cm ²). 2. Collagenous and vascular tissue appeared to be densely associated in the ultrasound group. 3. Significantly greater in ultrasound group than the sham group (E: 0.92 ± 0.06 vs C: 0.82 ± 0.14). 4. Significantly more blood vessels in the granulation tissue (E: 41.3 ± 23.0 vs C: 25.7 ± 20.3). (<i>p</i> < 0.05).
Mann et al., 2014 [25]	In vivo	Male BKS.Cg-Dock7m +/+ Leprdb /J) mice (<i>n</i> = 3 mice and <i>n</i> = 6 wound per group per time point)	E: 40 kHz with saline vapor, at distance 5 to 15 mm, 3 min, 3 times/week C: Change dressing	1. Wound area 2. Wound closure duration 3. Collagen deposition 4. VEGF expression 5. SDF-1 expression	1. On Day 9, mean wound area relative to original size decreased (E: 68 ± 3.4% vs C: 80 ± 3.2%; <i>p</i> = 0.003). 2. Decreased wound closure duration (E: 17.3 ± 1.5 vs C: 24 ± 1.0 days; <i>p</i> < 0.05). 3. Increased collagen deposition in ultrasound group (E: 32.8 ± 1.5 vs C: 21.0 ± 3.2; <i>p</i> < 0.05). 4. Increased VEGF expression in ultrasound group (E: 100 ± 15.4 vs C: 41.4 ± 5.7; <i>p</i> = 0.008). 5. Increased SDF-1 expression in ultrasound group (E: 100 ± 7.7 vs C: 53 ± 3.3; <i>p</i> = 0.003).
Roper et al., 2015 [26]	In vitro	Dermal fibroblasts from db/db mice		Cell proliferation	Increased fibroblast proliferation (E: 42 ± 2 vs C: 22 ± 2; <i>p</i> < 0.001)
	In vivo	Male Syndecan-4 wild-type; knockout C57BL/6J mice	E: 2.5 cm diameter transducer; water-based gel; 30 mWcm ⁻² ; 1.5 MHz; pulsed at 1 kHz, 20 min C: transducer applied but not activated	1. Wound size 2. Wound closure time	1. Wound size significantly reduced in ultrasound group on Days 6 and 7. 2. Wound closure time reduced 33% in ultrasound group.
	In vitro	Fibroblasts from wound tissue		Speed and persistent migration	Ultrasound switched the random migration to persistent migration in Sdc4 -/- fibroblasts.

E, Experimental group; C, Control group.

Table 3. Outcomes of ECSW energy for treating diabetic ulcers.

Reference	Study Type	Sample Type	Parameters	Outcome Measure	Main Results
Kuo et al., 2009 [27]	In vivo	Male Wistar Rats	E1 (<i>n</i> = 10): 1 session of defocused ESWT on postoperative Day 3 E2 (<i>n</i> = 10): 2 sessions of defocused ESWT on postoperative Day 3 and 7 E3 (<i>n</i> = 10): 3 sessions of defocused ESWT on postoperative Day 3, 7 and 10 C1 (<i>n</i> = 10): normal control without shockwave C2 (<i>n</i> = 10): diabetic control without shockwave [E1–E3: 100 impulses/area, 8 areas in all wound edges]	1. Wound healing time 2. Topical blood perfusion by laser Doppler flowmetry 3. Leukocyte infiltration by H&E staining 4. Cell proliferation and regeneration 5. Angiogenesis	1. Time course significantly reduced in E1 (8.2 ± 0.3 weeks), E2 (5.7 ± 0.6 weeks) and E3 (5.6 ± 0.4 weeks), as compared to C2 (9.8 ± 0.3 weeks) ($p < 0.05$). 2. E2 showed significant increase in wound area perfusion compared with C2 ($p = 0.023$). 3. Reduced in E1, E2 and E3 as compared to C1 and C2 on Day 3. 4. Increase in fibroblasts in E1, E2 and E3 on Days 3 and 10 compared to C1 and C2. 5. Up-regulated VEGF in E1, E2 and E3 on Day 3 and Day 10 as compared to C1 and C2.
Zins et al., 2010 [30]	In vivo	Female BALB/c, homozygous Bk.Cg-m Lepr db+/db+	E: 200 impulses, 0.1 mJ/mm ² , 5 pulses per second, 45 s C: sham treatment	1. Wound closure 2. Gene expression 3. Angiogenesis	1. Shockwave does not accelerate cutaneous wound closure in wildtype normal mice or db+/db+ diabetic mice. 2. Gene expression was augmented in both types of wound in PECAM-1 after shockwave. 3. 44% and significant 202% increase in blood vessel density observed in shockwave-treated BALB/c and db+/db+ mice, when compared to their respective control.
Yang et al., 2011 [28]	In vivo	Male Sprague-Dawley rats	E1 (<i>n</i> = 12): 1 session of ECSW on Day 1 E2 (<i>n</i> = 12): 3 sessions of ECSW on Days 1, 3 and 5 C1 (<i>n</i> = 12): normal control without shockwave C2 (<i>n</i> = 12): diabetic control without shockwave [E1–E2: 100 impulses per cm wound length; 0.11 mJ/mm ² ; 3 Hz]	1. Wound breaking strength 2. Collagen content 3. Fibroblast proliferation 4. TGF-β1-positive fibroblast expression	1. Significantly increased in E1 and E2 as compared to C2 ($p < 0.05$). 2. Hydroxyproline content significantly increased in E1 and E2 ($p < 0.05$). 3. Histological scores indicated ECSW-treated wounds epithelialized more rapidly and collagen fibers are more abundant at the wound site. 4. Up-regulated significantly in E1 and E2 on Day 7 post wounding ($p < 0.05$).

Table 3. Cont.

Reference	Study Type	Sample Type	Parameters	Outcome Measure	Main Results
Hayashi et al., 2012 [29]	In vivo	Endothelial nitric oxide synthase-knockout (eNOS-KO) mice; C5781/6 mice	E1 (n = 7): eNOS-KO E2 (n = 11): C5781/6 C1 (n = 6): eNOS-KO, sham C2 (n = 8): C5781/6, sham [E1–E2: 70.25 mJ/mm ² ; 4 Hz; 100 impulses on surface of 4 cm ² per side]	1. Wound closure 2. Myofibroblast accumulation 3. eNOS expression 4. Angiogenesis	1. Wound closure relative to Day 0 significantly increased in E2 than C2 (88.2 ± 14.5 vs 71.1 ± 13.6%), but not in E1 and C1 (71.4 ± 12.4 vs 71.9 ± 18.6%). 2. α-SMA-expressing myofibroblast accumulated more pronounce in E2 than C2, but did not differ between E1 and C1. 3. eNOS increased in E2 compared to C2; CD31 ⁺ cells in E2 is more profound than C2 (65.9 ± 10.6 vs 50.1 ± 11.0 count/mm ²). 4. Vascular density significantly higher in E2 than C2 (18.9 ± 7.4 vs 10.5 ± 4.8 count/mm ²). The difference was not seen in E1 and C1.

E, Experimental group; C, Control group; ECSW, extracorporeal shock-wave.

Table 4. Outcomes of ES energy for treating diabetic ulcers.

Reference	Study Type	Sample Type	Parameters	Outcome Measure	Main Results
Smith et al., 1984 [31]	In vivo	Male mice	E1 (<i>n</i> = 15): Diabetic mice, 20 volt, 20 ma E2 (<i>n</i> = 10): Diabetic mice, 1 volt, 10 ma E3 (<i>n</i> = 10): Normal mice, 20 volt, 20 ma E4 (<i>n</i> = 10): Normal mice, 1 volt, 10 ma C1 (<i>n</i> = 10): Diabetic mice, no charge C2 (<i>n</i> = 10): Normal mice without ES [E1–E3: Daily, 1 min interval, 5 days a week for 2 weeks; C1–C2: Electrode placement without charge]	1. Tensile strength 2. Histology	1. Tensile strength in E1 and E2 is greater than C1. 2. Longitudinal sections show restoration of hair follicles and sebaceous glands after ES than controls.
Thawer et al., 2001 [32]	In vivo	CD-1 mice (<i>n</i> = 55)	E1: Diabetic 12.5 V E2: Normal 12.5 V C1: Diabetic 0 V C2: Normal 0 V [E1–E2: restrained by flexible fiberglass narrow cone; monophasic pulsed current; pulse duration 200 ms, 200 Hz; negative electrode as treatment probe soaked in saline; 15 mins; alternate days; C1–C2: same setting except the electrode was not activated]	1. Histology 2. Collagen content 3. Correlation between collagen deposition and surface area of wounds	1. No statistical difference found in epidermis thickness in all groups. 2. ES energy decrease collagen amount in superficial scar in E2 as compared to C2; E1 and E2 has significantly greater collagen/non-collagenous protein ratios in deep scar than C1 and C2. 3. Fair degrees of association between collagen deposition and surface area of wounds was found on Day 16 (<i>p</i> < 0.01).
Kim et al., 2014 [33]	In vivo	Male Sprague-Dawley rats	E (<i>n</i> = 10): diabetic rats with high voltage pulsed current stimulation daily, 100 pps, 40 min, monophasic, twin-peak pulses for 140 μs, voltage from 35 to 50 V; negative pole for first 3 days and positive for next 4 days C1 (<i>n</i> = 10): diabetic rats with sham stimulation C2 (<i>n</i> = 10): normal rats with sham stimulation	1. Wound healing rate 2. Collagen-I expression 3. α-SMA 4. TGF-β1 mRNAs	1. E and C2 exhibited good wound healing as compared to C1 (<i>p</i> < 0.05). 2. E and C2 showed significantly higher collagen-I as compared to C1 (<i>p</i> < 0.02), whereas E is highest among the groups (<i>p</i> < 0.05). 3. E and C2 showed significantly higher α-SMA as compared to C1 (<i>p</i> = 0.04), whereas E is highest among the groups (<i>p</i> < 0.05). 4. E and C2 showed significantly higher TGF-β1 as compared to C1 (<i>p</i> = 0.01), whereas E is highest among the groups (<i>p</i> < 0.01).
Langoni Cassetari et al., 2014 [34]	In vivo	Male Wistar rats	E1 (<i>n</i> = 20): normal with continuous ES E2 (<i>n</i> = 20): diabetic with continuous ES C1 (<i>n</i> = 20): normal without stimulation C2 (<i>n</i> = 20): diabetic without stimulation C3 (<i>n</i> = 20): normal with zinc sulfate by transdermal iontophoresis C4 (<i>n</i> = 20): diabetic with zinc sulfate by transdermal iontophoresis [E1–E2: 2 mA, 10 min; at immediate after surgical incision, Days 1, 2 and 3]	1. Wound contraction 2. Fibroblasts and vascular endothelial cells proliferation 3. Collagen fibers deposition 4. Correlation of breaking strength and morphological findings	1. Wound contraction accelerated in E2 and C4 as compared to C2. 2. Morphological inflammatory process in E2 and C4 does not differ with E1, C1, C2 and C3. 3. Dense, progressive deposition of collagen fibers with few fenestrations on Day 4 in E2 and C4. C4 has more organizational pattern than E2. 4. Breaking strength in C2 was significantly lower than all other groups.

E, Experimental group; C, Control group; ES, Electrical stimulation.

Table 5. Outcomes of in vivo studies on photo energies (PE) for treating diabetic ulcers.

Reference	Sample Type	Parameters	Outcome Measure	Main Results
Low-level laser				
Yu et al., 1997 [35]	C57BL/Ksj/db/db mice ($n = 40$, wound = 80)	630 nm, 20 ± 8 mW/cm ² , 2 cm diameter, 250 s at each treatment session and received fluence of 5 J/cm ²	1. Percentage of wound closure 2. Histologic evaluation	1. On Day 10, significantly greater wound closure percentage in E ($58.4 \pm 2.6\%$) as compared to control ($40.8 \pm 3.4\%$). On Day 14, significantly greater wound closure percentage in E ($95.7 \pm 2\%$) as compared to C ($82.3 \pm 3.6\%$). 2. On Day 10, significantly higher histological score in laser-treated group (6.4 ± 0.16). On Day 14, significantly higher histological score in E (12.0 ± 0.21).
Reddy et al., 2001 [37]	Male Sprague-Dawley rats	Left side wounds; 1.0 J/cm ² He-Ne laser at 632.8 nm; 5 days/week until wound closed	1. Biomechanical analysis 2. Biochemical analyses	1. Maximum load and stress increased by 16%. An increase in maximum strain by 27%. No significant between-group difference found for Young's modulus of elasticity. Energy absorption capacity increased by 47% and overall toughness increased to 84%. 2. Total collagen for was significantly higher. There was 15% increase in neutral salt soluble collagen, 16% increase in insoluble collagen and 19% decrease in pepsin soluble collagen.
Reddy, 2003 [40]	Male Sprague-Dawley rats ($n = 15$)	Continuous infrared radiation at 904 nm produced by Ga-As laser, 7 mW, 1.0 J/cm ² , once a day, 5 days/week until wound closed	1. Biomechanical analysis 2. Biochemical analyses 3. Hydroxyproline 4. Collagen maturation	1. Significant increase in tensile strain. Marginal increases were observed in tensile strength and stress indices. 2. Total collagen increased by 14%. 3. Collagen deposition increased. 4. Insoluble collagen increased by 50%.
Danno et al., 2001 [36]	Male ICR mice ($n = 20$); Female C57BL/KsJ-db/db mice ($n = 20$)	Daily, 30 min, at distance of 20 cm, 54 J/cm ²	Wound area	The rate of wound closure significantly accelerated.
Stadler et al., 2001 [38]	C57BL/Ksj/db/db mice; Heterozygous littermates as control ($n = 20$)	Class IIIb 830 nm laser; 79 mW/cm ² , daily, 5 J/cm ² /wound; 5 consecutive days; 0–4 days or 3–7 days	Tensile strength	Tensile strength at 11 days was significant between diabetic laser group (2.16 ± 0.47 g/mm ²) and sham (1.28 ± 0.32 g/mm ²). Tensile strength at 23 days E than in C (2.72 ± 0.56 g/mm ² vs 1.5 ± 0.3 g/mm ²).
Byrnes et al., 2004 [42]	Psammomys obesus (Sand rats)	Diabetic, 4 J/cm ² , He-Ne gas laser: 632.8 nm, daily for 3 consecutive days, at left wound	1. Wound closure percentage 2. Histological characteristics	1. Wound closure was significantly faster in E (34.3 ± 10.5 , $68.4 \pm 10.4\%$) than C (-42.0 ± 23.3 , $28.5 \pm 10.8\%$) on Days 2 and 10. 2. Three-fold increase in bFGF in E as compared to C.

Table 5. Cont.

Reference	Sample Type	Parameters	Outcome Measure	Main Results
Kawalec et al., 2004 [43]	C57BLKS/J mice ($n = 56$)	E1: 5 W every 2 days, 18 J/cm ² E2: 5 W every 4 days, 18 J/cm ² E3: 10 W every 2 days, 36 J/cm ² E4: 10 W every 4 days, 36 J/cm ² GaAlAs diode laser, 980 nm, 1 s	1. Wound closure percentage 2. Histological characteristics	1. Wound closure percentage was only significant in E2 and E3 on Day 5. 2. Average score of 5.8 on Day 7 and 15.5 on Day 14 in E1.
Maiya et al., 2005 [44]	Male Wistar rats ($n = 48$)	632.8 nm, 4.8 J/cm ² , He-Ne laser, 5 days per week until closed	1. Biochemical analysis 2. Histopathological analysis	1. Total collagen for E was significantly higher. 2. Significant increase in fibroblastic proliferation, capillary proliferation, granulation tissue formation, vascularity and epithelization on Day 4.
Carvalho et al., 2006 [47]	Male Wistarrats	632.8 nm HeNe laser, 4 J/cm ² , 60 s/wound, continuous, 5 mW	Histology	Significant difference in collagen.
Rabelo et al., 2006 [48]	Male Wistar rats ($n = 50$)	3 times/week, continuous, 632.8 nm HeNe laser, 10 J/cm ² , 17 s	1. Qualitative histopathological analysis 2. Quantitative histological analysis	1. Less intense inflammatory process 2. Significant decrease of the inflammatory cell density and significant increase in capillarity.
AI-Watban et al., 2007 [49]	Male Sprague-Dawley rats ($n = 52$)	E1: 532 nm, 5 J/cm ² E2: 633 nm, 5 J/cm ² E3: 810 nm, 5 J/cm ² E4: 980 nm, 5 J/cm ² E5: 532 nm, 10 J/cm ² E6: 633 nm, 10 J/cm ² E7: 810 nm, 10 J/cm ² E8: 980 nm, 10 J/cm ² E9: 532 nm, 20 J/cm ² E10: 633 nm, 20 J/cm ² E11: 810 nm, 20 J/cm ² E12: 980 nm, 20 J/cm ² E13: 532 nm, 30 J/cm ² E14: 633 nm, 30 J/cm ² E15: 810 nm, 30 J/cm ² E16: 980 nm, 30 J/cm ²	Wound healing percentage	The percentage of wound healing acceleration is higher in all treatment groups than the control groups. The optimum wavelength and incident dose was at E6.
Meireles et al., 2008 [55]	Male Wistar rats ($n = 55$)	E1: 660 nm, 20 J/cm ² E2: 780 nm, 20 J/cm ²	Histology	At Day 7, E1 as necrosis extended down to epidermis, and E2 has extending down to dermis. On Day 14, E1 and E2 showed moderate amount of neo-angiogenesis. On Day 21, E1 showed advanced re-epithelialization, but E2 showed no epithelialization.
Gungormus and Akyol, 2009 [59]	Female Wistar rats	Class IV, medical class IIB, 20 W, 50 Hz, GaAlAs 808 nm, continuous, 0.1 W/cm ² , 10 J/cm ² , on Days 2, 4, 6, and 8	Degree of re-epithelialization and inflammation	Significant between-group difference was found in re-epithelialization and inflammation on Day 10, but not on Day 20.

Table 5. Cont.

Reference	Sample Type	Parameters	Outcome Measure	Main Results
Akyol and Gungörmus, 2010 [60]	Wistar rats ($n = 54$)	Diode laser; 808 nm, 0.1 W/cm ² , Day 0,2,4,6 and 8, 10 J/cm ² , 20 s per session	Histology analysis	Significant difference found in post hoc analysis between E and C in re-epithelialization and inflammation on Day 10.
Carvalho pde et al., 2010 [61]	Male Wistar rats	InGaAlP diode laser, continuous, 100 mW, 660 nm, 10 J/cm ²	1. Histology analysis 2. Morphometric analysis	1. Significant difference in mean collagen between E and C (19.96 ± 1.89 vs 13.19 ± 3.70 ; $p = 0.0457$) on Day 3, and on Day 5 (30.95 ± 4.14 vs 16.95 ± 2.36). 2. Significant difference was found in mean number of macrophages between E and C on Day 3, Day 5 and Day 7.
Chung et al., 2010a [63]	BKS.Cg-m+/+Leprdb/J ($n = 47$)	E1: 660 nm, 20 s, 18 mW, 7 consecutive days, 0.36 J/day E2: 660 nm, 20 s, 80 mW, 7 consecutive days, 1.6 J/day	1. Wound area 2. Histological analysis	1. E2 increased the mean wound area on Day 4, but decreased in wound area on Day 14 as compared to E1 and C. 2. The mean dermal gap and epithelial gap for E2 was significantly different from C but not E1.
Chung et al., 2010b [62]	BKS.Cg-m+/+Leprdb/J	E1: 660 nm, 0 s, 80 mW, 7 consecutive days, 0 J/day E2: 660 nm, 10 s, 80 mW, 7 consecutive days, 0.8 J/day E3: 660 nm, 20 s, 80 mW, 7 consecutive days, 1.6 J/day E4: 660 nm, 30 s, 80 mW, 7 consecutive days, 3.2 J/day	Histological analysis	In splinted wound, the mean dermal gap and epithelial gap for E3 was significantly different from E1, 2 and 3. All wounds in E3 completely re-epithelized, and granulation tissue with collagen fibers filled or almost filled the whole of wound bed in splinted wound.
Jahangiri Noudeh et al., 2010 [66]	Male Wistar rats ($n = 19$)	GaAlInP laser, 670 nm, 10 J/cm ² ; combined with 810 nm GaAlAs laser, 250 mW, 12 J, 50 s, 1.33 J/cm ² , performed every 3 days	Wound area	No statistical significance in wound area throughout repeated measurements in the study time period.
Santos et al., 2010 [68]	Male Wistar rats ($n = 12$)	E1: 680 nm, 40 J/cm ² per session E2: 790 nm, 40 J/cm ² per session	Histological analysis	Fibroblast number and angiogenesis was higher in E2. Necrosis was more evident in E1.
Hegde et al., 2011 [69]	Male Swiss albino mice	E1: 4 min, 15 s ⁻¹ J cm ⁻² E2: 8 min, 32 s ⁻² J cm ⁻² E3: 12 min, 46 s ⁻³ J cm ⁻² E4: 17 min, 3 s ⁻⁴ J cm ⁻² E5: 21 min, 17 s ⁻⁵ J cm ⁻² [E1–E5: 632.8 nm HeNe laser]	Biochemical analysis	Hydroxyproline content in granulation tissue on Day 6 and Day 12 revealed a significant increase in the collagen content in all treatment groups. Rise in glucosamine levels was observed in all experimental groups on Day 6 but subsequently decreased linearly.
Peplow et al., 2011 [71]	BKS.Cg-m+/+Leprdb/J	E1: 100 mW, 233–313 mW/cm ² E2: 50 mW, 116–156 mW/cm ² E3: 25 mW, 58–78 mW/cm ² [E1–E3: 660 nm]	Histological analysis	All splinted wounds were completely re-epithelized, and granulation tissue with collage fibers filled or almost filled the whole wound bed.

Table 5. Cont.

Reference	Sample Type	Parameters	Outcome Measure	Main Results
Dadpay et al., 2012 [74]	Male Wistar rats ($n = 18$)	0.2 J/cm ² , pulsed infrared diode laser, 1.08 W/cm ⁻² , 890 nm, 80 Hz	Biomechanical examination	Significant increases in maximum load and accelerate wound healing.
Park and Kang, 2012 [89]	Male Sprague-Dawley rats ($n = 48$)	980 GaAlAs diode laser, 60 s every day, 0.01 W, 13.95 J/cm ²	1. Histological analyses 2. Gene expression	Histological observations and gene expression analyses revealed a faster initial healing and more alveolar bone formation.
Peplow et al., 2012 [76]	BKS.Cg-m+/+Leprdb/J	660 nm, 100 mW, 20 s/day, 7 days	1. Body weight and water intake 2. Glucose and GHB1c levels in blood plasma	1. There were no significant differences in body weight and water intake over 22 days. 2. On Day 14, the mean blood plasma glucose level was not significantly different between E and C. Ghb1c was not detected.
Aparecida Da Silva et al., 2013 [77]	Male Wistar rats ($n = 120$)	InGaAlP, 50 mW, 660 nm, 4 J/cm ²	1. Histological analysis 2. Morphometric analysis 3. MMP-2 and MMP-9 synthesis	1. The density of total collagen of E was significantly higher than C. 2. Collagen I was always greater than that observed in collagen III in all groups. 3. Significant increase in MMP-2 and MMP-9 expression in C than E.
Fathabadie et al., 2013 [78]	Male Wistar rats ($n = 72$)	Once daily for 6 days a week, pulsed infrared laser, 75 W, 1.08 W/cm ² , 890 nm, 80 Hz, 180 ns pulse duration, 200 s, 0.2 J/cm ²	Morphometric examination	Significantly increased the number of mast cells on Days 4 and 15 after surgery.
Firat et al., 2013 [86]	Male Wistar rats ($n = 42$)	GaAlAs laser, 940 nm, 10 J/cm ² , 0.1 W, continuous for 9 s, first dose at 2 h after wounding, then at 2 days interval for 4 sessions	1. Histological analysis 2. Biochemical analysis	1. Histopathological findings revealed a decrease in number of inflammatory cells, and increased mitotic activity of fibroblasts, collagen synthesis, and vascularization. 2. The total oxidative status was significantly decreased on Day 21.
Franca et al., 2013 [87]	Male Wistar rats ($n = 65$)	780 nm, 5 J/cm ² , 10 s/point, 0.2 J	1. Morphologic evaluation 2. Collagen analysis 3. Muscle fiber area	1. On Day 14, E was in the remodeling phase, C was still in the proliferative phase, with fibrosis, chronic inflammation, and granulation tissue. 2. Under polarized light, on Day 14, E had organized collagen bundles in the perimysium. 3. C exhibited more myonecrosis than E.
Dancáková et al., 2014 [80]	Male Sprague-Dawley rats ($n = 21$)	810 nm laser	1. Tensile strength 2. Histological evaluation and morphometry	1. Reduced the loss of tensile strength and increased the wound stiffness significantly. 2. Significantly more mature granulation tissue.
Kilík et al., 2014 [82]	Male Sprague-Dawley rats ($n = 48$)	GaAlAs 635 nm, three times daily, 5 J/cm ² ; 1st wound: 1 mW/cm ² ; 2nd wound: 5 mW/cm ² ; 3rd wound: 15 mW/cm ²	Histopathological evaluation	The synthesis and organization of collagen fibers were consecutively enhanced in the 15 mW/cm ² group. A significant difference in the number of newly formed capillaries.

Table 5. Cont.

Reference	Sample Type	Parameters	Outcome Measure	Main Results
Sharifian et al., 2014 [83]	Male Wistar rats ($n = 24$)	890 nm, 6 days per week, pulsed infrared laser, 80 Hz, 0.2 J/cm ²	1. Histomorphometry 2. bFGF gene expression	1. Laser significantly increased the numbers of macrophages, fibroblasts, and blood vessel sections. 2. bFGF expression at 48 h revealed a significant increase in gene expression.
De Loura Santana et al., 2015 [84]	Female Wistar rats ($n = 90$)	E1: laser 1 J/cm ² , 26 s, 4 times E2: laser 4 J/cm ² , 26 s, 1 time Gallium-aluminum-arsenide diode laser, 660 nm	1. Wound closure rate 2. Healing morphology, inflammatory infiltrate and myofibroblasts count 3. Collagen deposition and optical retardation of collagen	1. Laser accelerated wound closure by 40% in first 3 days. 2. Laser increased acute inflammatory infiltrate until Day 3. 3. More myofibroblasts and better collagen organization.
Lau et al., 2015 [85]	Male Sprague Dawley rats ($n = 120$)	E1: 100 mW, 50 s, 0.1 W/cm ² E2: 200 mW, 25 s, 0.2 W/cm ² E3: 300 mW, 17 s, 0.3 W/cm ² 808 nm diode laser, continuous mode, 5 J/cm ² , once daily	1. Wound contracture 2. Histology	1. The wound contracture was found optimized. 2. Laser therapy enhanced epithelialization and collagen fiber synthesis.
Lau et al., 2015 [90]	Male rats ($n = 21$)	E1: 110 mW, 30 s E2: 110 mW, 60 s E3: 110 mW, 120 s E4: 510 mW, 30 s E5: 510 mW, 60 s E6: 510 mW, 120 s 808 nm diode laser, continuous mode	1. Tensile strength	1. Tensile strength in E4–E6 enhanced as compared to control and E1–E3.
Fekrazad et al., 2015 [92]	Male Wistar rats ($n = 40$)	E1: blue (425 nm) laser, 50 mW/cm ² , 2 J/cm ² E2: green (532 nm) laser, 55 mW/cm ² , 2 J/cm ² E3: red (630 nm) laser, 50 mW/cm ² , 2 J/cm ²	Wound healing	Significant difference in the mean slope of wound healing between E and C.
de Loura Santana et al., 2016 [95]	Female Wistar rats ($n = 90$)	E1: Single dose laser, 4 J/cm ² , 104 s, 3.12 J, Day 1 E2: Fractionated-dose laser, 1 J/cm ² , 26 s, 0.78 J, Days 1, 3, 8 and 10 660 nm, 30 mW, 38 mW/cm ²	1. Immunohistochemistry 2. Inflammatory cell counts	1. Neutrophils were predominant in E1 on Day 1. E1 exhibited greater number of total macrophages on Day 3. 2. CD206+ cell counts revealed that E1 had more M2 macrophages on Day 8, whereas E2 exhibited more M2 macrophages on Day 10.

Table 5. Cont.

Reference	Sample Type	Parameters	Outcome Measure	Main Results
Ranjbar et al., 2016 [99]	Male Wistar rats (n = 30)	685 nm InGaAlP laser, 15 mW, 3 J/cm ² , 0.028 cm ²	<ol style="list-style-type: none"> 1. Bacterial growth 2. Wound length 3. Histological structures 4. Breaking strength 	<ol style="list-style-type: none"> 1. Mean bacterial numbers (0.51 × 10¹ ± 0.2 × 10¹ CFU/mL) were significantly lower). 2. Length of wounds in E were significantly shorter on Days 14 and 21. 3. Significant increase in number of macrophages and new blood vessels, and also significant elevated fibroblast number and collagen deposition. 4. E significantly increased in breaking strength.
Tatmatsu Rocha et al., 2016 [100]	Male Swiss mice (n = 20)	904 nm GaAs diode laser, 5 days, 40 mW, 60 s	<ol style="list-style-type: none"> 1. Histopathological analysis 2. Collagen amount 3. Catalase activity 4. Nitrite 5. Thiobarbituric acid reactive substances 	<ol style="list-style-type: none"> 1. Moderate amount of fusiform fibroblasts, an increased density of blood vessels and intense deposition of a more organized collagen matrix was observed. 2. Significant differences in type II fibers. 3. Higher catalase activity. 4. Decreased concentration of nitrite and nitrite concentration compared. 5. Significantly lower levels of thiobarbituric acid reactive substances.
Denadai et al., 2017 [96]	Wistar rats (n = 36)	660 nm InGaAlP, 100 mW, 60 s, 6 J/cm ² , 0.028 cm ²	Malondialdehyde levels	Significant lower level of malondialdehyde.
Eissa and Salih, 2017 [97]	Wistar rats (n = 14; 6 males, 8 females)	632.8 nm He-Ne laser, continuous, aperture ~2.3 × 10 ⁻⁶ mm, 4 mW/cm ² , 4 min, 6 mm away from skin, 5 days/week until wound healed	Wound diameter	E healed on average on Day 21, whereas C healed after 40 days of 60 days.
AI-Watban and Andres, 2003 [39]	Sprague-Dawley rats (n = 30)	Polychromatic light emitting diodes (LED) energy E1: 5 J/cm ² E2: 10 J/cm ² E3: 20 J/cm ² E4: 30 J/cm ² 25-LED array (510–543 nm; 594–599 nm; 626–639 nm; 640–670 nm; 842–872 nm); 13.6 mW/cm ² ; 3 times/week; 3 consecutive weeks	Healing rate	Healing accelerated at 5 and 10 J/cm ² , but no significant inhibition seen at 20 and 30 J/cm ² .
Whelan et al., 2003 [41]	BKS.Cg-m +/+Leprdb (n = 80)	670 nm LED with restrainer; daily for 14 days; 4 J/cm ² ; 28 mW/cm ² for 2 min and 24 s	<ol style="list-style-type: none"> 1. Wound healing rate 2. RNA 	<ol style="list-style-type: none"> 1. Wound healing rate increased. 2. Galectin-7 is upregulated at Day 2 and continued to be elevated after 14 days of treatment. Fibroblast growth factor 7 and 12 were upregulated by 2 days. Genes of TGF-Beta 1 and thrombospondin 1 were upregulated by 14 days of treatment.
Oliveira et al., 2010 [67]	Male Wistar rats (n = 30)	E1: Polarized light 400–2000 nm, 20 J/cm ² E2: Polarized light 400–2000 nm, 40 J/cm ²	Histological analysis	Significant difference in revascularization and re-epithelialization.

Table 5. Cont.

Reference	Sample Type	Parameters	Outcome Measure	Main Results
Oliveira et al., 2011 [70]	Male Wistar rats ($n = 90$)	E1: polarized light 400–2000 nm, 10.2 J/cm ² E2: polarized light 400–2000 nm, 20.4 J/cm ²	Histological analysis	10.2 J/cm ² caused higher deposition of collagen, quicker inflammatory reaction and improved revascularization than 20.4 J/cm ² .
Monochromatic infrared energy (MIRE)				
He et al., 2013 [79]	Male Sprague-Dawley rats ($n = 30$)	890 nm, intensity set at level 6, 85% of full power, 30 min, three times a week before euthanized	1. Wound closure percentage 2. Histological analysis	1. No significant difference was found between E and C for wound closure. 2. No significant difference was found between E and C for re-epithelialization, cellular content, myofibroblast population and granulation tissue formation at each time point. Greater deposition of type I collagen was found in E as compared to C at end of Week 2.
Al-Watban and Andres, 2006 [46]	Male Sprague-Dawley rats ($n = 61$)	E1: 5 J/cm ² E2: 10 J/cm ² E3: 20 J/cm ² E4: 30 J/cm ² 25-LED array (510–543 nm; 594–599 nm; 626–639 nm; 640–670 nm; 842–872 nm); 13.6 mW/cm ² ; 3 times/week; 3 consecutive weeks	Wound healing percentage	Wound healing percentage was significant for E1 ($16 \pm 3.1\%$, $p = 0.01$) but not significant for E2, 3 and 4 (7 ± 3.4 , 3.4 ± 3.5 , $0.9 \pm 3.6\%$).
Comparing different photo energies				
Al-Watban, 2009 [56]	Sprague-Dawley rats ($n = 893$)	E1: 5 J/cm ² E2: 10 J/cm ² E3: 20 J/cm ² E4: 30 J/cm ² [E1–E4: laser 532 nm, 143 mW, 20.4 mW/cm ²] E5: 5 J/cm ² E6: 10 J/cm ² E7: 20 J/cm ² E8: 30 J/cm ² [E5–E8: laser 633 nm, 140 mW, 15.56 mW/cm ²] E9: 5 J/cm ² E10: 10 J/cm ² E11: 20 J/cm ² E12: 30 J/cm ² [E9–E12: laser 810 nm, 200 mW, 22.22 mW/cm ²] E13: 5 J/cm ²	Wound area	The best effects on wound healing was shown in E5–E8, followed by E1–E4 > E13–E16 > E9–E12 > E21–E24 > E17–E20. [E17–E20: laser 10,600 nm, 300 mW, 66.37 mW/cm ²] E21: 5 J/cm ² E22: 10 J/cm ² E23: 20 J/cm ² E24: 30 J/cm ² [E21–E24: Polychromatic LEDs 510–872 nm, 272 mW, 13.6 mW/cm ²] [three times per week]

Table 5. Cont.

Reference	Sample Type	Parameters	Outcome Measure	Main Results
Al-Watban et al., 2009 [57]	Male Sprague-Dawley rats	E14: 10 J/cm ² E15: 20 J/cm ² E16: 30 J/cm ² [E13–E16: laser 980 nm, 200 mW, 22.22 mW/cm ²] E17: 5 J/cm ² E18: 10 J/cm ² E19: 20 J/cm ² E20: 30 J/cm ² E1: 5 J/cm ² E2: 10 J/cm ² E3: 20 J/cm ² E4: 30 J/cm ² [E1–E4: laser 532 nm, 143 mW, 20.4 mW/cm ²] E5: 5 J/cm ² E6: 10 J/cm ² E7: 20 J/cm ² E8: 30 J/cm ² [E5–E8: laser 633 nm, 140 mW, 15.56 mW/cm ²] E9: 5 J/cm ² E10: 10 J/cm ² E11: 20 J/cm ² E12: 30 J/cm ² [E9–E12: laser 670 nm, 120 mW, 22.86 mW/cm ²] E13: 5 J/cm ² E14: 10 J/cm ² E15: 20 J/cm ² E16: 30 J/cm ² [E13–E16: laser 810 nm, 200 mW, 22.22 mW/cm ²] E17: 5 J/cm ² E18: 10 J/cm ² E19: 20 J/cm ² E20: 30 J/cm ² [E17–E20: laser 980 nm, 200 mW, 22.22 mW/cm ²] [three times per week]	Relative healing	Significant difference in the mean percentage of healing acceleration between the visible laser and invisible laser.

Table 5. Cont.

Reference	Sample Type	Parameters	Outcome Measure	Main Results
Dall Agnol et al., 2009 [58]	Male Wistar rats	E1: GaAlAs LED, 40 nm bandwidth centered at 640 nm, 30 mW E2: indium-gallium-aluminum-phosphide (InGaAlP) laser, 660 nm, 30 mW, 6 J/cm ²	1. Wound diameter 2. Microscopic evolution 3. Qualitative microscopic analysis	1. Significantly reduced in wound diameter: 45% in E1 and 44.5% in E2. 2. The number of inflammatory cells in E1 and E2 was reduced by 23% at the shallow dermis region, and 19% in the deep dermis. 3. Histological characteristics indicated an acceleration of the cicatrization process by the phototherapy.
Wu et al., 2015 [91]	Male Zucker Diabetic Fatty rats (<i>n</i> = 30)	E1: Organic light-emitting diode E2: 635 nm laser [10 mW/cm ² , 5 J/cm ² , 8 mins 20 s, Daily for 7 consecutive days]	1. Wound closure measurement 2. Histological score 3. Immunohistochemistry	1. Percentage wound closure significantly higher in E1 (40.94 ± 3.49%). 2. E1 and E2 had significantly higher histological scores. 3. Significantly higher level of FGF2 expression.

E, Experimental group; C, Control group.

Table 6. Outcomes of in vitro studies on photo energies for treating diabetic ulcers.

Reference	Sample Type	Parameters	Outcome Measure	Main Results
Low-level laser				
Hourelid and Abrahamse, 2007a [50]	Human skin fibroblast cells	E1: 26 min 33 s, 5 J/cm ² E2: 84 min 23 s, 16 J/cm ² Exposed once on Days 1 and 4, HeNe laser 632.8 nm, 3 mW/cm ²	1. Cell morphology 2. Cytotoxicity 3. Apoptosis 4. Genetic integrity	1. No marked morphological changes were observed in cells following laser. 2. Exposure of E1 did not induce additional damage to cells; Exposure to E2 significantly increased amount of cellular lysis. 3. Apoptosis was significantly increased. 4. Additional DNA damage was not seen in E1, but in E2.
Hourelid and Abrahamse, 2007b [51]	Human skin fibroblast cells	E1: 37 min, 5 J/cm ² E2: 2 h, 16 J/cm ² HeNe laser 632.8 nm, 2.206 mW/cm ²	1. Cell morphology 2. Expression of human IL-6 3. Neutral red assay	1. No marked morphological changes were observed in E1; cells in E2 showed sign of stress with open spaces. 2. Significant increase in human IL-6 in E1, but no significant changes in E2. 3. Significant increase in neutral assay in, significant decrease in neutral assay was shown in E2.
Hourelid and Abrahamse, 2007c [52]	Human skin fibroblast cells	E1: 27 min 46 s, 5 J/cm ² , at 30 min and 24 h E2: 2 h, 16 J/cm ² , at 30 min and 72 h HeNe laser 632.8 nm, 3.034 mW/cm ²	1. Cell morphology 2. Cell viability 3. Cytotoxicity and genetic integrity	1. E1 and E2 showed more chemotaxis and haptotaxis at 30 min. 2. No significant change in percentage of ATP viability in E1 and E2 after 30 min. Decrease in viability at E1 at 24 h. 3. Significant increase in cytotoxicity and DNA damage in E1 and E2 after 30 min. Significant damage in DNA seen at 24 h and 72 h in E1 and E2.
Mirzaei et al., 2007 [53]	Cultures of fibroblast-like cells from Wistar rats	E1 (wells n = 10): 0.09 J/cm ² , 30 s, 4 times/day E2 (wells n = 10): 0.09 J/cm ² , 30 s, 4 times at 2 days E3 (wells n = 10): 1 J/cm ² , 330 s, 4 times at 2 days E4 (wells n = 10): 1 J/cm ² , 100 s, 4 times at 4 days E5 (wells n = 10): 4 J/cm ² , 1320 s, 4 times at 4 days [E1–E5: HeNe laser 632.8 nm, 0.6 mW]	1. Viability 2. Number of cells 3. Transmission electron microscopy	1. More bipolar and spindle-shaped fibroblasts in the laser-treated cultures than in the sham-exposed. 2. Significant increase in the number of cells in E5. 3. Ultrastructure features of fibroblasts in the sham-exposed and laser-treated cultures were similar.

Table 6. Cont.

Reference	Sample Type	Parameters	Outcome Measure	Main Results
Hourel and Abrahamse, 2008 [54]	Human skin fibroblast cells	E1: HeNe 632.8 nm, 5 J/cm ² , 23 mW, 2.206 mW/cm ² E2: HeNe 632.8 nm, 16 J/cm ² , 23 mW, 2.206 mW/cm ² E3: diode 830 nm, 5 J/cm ² , 55 mW, 6 mW/cm ² E4: diode 830 nm, 16 J/cm ² , 55 mW, 6 mW/cm ² E5: Nd:YAG 1064 nm, 5 J/cm ² , 1 W, 12.7 mW/cm ² E6: Nd:YAG 1064 nm, 16 J/cm ² , 1 W, 12.7 mW/cm ²	1. Morphology 2. Cellular viability 3. Cellular proliferation	1. The rate of cellular migration into the central scratch was significantly higher in E1 than C. Cells radiated at E3 showed more migration into the central scratch compared to E4. E4 and E5 did not show an increased rate of cellular migration. 2. E1 showed a significant increase in percentage viability compared to E2. Cells radiated with E2 showed a decrease in percentage viability but was not significant. Cells radiated in E3, E4, E5 and E6 show no significant change in percentage viability. 3. E1 and E3 showed a significant increase in bFGF expression.
Hourel and Abrahamse, 2010 [64]	Human skin fibroblast cells	E1: HeNe 632.8 nm, 5 J/cm ² , 23 mW, 2.206 mW/cm ² E2: diode 830 nm, 5 J/cm ² , 55 mW, 6 mW/cm ² E3: Nd:YAG 1064 nm, 5 J/cm ² , 1 W, 12.7 mW/cm ²	1. Morphology 2. Cellular viability 3. Cellular proliferation	1. E3 showed less migration into the central scratch and incomplete wound healing. E1 and E2 showed higher rate of migration and haptotaxis with complete wound closure. 2. No significant change in ATP luminescence in E1 and E2, whereas E3 showed a significant decrease to all other groups. 3. Significant increase in bFGF in E1 and E2.
Hourel et al., 2010 [65]	Human skin fibroblast cells (n = 6)	830 nm, 40 mW, 5 J/cm ²	1. Cellular viability 2. Apoptosis 3. Cellular proliferation 4. Cytokine expression 5. Nitric oxide 6. Reactive oxygen species	1. No significant change in viability 2. A decrease in apoptosis 24 h post irradiation. 3. Significant increase in proliferation at 24 and 48 h. 4. TNF- α were significantly decreased at both 1 and 24 h. No significant change in IL-6. 5. An increase in NO 15 min post irradiation. 6. An increase in ROS 15 min post irradiation.
Sekhejane et al., 2011 [72]	Diabetic wounded and hypoxic human skin fibroblast cells (WS1)	636 nm, continuous, 5 J/cm ² , 476 s and incubated for 1 or 24 h	1. Cellular morphology 2. Viability 3. Apoptosis 4. Proliferation 5. Cytokine expression	1. Regained in cellular morphology. 2. Increase in cellular viability. 3. Decrease in apoptosis. 4. All cells model showed an increase in proliferation. 5. Decrease in TNF- α and proinflammatory cytokine interleukin IL-1 β . E3 showed a decrease in TNF- α .

Table 6. Cont.

Reference	Sample Type	Parameters	Outcome Measure	Main Results
Ayuk et al., 2012 [73]	Diabetic wounded human skin fibroblast	660 nm, continuous, 10.22 mW/cm ² , 5 J/cm ² , 8 min 9 s and incubated for 48 or 72 h	1. Cellular morphology 2. Cellular viability 3. Cellular proliferation 4. Collagen-I	Significant increase in cell migration, viability, proliferation and collagen production.
Hourelid et al., 2012 [75]	Human skin fibroblast	E1: 5 J/cm ² E2: 15 J/cm ² 660 nm, continuous, 11 mW/cm ²	1. Enzymatic activities 2. ATP luminescent assay 3. Mitochondrial staining	1. E2 showed a significant decrease in complex III activity. 2. ATP showed a significant increase in E2. 3. There are higher accumulations of active mitochondria.
Esmaeelinejad et al., 2014 [81]	Human skin fibroblasts	E1: 757 s, 0.5 J/cm ² E2: 1512 s, 1 J/cm ² E3: 3024 s, 2 J/cm ² HeNe laser, 1.5 mW, 632.8 nm, 0.66 mW/cm ²	1. Cell morphology 2. Proliferation rate and cell viability	1. Biological changes in cell morphology were clearly visible in laser-treated human skin fibroblasts at energy densities of 0.5, 1 and 2 J/cm ² . 2. Laser delivered at densities of 0.5 and 1 J/cm ² had stimulatory effects on the viability and proliferation rate of human skin fibroblasts cultured in physiologic glucose concentration.
Masha et al., 2013 [88]	Human skin fibroblast cells (WS1)	660 nm, continuous, 100 mW, 11 mW/cm ² , 5 J/cm ² , 7 min 35 s	Gene expression	Upregulated the expression of mitochondrial genes COX6B2 (complex IV), COX6C (complex IV), PPA1 (complex V), ATP4B (complex V) and ATP5G2 (complex V), ATP5F1 (complex V), NDUFA11 (complex I), and NDUF57 (complex I).
Goralczyk et al., 2016 [98]	Human umbilical vein endothelial cells	E1: 635 nm, 30 mW, 1066 s, 1.875 mW/cm ² E2: 830 nm, 60 mW, 533 s, 3.75 mW/cm ² 80 cm ² irradiated area, 10 cm distance	1. TNF- α concentration 2. IL-6 concentration	1. TNF- α level decreased. 2. LLLT did not cause significant changes in concentration of IL-6 in the endothelial cell culture.
Ayuk et al., 2016 [93]	Human skin fibroblasts	830 nm, 5 J/cm ² , continuous, 98 mW, 9.1 cm ² , 10.76 mW/cm ² , 7 min 43 s	Gene expression profiling	Stimulatory effect on cadherins, integrins, selectins and immunoglobulins.
Ayuk et al., 2018 [94]	Human skin fibroblast cells (WS1)	660 nm, 5 J/cm ² , continuous, 102 mW, 9.1 cm ² , 11.23 mW/cm ² , 7 min 25 s	1. Cell migration 2. Cell viability 3. Cell proliferation	1. Wound closure at 24 h as compared to 0 h. 2. Significant increase in cell at 24 h as compared to 0 h. 3. Increase in S-phase and decrease in G2M phase.

Table 6. Cont.

Reference	Sample Type	Parameters	Outcome Measure	Main Results
Near-infrared				
Danno et al., 2001 [36]	Human foreskin keratinocytes; human foreskin microvascular endothelial cells; human newborn foreskin fibroblasts	Halolamps with 0.7–1.3 μm near infrared, 30 mW/cm^2 , 20–60 min at distance of 20 cm	1. TGF- β 1 2. Matrix metalloproteinase (MMP)-2	1. TGF- β 1 significantly more elevated after irradiation than sham-irradiated controls. 2. Greater increase in MMP-2 was found after irradiation than sham-irradiated controls.
Polychromatic light emitting diode (LED) energy				
Vinck et al., 2005 [45]	Chicken embryos fibroblast cultures ($n = 256$)	Green light of 570 nm, continuous mode, 0.1 J/cm^2 , 3 min, 10 mW, once per day for 3 days	Fibroblast survival and proliferation	Significantly higher rate of proliferation in hyperglycemia circumstances after irradiation.
Wu et al., 2015 [91]	Primary human dermal fibroblasts in 180 mM glucose concentration	Organic light-emitting diode, 623 nm peak wavelength; 7 or 10 mW/cm^2 , 0.2, 1 or 5 J/cm^2	1. Adenosine triphosphate assay 2. MTS assay 3. CyQuant assay	1. Increase in total adenosine triphosphate production at both power densities except the power density of 10 mW/cm^2 and 5 J/cm^2 . 2. Mitochondrial metabolism was significantly higher. 3. Significantly higher cellular proliferation with groups irradiated with 10 mW/cm^2 .

E, Experimental group; C, Control group.

3.3. Methodological Characteristics

The summary of methodological quality in animal studies is presented in Table 7. Only two trials have a detailed explanation of how randomization was carried out and provide an adequate report on the assignment of samples [39,46]. All trials provide baseline clinical characteristics including gender, age or weight of the subjects. In addition, all expected outcomes are reported [19–44,46–49,55–63,66–71,74,76–80,82–85,90–92,95–97,99,100]. Only one trial provides an adequate report on allocation concealment [24]. Five trials report the non-random approach when placing the animals within the facility [62,63,66,71,92]. None of the trials provide information about investigator blinding, but twenty trials report outcome assessor blinding [21,24,25,42–44,60,62,67,68,70,78,79,84,86,87,92,95,99,100]. Three trials report random outcome assessment, although no detailed method of randomization is provided [23,86,87]. Three trials did not include all subjects in the analysis [29,31,37]. Ten studies applied interventions to parts of the body in a single animal, accounting for the analysis bias [37,40,42,59,60,74,78,82,83,89,91].

Table 7. Characteristics of animal experimental studies.

Reference	(1)	(2)	(3)	(4)	(5)	(6)	(7)	(8)	(9)	(10)
Pulsed electromagnetic field										
Callaghan et al., 2008 [19]	Unclear	Yes	Unclear	Unclear	Unclear	Unclear	Unclear	Yes	Yes	Yes
Goudarzi et al., 2010 [20]	Unclear	Yes	Unclear	Unclear	Unclear	Unclear	Unclear	Yes	Yes	Yes
Cheing et al., 2014 [21]	Unclear	Yes	Unclear	Unclear	Unclear	Unclear	Yes	Yes	Yes	Yes
Choi et al., 2016 [22]	Unclear	Yes	Unclear	Unclear	Unclear	Unclear	Unclear	Yes	Yes	Yes
Choi et al., 2018 [23]	Yes	Yes	Unclear	Unclear	Unclear	Yes	Unclear	Yes	Yes	Yes
Ultrasound										
Thawer et al., 2004 [24]	Unclear	Yes	Yes	Unclear	Unclear	Unclear	Yes	Yes	Yes	Yes
Mann et al., 2014 [25]	Unclear	Yes	Unclear	Unclear	Unclear	Unclear	Yes	Yes	Yes	Yes
Roper et al., 2015 [26]	Unclear	Yes	Unclear	Unclear	Unclear	Unclear	Unclear	Yes	Yes	Yes
Shockwave										
Kuo et al., 2009 [27]	Unclear	Yes	Unclear	Unclear	Unclear	Unclear	Unclear	Yes	Yes	Yes
Zins et al., 2010 [30]	Unclear	Yes	Unclear	Unclear	Unclear	Unclear	Unclear	Yes	Yes	Yes
Yang et al., 2011 [28]	Unclear	Yes	Unclear	Unclear	Unclear	Unclear	Unclear	Yes	Yes	Yes
Hayashi et al., 2012 [29]	Unclear	Yes	Unclear	Unclear	Unclear	Unclear	Unclear	No	Yes	Yes
Electrical stimulation										
Smith et al., 1984 [31]	Unclear	Yes	Unclear	Unclear	Unclear	Unclear	Unclear	No	Yes	Yes
Thawer et al., 2001 [32]	Unclear	Yes	Unclear	Unclear	Unclear	Unclear	Unclear	Yes	Yes	Yes
Kim et al., 2014 [33]	Unclear	Yes	Unclear	Unclear	Unclear	Unclear	Unclear	Yes	Yes	Yes
Langoni et al., 2014 [34]	Unclear	Yes	Unclear	Unclear	Unclear	Unclear	Unclear	Yes	Yes	Yes
Photo energy										
Yu et al., 1997 [35]	Unclear	Yes	Unclear	Unclear	Unclear	Unclear	Unclear	Yes	Yes	Yes
Danno et al., 2001 [36]	Unclear	Yes	Unclear	Unclear	Unclear	Unclear	Unclear	Yes	Yes	Yes
Reddy et al., 2001 [37]	No	Yes	Unclear	Unclear	Unclear	Unclear	Unclear	Unclear	Yes	No
Stadler et al., 2001 [38]	Unclear	Yes	Unclear	Unclear	Unclear	Unclear	Unclear	Yes	Yes	Yes
AI-Watban and Andres, 2003 [39]	Yes	Yes	Unclear	Unclear	Unclear	Unclear	Unclear	Yes	Yes	Yes
Reddy, 2003 [40]	Unclear	Yes	Unclear	Unclear	Unclear	Unclear	Unclear	Yes	Yes	No
Whelan et al., 2003 [41]	Unclear	Yes	Unclear	Unclear	Unclear	Unclear	Unclear	Yes	Yes	Yes
Byrnes et al., 2004 [42]	No	Yes	Unclear	Unclear	Unclear	Unclear	Yes	Yes	Yes	No
Kawalec et al., 2004 [43]	Unclear	Yes	Unclear	Unclear	Unclear	Unclear	Yes	Yes	Yes	Yes
Maiya et al., 2005 [44]	Unclear	Yes	Unclear	Unclear	Unclear	Unclear	Yes	Yes	Yes	Yes
AI-Watban and Andres, 2006 [46]	Yes	Yes	Unclear	Unclear	Unclear	Unclear	Unclear	Yes	Yes	Yes
Carvalho et al., 2006 [47]	Unclear	Yes	Unclear	Unclear	Unclear	Unclear	Unclear	Yes	Yes	Yes
Rabelo et al., 2006 [48]	Unclear	Yes	Unclear	Unclear	Unclear	Unclear	Unclear	Yes	Yes	Yes
AI-Watban et al., 2007 [49]	Unclear	Yes	Unclear	Unclear	Unclear	Unclear	Unclear	Yes	Yes	Yes
Meireles et al., 2008 [55]	Unclear	Yes	Unclear	Unclear	Unclear	Unclear	Unclear	Yes	Yes	Yes

Table 7. Cont.

Reference	(1)	(2)	(3)	(4)	(5)	(6)	(7)	(8)	(9)	(10)
AI-Watban, 2009 [56]	Unclear	Yes	Unclear	Unclear	Unclear	Unclear	Unclear	Yes	Yes	Yes
AI-Watban et al., 2009 [57]	Unclear	Yes	Unclear	Unclear	Unclear	Unclear	Unclear	Yes	Yes	Yes
Dall Agnol et al., 2009 [58]	Unclear	Yes	Unclear	Unclear	Unclear	Unclear	Unclear	Yes	Yes	Yes
Gungormus and Akyol, 2009 [59]	Unclear	Yes	Unclear	Unclear	Unclear	Unclear	Unclear	Yes	Yes	No
Akyol and Gungörmuş, 2010 [60]	Unclear	Yes	Unclear	Unclear	Unclear	Unclear	Yes	Yes	Yes	No
Carvalho pde et al., 2010 [61]	Unclear	Yes	Unclear	Unclear	Unclear	Unclear	Unclear	Yes	Yes	Yes
Chung et al., 2010a [63]	Unclear	Yes	Unclear	No	Unclear	Unclear	Yes	Yes	Yes	Yes
Chung et al., 2010b [62]	Unclear	Yes	Unclear	No	Unclear	Unclear	Unclear	Yes	Yes	Yes
Jahangiri Noudeh et al., 2010 [66]	Unclear	Yes	Unclear	No	Unclear	Unclear	Unclear	Yes	Yes	Yes
Oliveira et al., 2010 [67]	Unclear	Yes	Unclear	Unclear	Unclear	Unclear	Yes	Yes	Yes	Yes
Santos et al., 2010 [68]	Unclear	Yes	Unclear	Unclear	Unclear	Unclear	Yes	Yes	Yes	Yes
Hegde et al., 2011 [69]	Unclear	Yes	Unclear	Unclear	Unclear	Unclear	Unclear	Yes	Yes	Yes
Oliveira et al., 2011 [70]	Unclear	Yes	Unclear	Unclear	Unclear	Unclear	Yes	Yes	Yes	Yes
Peplow et al., 2011 [71]	Unclear	Yes	Unclear	No	Unclear	Unclear	Unclear	Yes	Yes	Yes
Dadpay et al., 2012 [74]	No	Yes	Unclear	Unclear	Unclear	Unclear	Unclear	Yes	Yes	No
Park and Kang, 2012 [89]	No	Yes	Unclear	Unclear	Unclear	Unclear	Unclear	Yes	Yes	No
Peplow et al., 2012 [76]	Unclear	Yes	Unclear	Unclear	Unclear	Unclear	Unclear	Yes	Yes	Yes
Aparecida Da Silva et al., 2013 [77]	Unclear	Yes	Unclear	Unclear	Unclear	Unclear	Unclear	Yes	Yes	Yes
Firat et al., 2013 [86]	Unclear	Yes	Unclear	Unclear	Unclear	Yes	Yes	Yes	Yes	Yes
Franca et al., 2013 [87]	Unclear	Yes	Unclear	Unclear	Unclear	Yes	Yes	Yes	Yes	Yes
He et al., 2013 [79]	Unclear	Yes	Unclear	Unclear	Unclear	Unclear	Yes	Yes	Yes	Yes
Masha et al., 2013 [88]	Unclear	Yes	Unclear	Unclear	Unclear	Unclear	Unclear	Yes	Yes	Yes
Dancáková et al., 2014 [80]	Unclear	Yes	Unclear	Unclear	Unclear	Unclear	Unclear	Yes	Yes	Yes
Kilik et al., 2014 [82]	No	Yes	Unclear	Unclear	Unclear	Unclear	Unclear	Yes	Yes	No
Sharifian et al., 2014 [83]	No	Yes	Unclear	Unclear	Unclear	Unclear	Unclear	Yes	Yes	No
De Loura Santana et al., 2015 [84]	Unclear	Yes	Unclear	Unclear	Unclear	Unclear	Yes	Yes	Yes	Yes
Fekrazad et al., 2015 [92]	Unclear	Yes	Unclear	No	Unclear	Unclear	Yes	Unclear	Yes	Yes
Lau et al., 2015 [85]	Unclear	Yes	Unclear	Unclear	Unclear	Unclear	Unclear	Yes	Yes	Yes
Lau et al., 2015 [90]	Unclear	Yes	Unclear	Unclear	Unclear	Unclear	Unclear	Unclear	Yes	Yes
Wu et al., 2015 [91]	No	Yes	Unclear	Unclear	Unclear	Unclear	Unclear	Yes	Yes	No
de Loura Santana et al., 2016 [95]	Unclear	Yes	Unclear	Unclear	Unclear	Unclear	Yes	Unclear	Yes	Yes
Ranjbar et al., 2016 [99]	Unclear	Yes	Unclear	Unclear	Unclear	Unclear	Yes	Unclear	Yes	Yes
Tatmatsu Rocha et al., 2016 [100]	Yes	Yes	Unclear	Unclear	Unclear	Unclear	Yes	Unclear	Yes	Yes
Denadai et al., 2017 [96]	Yes	Yes	Unclear	Unclear	Unclear	Unclear	Unclear	Unclear	Yes	Yes
Eissa and Salih, 2017 [97]	Yes	Yes	Unclear	Unclear	Unclear	Unclear	Unclear	Unclear	Yes	Yes

Studies fulfilling the criteria of: (1) sequence generation; (2) baseline characteristics; (3) allocation concealment; (4) random housing; (5) investigator blinding; (6) random outcome assessment; (7) assessor blinding; (8) incomplete outcome data addressed; (9) free of selective outcome reporting; and (10) free of other source of bias.

3.4. Efficacy of Biophysical Energy (BPEs) Stimulation

3.4.1. Pulsed Electromagnetic Field (PEMF)

The five PEMF trials compared pulsed electromagnetic fields with the sham treatment [19–23] (Table 1). Three trials conducted by the same researchers compared 2 mT, 5 mT and 10 mT of 25 Hz sinusoidal PEMF in male SD rats with the sham treatment [21–23]. One trial compared 8 mT, 20 Hz PEMF in male Wistar rats with the sham treatment [20]. Another trial involved both in vitro and in vivo studies using human umbilical vein endothelial cells, db/db mice, C57BL6 mice and FGF-2 knockout mice [19].

Wound closure percentage was the main outcome measure for all five trials. Other measures included overall wound closure time, cell proliferation, vascularity, murine endothelial cell culture, FGF-2 secretion, wound tensile strength, myofibroblast production, type 1 collagen fiber deposition, collagen fibril alignment, collagen fiber anisotropy and orientation, energy absorption capacity, Young's modulus, wound thickness, and maximum stress of wound tissue. Four trials report significant between-group difference in the percentage of original wound size, and the experimental groups in all these studies demonstrated improved wound healing compared to the control groups [19–21,23].

3.4.2. Ultrasound (US)

Two trials compared ultrasound with sham treatment [24,26], whereas one trial compared ultrasound with dressing changing [25]. The wound size was the main outcome measure for all three ultrasound trials. Other measures included wound closure duration, granulation tissue, collagen deposition, angiogenesis, VEGF expression, SDF-1 expression, fibroblast proliferation, speed and persistency of fibroblast migration (Table 2).

Male CD-1 mice, BKS.Cg-Dock7m+/+Leprdb/J mice, Syndecan-4 wild-type and knockout C57BL/6J mice were used in the animal models. Fibroblasts from wound tissues and db/db mouse skins were used as the cellular model. Thawer et al. and Mann et al. delivered ultrasound with saline vapor at 45 kHz and 40 kHz, respectively, while Roper et al. delivered 1 kHz ultrasound through water-based gel. Two out of three trials revealed significant between-group differences in wound size in favor of the experimental groups over the control groups in these studies [25,26]. The exception was the trial reported by Thawer and collaborators, which showed no significant between-group differences in wound size after ultrasound treatment.

3.4.3. Extracorporeal Shockwave (ECSW)

Four trials on the efficacy of shock wave used male Wistar rats, SD rats, endothelial nitric oxide synthase-knockout mice, C5781/6 mice BALB/c and Bk.Cg-m Lepr (db+/db+) mice. Outcome measures included wound healing area, topical blood perfusion, leukocyte infiltration, cell proliferation, angiogenesis, wound breaking strength, collagen content, fibroblast proliferation, TGF- β 1 expression in fibroblasts, myofibroblast accumulation, eNOS expression and angiogenic gene expression (Table 3).

Kuo and colleagues compared three different protocols of shockwave with the control group receiving no shockwave energy and reported a significant acceleration in wound healing ($p < 0.05$). The perfusion in wound area was significantly higher in the experimental group treated with two sessions of defocused shockwave (on postoperative Days 3 and 7) than the diabetic control group ($p = 0.023$). In addition, fibroblast count and VEGF level were upregulated in experimental groups compared to control groups. The authors concluded that treatment with an optimal session of ECSW significantly enhanced diabetic wound healing associated with increased neo-angiogenesis, tissue regeneration and topical anti-inflammatory response. However, they did not provide details on the randomization method, allocation concealment, random housing, outcome assessment, and investigator and assessor blinding [27].

Yang and colleagues compared two different protocols of shockwave with the control groups, and they reported a significant improvement evident by increased wound breaking strength, number of fibroblasts and collagen fibers. The authors concluded that low energy ECSW can improve the healing of incisional wound in diabetic rats [28]. Zins et al. investigated the angiogenic gene expressions and wound closure kinetics during diabetic wound healing with or without ECSW therapy. The expression of certain genes in the diabetic wound was augmented by shockwave, especially PECAM-1; however, they found that shockwave had no effect on wound closure in both normal and diabetic models [30].

Hayashi et al. investigated the role of endothelial nitric oxide synthase with shockwave energy for diabetic wounds. A single session of ECSW accelerated wound healing in a streptozotocin-induced diabetic mouse model, accompanied by an increased expression of eNOS and vascular endothelial growth factor (VEGF). However, the efficacy of ECSW was attenuated in eNOS-KO mice. The authors concluded that eNOS played a critical role in the therapeutic effects of shockwave by accelerating the wound healing through VEGF upregulation and neovascularization [29].

3.4.4. Electrical Stimulation (ES)

The four ES trials used different types of protocols. Two trials compared ES with sham treatment [32,33]. One trial compared two different ES protocols with control receiving no ES [31]. Another trial compared ES with the control group receiving no ES or with transdermal iontophoresis by zinc sulfate [34]. None of these studies provided information about randomization, allocation concealment, investigator and assessor blinding, random housing and outcome assessment (Table 4).

Monophasic pulse wave is reported in two trials [32,33]. The outcome measures included wound healing rate, wound contraction, tensile strength, histology, collagen deposition, fibroblast proliferation and morphological analysis. Smith et al. classified the tensile strength into “poor”, “moderate” and “good” after 10 days of stimulation, and they showed that ES enhanced diabetic wound healing. However, no statistical analysis is provided in their study [31].

Thawer et al. compared wound healing in diabetic mice with ES at 12.5 V and sham treatment (0 V). No statistical difference was found in epidermis thickness between groups. The authors suggested that ES at a high dose can alter collagen deposition in excisional wounds of diabetic mice; however, they found the effect of ES on wound healing to be disease-specific [32]. Kim and colleagues compared experimental groups receiving ES at 35–50 V with a control group receiving sham ES. Significant difference was found in wound healing rate between groups. In addition, elevated levels of collagen-I, α -SMA and TGF- β 1 were found in experimental groups (all $p < 0.05$) [33].

Langoni Cassettari and collaborators divided the normal and diabetic Wistar rats into six experimental groups to study the effect of ES with direct current (DC) and zinc sulfate treatment by transdermal iontophoresis. The authors concluded that DC alone or used in association with zinc by transdermal iontophoresis was able to induce the morphological and ultrastructural changes observed during surgical wound healing in diabetic animals [34].

3.4.5. Photo Energies (PE)

The photo energies reported for treating diabetic wounds encompass low-level laser energy [35, 37,38,40,42–44,47–55,59–66,68,69,71–78,80–90,92,93,97,99,100], near-infrared [36], polychromatic light emitting diodes [39,41,45,67,70] and monochromatic infrared energy [79]. Some studies also compared different types of photo energy [46,56–58] (Tables 5 and 6).

Low Level Laser Therapy (LLL)

A broad spectrum of laser wavelengths has been reported by different studies, whereas wavelengths in the visible red range (630–685 nm) were most commonly investigated either in isolation or in combination with other wavelengths ranging from 425 nm to 1064 nm. Power density in mWcm² was not specified in some of the reviewed studies, even though this represents an important parameter. The irradiance ranged widely from 4 to 79 mWcm². Peplow et al. reported a range of irradiance

instead of a specific density [71]. Similarly, a large variety of animal models have been used, including C57BL/Ksj/db/db mice, SD rats, Sand rats, Wistar rats, BKS.Cg-m+/+Leprdb/J mice, Zucker diabetic rats and Swiss albino mice. Several wound healing outcomes were measured using various techniques, most commonly wound size and histology. However, nine of our surveyed trials applied laser to parts of the body of a single animal for both experiment and control, and analysis was conducted as if every single wound were from an individual animal [37,40,42,59,60,74,78,82,83,89].

Polychromatic Light Emitting Diodes (LED)

In six trials that investigated effects of polychromatic light emitting diodes (LED), three trials studied burn healing in diabetic rats [39,67,70]. Al-Watban et al. compared the efficacy of LED (wavelength 510–543, 594–599, 626–639, 640–670 and 842–879 nm) on burn wound at four different doses with the sham treatment. Significant burn healing was found from 48.77% to 76.77% after LED stimulation at different doses in diabetic rats [39]. The same research group also compared the efficacy of laser of different wavelengths (532, 633, 810, 980, 10600 nm) to LED clusters (510–872 nm) with incident doses of 5, 10, 20 and 30 J/cm² in SD rats (*n* = 893) [56]. Their results showed that phototherapy at 633 nm should be given three times a week at a fluence of 2.35 J/cm² each time for diabetic wound treatment. Wu et al. [91] compared the 635 nm laser with organic LED and showed that the organic LED significantly increased fibroblast growth factor-2 expression and macrophage activation during the initial stages of wound healing. In addition, they also found that organic LED and laser had comparative effects on promoting diabetic wound healing in rats.

Infrared (IR)

Danno and colleagues conducted both *in vitro* and *in vivo* studies to compare the infrared irradiation treatment with sham irradiation control or thermal control [36]. The TGF- β 1 and MMP-2 content in the medium of cultured cells was significantly elevated after irradiation. Negative results in thermal controls suggested that the action of the light was athermic in nature. In animal models, the rate of wound closure was significantly accelerated after repeated exposures. Cheing and collaborators compared the efficacy of managing acute wounds in male diabetic SD rats between groups of monochromatic infrared energy (MIRE) at 890 nm and the sham group without receiving infrared energy [79]. Both experimental and sham groups showed improvement in terms of wound closure percentage; however, no statistical difference was found between groups.

4. Discussion

Preclinical research is important for expanding knowledge and provides insights into the cellular and physiological mechanisms on how BPEs enhance diabetic wound healing. Two trials have investigated how cells respond when exposed to electrical currents [101,102]; however, research evidence showing its effects on diabetic wound healing is limited. Four *in vivo* studies described here present inconsistent results regarding the value of ES in acute diabetic wound healing in animals. Thawer et al. showed no statistical difference in epidermis thickness between groups, but they did find a significant increase in collagen deposition [32]. Findings reported by Kim et al. are consistent with those found by Thawer's team, in which collagen-I expression was higher after ES. In addition, α -SMA and TGF- β 1 expression were also enhanced after daily ES [33]. Langoni Cassettari et al. found accelerated wound contraction, but the morphology of inflammation was not altered after ES [34]. Statistical analysis was not available in one of the studies examined [31], making it difficult to draw conclusions on the ES' benefits in diabetic wound healing from this animal study.

Extracorporeal shockwave (ECSW) has been used clinically for treating musculoskeletal disorders and diabetic ulcers for some years [103]. However, preclinical studies examined in this review reported contradictory findings in supporting the use of ECSW on diabetic wound healing. Two studies showed that ECSW significantly reduced wound size compared to sham treatment groups in diabetic rats [27,29]. On the contrary, a recent study by Zins et al. found that ECSW did not accelerate wound

closure in wildtype (non-diabetic) mice or db/db diabetic mice [30]. Another study found that diabetic mice treated with ECSW significantly increased the wound breaking strength and the collagen fiber content [28]. However, this effect was attenuated in endothelial nitric oxide synthase-knockout mice, suggesting that nitric oxide synthesis plays a critical role in the therapeutic effects of ECSW in diabetic wound healing [29].

Pulsed electromagnetic field (PEMF) energy has been used to treat diabetic stump wounds [104] and chronic diabetic ulcers [9]. All five studies included in our review showed positive findings that supported the use of PEMF in promotion of diabetic wound healing in animal models [19–23]. However, when Callaghan et al. repeated the same protocol on FGF-2 knockout mice, there was no significant improvement found in wound closure rate, suggesting FGF-2 might be a crucial factor in PEMF stimulated diabetic wound healing [19].

Sixty-six studies concerning photo energies are included in the present review. Different types of photo energies with different frequencies have been used in various studies. The wavelengths used range from visible red to infrared, power values from milliwatt to watt, and irradiation from seconds to hours. The wide range of irradiation parameters from the current review suggests the bio-modulatory potential of laser therapy [105]. In addition, these studies were conducted using various diabetic wound models, and different outcome measures were used. The findings show that irradiation by laser accelerated wound closure and collagen production, and there were increases in cellular migration, tissue viability, growth factors and gene expression. Histopathological analysis also showed a decrease in inflammatory cells and an increase in vascularization after irradiation compared to the sham control. Most trials report positive results, except Jahangiri Noudeh et al. who found no statistical significance by repeated measurements throughout the entire study period when a combined 670 nm and 810 nm laser was applied to wound areas [66]. Histological analysis revealed that there was an increase in macrophages [61,95,99], fibroblasts [47,53,63,67,68,81,84,99,100], neutrophils [95], T lymphocyte [95], collagen deposition [37,40,70,77,82,85,99,100], nitrite [100] and nitric oxide level [65], catalase activity [100], thiobarbituric acid reactive substances [100] and vascularization [44,68,70,99] after irradiation. Chung et al. adopted a splinted diabetic wound model to minimize mouse skin contraction during wound healing [62]. Seven-day treatment of 3.7–5.0 J/cm² caused maximum stimulation of wound healing in diabetic mice compared to the mice receiving no irradiation. Laser irradiation of wavelength at 780 nm improved muscle repair by enhancing reorganization of myofibers and perimysium in cryoinjured diabetic rats [87]. However, not all studies demonstrated a positive result due to the specificity of absorption spectrum and laser intensity. For instance, higher frequencies might cause a negative effect on cells. Houreld and Abrahamse compared the cell morphology and expression of human IL-6 between groups receiving 5 and 16 J/cm². They found that subjects treated with 16 J/cm² demonstrated signs of stress without a significant increase in IL-6 expression [51]. Therefore, the optimal protocol of laser therapy for enhancing diabetic wound healing should be further investigated.

The present review does not support the use of ultrasound (US) in promoting diabetic wound healing using animal models [24–26]. Thawer and collaborators [24] demonstrated no significant between-group difference in wound size reduction after US, however, a significant improvement was shown by Mann et al. and Roper et al. after treatment [25,26]. Fibroblast migration and proliferation [24–26], as well as vascular density [24,25], were enhanced by the use of US compared to the sham groups. Interestingly, these two studies applied 40 and 45 kHz US to wounds through saline vapour or mist (as the coupling medium) for 1.5 and 3 min, respectively [24,25]. Another study utilized US at 1.5 MHz applied via traditional coupling gel for 20 min [26]. The optimal protocol for using ultrasound for enhancing diabetic wound healing should be further evaluated in future studies.

Most research on BPEs have been conducted on animal models consisting of surgically excised skin or burn wounds. However, no animal tissue model could possibly replicate the clinical situation in humans because different species may involve different healing mechanisms in skin wound, therefore, treatments with different BPEs are likely to yield different cellular responses when compared to human

skin [106]. These experimental wounds excluded common problems associated with delays in healing including ischemia and infection, thus they might not present the real situation in humans [107]. In addition, Wang et al. commented that most in vitro data derived from fibroblasts of abnormal wound lesions only represent the terminal stage of the disease [107]. Therefore, these wound models may not be ideal to study the effect of BPEs on human diabetic ulcer healing. Recently, a reproducible chronic diabetic wound model that had low mortality rate was established by using *Pseudomonas aeruginosa* biofilm in db/db mice [108,109]. This model could be adopted in future studies to evaluate the antibiofilm effectiveness of BPEs in chronic wounds, which simulate infected diabetic ulcerations commonly seen in clinical settings. It should be noted that humane issue is always a concern of animal studies, in particular for experiments involving burn and wound. Therefore, in vitro methods might be an alternative because not only the humane concerns are circumvented but also the human cells instead of animal cells can be directly tested. Due to the shortcomings of animal studies, well-designed human studies are still the gold standard in clinical practice.

5. Conclusions

The present review demonstrates methodological shortcomings in animal studies that have studied the efficacy of BPEs in diabetic wound healing. One major limitation exhibited in animal experiments is that random allocation of animals to experimental and control groups and blinding is not yet a standard practice [110]. In addition, critical information for animal housing conditions and dropouts are unreported. Investigators should consider the findings of this systematic review when designing future studies and attempting to improve the internal validity of the studies by using true randomization in group allocation and outcome assessment, investigator and assessor blinding, allocation concealment, random housing, and reporting accurately on the number of animals used. In this review, the search was restricted to English publications as the translation was not available for full text review, which may have resulted in language bias. Notably, a variety of animal models were used for in vivo wound healing studies, but the physiology and healing mechanisms may not be the same across different species, and they are even more distinct compared to humans. There was considerable variation in research design, methodology, and parameters which limited comparison of research findings between studies. Therefore, findings obtained from even well-controlled animal studies may not be readily translated into clinical practice for people with diabetes management. Based on positive effects of PEMF and photo energies towards diabetic wound healing, more high-quality human clinical trials to assess the effects of those biophysical energies are warranted in the future.

Author Contributions: Conceptualization, R.L.-C.K. and G.L.-Y.C.; Methodology, R.L.-C.K.; Formal Analysis, R.L.-C.K.; Investigation, R.L.-C.K. and H.M.-C.C.; Resources, R.L.-C.K.; Data Curation, R.L.-C.K. and H.M.-C.C.; Writing—Original Draft Preparation, R.L.-C.K.; Writing—Review and Editing, R.L.-C.K., S.L., H.M.-C.C., L.C.K. and G.L.-Y.C.; Supervision, L.C.K. and G.L.-Y.C.; Project Administration, R.L.-C.K. and G.C.; and Funding Acquisition, G.L.-Y.C.

Funding: This research was funded by the General Research Fund provided by the Research Grants Council of the Hong Kong SAR Government grant number (PolyU151003/14M).

Conflicts of Interest: The authors declare no conflict of interest.

Abbreviations

BPEs	biophysical energies
ES	electrical stimulation
PEMF	pulsed electromagnetic field
ECSW	extracorporeal shockwave
LLL	low-level laser therapy
US	ultrasound
LED	light emitting diode
NIR	infrared
E	experimental group
C	control group

Appendix A

Detailed search strings

Basic search was combined with searches for interventions by adding the search term AND.

Basic search

(Diabetes Mellitus [MeSH]) OR (Diabetes Mellitus) OR (Diabetes) OR (Diabetic) OR (Diabetes Mellitus, Type 2) OR (Diabetes Complications [MeSH]) AND (ulcer [MeSH]) OR ((Foot ulcer) OR (diabetic foot) OR (wound) OR (wound healing [MeSH]) OR (wounds and injuries [MeSH])).

Model

(Animal) OR (Animals [MeSH]) OR (mouse) OR (Mice [MeSH]) OR (murine) OR (Rats [MeSH]) OR (rodent) OR (Hamster) OR (Cricetulus [MeSH]) OR (Rabbits [MeSH]) OR (Guinea pigs [MeSH]) OR (Swine [MeSH]) OR (dog) OR (porcine) OR (Sprague-Dawley) OR (Transgenic) OR (Sheep [MeSH]) OR (pig) OR (*In Vitro* [MeSH]) OR (*In vivo*) OR (Cells [MeSH]) OR (macrophages) OR (fibroblasts) OR (Adenosine triphosphate) OR (Collagen).

Electrical stimulation

(Physical therapy modalities [MeSH]) OR (Electric stimulation therapy [MeSH]) OR (Electric* therapy) OR (Microamperage stimulation) OR (Low intensity direct current) OR (High voltage) OR (electrotherapy) OR (direct current) OR (microcurrent).

Electromagnetics

(Electromagnetic*) OR (Electromagnetic Fields [MeSH]) OR (Magnetic Field Therapy [MeSH]) OR (Pulsed electromagnetic therapy) OR (diathermy) OR (shortwave).

Phototherapy

(Ultraviolet rays [MeSH]) OR (Lasers [MeSH]) OR (Laser Therapy [MeSH]) OR (Laser Therapy, Low-Level [MeSH]) OR (MIRE) OR (monochromatic infrared energy) OR (Phototherapy [MeSH]) OR (Infrared Rays [MeSH]) OR (Anodyne) OR (near infrared) OR (near-infrared).

Ultrasound

(Ultrasound [MeSH]) OR (Ultrasonic Therapy [MeSH]) OR (Ultrasonic Therap*) OR (ultrasonic).

Extracorporeal shockwave therapy

(extracorporeal shockwave) OR (shockwave).

Filter

NOT ("review" [Publication Type]) OR (review literature as topic [MeSH]) OR (reviews).

References

1. American Diabetes Association. FAST FACTS—Data and Statistics about Diabetes. Available online: http://professional.diabetes.org/admin/UserFiles/0%20-%20Sean/Documents/Fast_Facts_3-2015.pdf (accessed on 18 December 2017).
2. Margolis, D.J.; Malay, D.S.; Hoffstad, O.J.; Leonard, C.E.; MaCurdy, T.; de Nava, K.L.; Tan, Y.; Molina, T.; Siegel, K.L. Incidence of Diabetic Foot Ulcer and Lower Extremity Amputation among Medicare Beneficiaries, 2006 to 2008: Data Points #2. Available online: <http://www.ncbi.nlm.nih.gov/books/NBK65149/> (accessed on 18 December 2017).
3. Johannesson, A.; Larsson, G.U.; Ramstrand, N.; Turkiewicz, A.; Wirehn, A.B.; Atroshi, I. Incidence of lower-limb amputation in the diabetic and nondiabetic general population: A 10-year population-based cohort study of initial unilateral and contralateral amputations and reamputations. *Diabetes Care* **2009**, *32*, 275–280. [[CrossRef](#)] [[PubMed](#)]

4. Dubský, M.; Jirkovská, A.; Bem, R.; Fejfarová, V.; Skibová, J.; Schaper, N.C.; Lipsky, B.A. Risk factors for recurrence of diabetic foot ulcers: Prospective follow-up analysis in the Eurodiale subgroup. *Int. Wound J.* **2013**, *10*, 555–561. [[CrossRef](#)] [[PubMed](#)]
5. Dinh, T.; Tecilazich, F.; Kafanas, A.; Doupis, J.; Gnardellis, C.; Leal, E.; Tellechea, A.; Pradhan, L.; Lyons, T.E.; Giurini, J.M.; et al. Mechanisms Involved in the Development and Healing of Diabetic Foot Ulceration. *Diabetes* **2012**, *61*, 2937–2947. [[CrossRef](#)] [[PubMed](#)]
6. Kloth, L.C. Electrical Stimulation Technologies for Wound Healing. *Adv. Wound Care* **2014**, *3*, 81–90. [[CrossRef](#)]
7. Kwan, R.L.; Cheing, G.L.; Vong, S.K.; Lo, S.K. Electrophysical therapy for managing diabetic foot ulcers: A systematic review. *Int. Wound J.* **2013**, *10*, 121–131. [[CrossRef](#)]
8. Thakral, G.; Kim, P.J.; LaFontaine, J.; Menzies, R.; Najafi, B.; Lavery, L.A. Electrical Stimulation as an Adjunctive Treatment of Painful and Sensory Diabetic Neuropathy. *J. Diabetes Sci. Technol.* **2013**, *7*, 1202–1209. [[CrossRef](#)]
9. Kwan, R.L.; Wong, W.C.; Yip, S.L.; Chan, K.L.; Zheng, Y.P.; Cheing, G.L. Pulsed electromagnetic field therapy promotes healing and microcirculation of chronic diabetic foot ulcers: A pilot study. *Adv. Skin Wound Care* **2015**, *28*, 212–219. [[CrossRef](#)]
10. Santamato, A.; Panza, F.; Fortunato, F.; Portincasa, A.; Frisardi, V.; Cassatella, G.; Valente, M.; Seripa, D.; Ranieri, M.; Fiore, P. Effectiveness of the frequency rhythmic electrical modulation system for the treatment of chronic and painful venous leg ulcers in older adults. *Rejuvenation Res.* **2012**, *15*, 281–287. [[CrossRef](#)]
11. Musaev, A.V.; Guseinova, S.G.; Imamverdieva, S.S. The use of pulsed electromagnetic fields with complex modulation in the treatment of patients with diabetic polyneuropathy. *Neurosci. Behav. Physiol.* **2003**, *33*, 745–752. [[CrossRef](#)]
12. Cho, M.R.; Thatte, H.S.; Lee, R.C.; Golan, D.E. Integrin-dependent human macrophage migration induced by oscillatory electrical stimulation. *Ann. Biomed. Eng.* **2000**, *28*, 234–243. [[CrossRef](#)]
13. Ercan, B.; Kummer, K.M.; Tarquinio, K.M.; Webster, T.J. Decreased Staphylococcus aureus biofilm growth on anodized nanotubular titanium and the effect of electrical stimulation. *Acta Biomater.* **2011**, *7*, 3003–3012. [[CrossRef](#)]
14. Lee, J.-H.; Jekal, S.-J.; Kwon, P.-S. 630 nm Light Emitting Diode Irradiation Improves Dermal Wound Healing in Rats. *JKPT* **2015**, *27*, 140–146. [[CrossRef](#)]
15. de Vries, R.B.M.; Hooijmans, C.R.; Langendam, M.W.; van Luijk, J.; Leenaars, M.; Ritskes-Hoitinga, M.; Wever, K.E. A protocol format for the preparation, registration and publication of systematic reviews of animal intervention studies. *Evid. Based Preclin. Med.* **2015**, *2*, 1–9. [[CrossRef](#)]
16. Hooijmans, C.R.; Rovers, M.M.; de Vries, R.B.; Leenaars, M.; Ritskes-Hoitinga, M.; Langendam, M.W. SYRCLE's risk of bias tool for animal studies. *BMC Med. Res. Methodol.* **2014**, *14*, 43. [[CrossRef](#)]
17. Hass, H.L. The therapeutic activity of the BIOPTRON-lamp in the treatment of disorders of wound healing. Diabetic gangrene. *Krankenpf. J.* **1998**, *36*, 494–496. [[PubMed](#)]
18. Kilik, R.; Bober, J.; Gal, P.; Vidinsky, B.; Mokry, M.; Longauer, F.; Sabo, J. The influence of laser irradiation with different power densities on incisional wound healing in healthy and diabetic rats. *Rozhl Chir* **2007**, *86*, 384–387. [[PubMed](#)]
19. Callaghan, M.J.; Chang, E.I.; Seiser, N.; Aarabi, S.; Ghali, S.; Kinnucan, E.R.; Simon, B.J.; Gurtner, G.C. Pulsed electromagnetic fields accelerate normal and diabetic wound healing by increasing endogenous FGF-2 release. *Plast. Reconstr. Surg.* **2008**, *121*, 130–141. [[CrossRef](#)] [[PubMed](#)]
20. Goudarzi, I.; Hajizadeh, S.; Salmani, M.E.; Abrari, K. Pulsed electromagnetic fields accelerate wound healing in the skin of diabetic rats. *Bioelectromagnetics* **2010**, *31*, 318–323. [[CrossRef](#)] [[PubMed](#)]
21. Cheing, G.L.; Li, X.; Huang, L.; Kwan, R.L.; Cheung, K.K. Pulsed electromagnetic fields (PEMF) promote early wound healing and myofibroblast proliferation in diabetic rats. *Bioelectromagnetics* **2014**, *35*, 161–169. [[CrossRef](#)]
22. Choi, M.C.; Cheung, K.K.; Li, X.; Cheing, G.L. Pulsed electromagnetic field (PEMF) promotes collagen fibre deposition associated with increased myofibroblast population in the early healing phase of diabetic wound. *Arch. Dermatol. Res.* **2016**, *308*, 21–29. [[CrossRef](#)]
23. Choi, H.M.C.; Cheing, A.K.K.; Ng, G.Y.F.; Cheing, G.L.Y. Effects of pulsed electromagnetic field (PEMF) on the tensile biomechanical properties of diabetic wounds at different phases of healing. *PLoS ONE* **2018**, *13*, e0191074. [[CrossRef](#)]

24. Thawer, H.A.; Houghton, P.E. Effects of ultrasound delivered through a mist of saline to wounds in mice with diabetes mellitus. *J. Wound Care* **2004**, *13*, 171–176. [[CrossRef](#)] [[PubMed](#)]
25. Maan, Z.N.; Januszyk, M.; Rennert, R.C.; Duscher, D.; Rodrigues, M.; Fujiwara, T.; Ho, N.; Whitmore, A.; Hu, M.S.; Longaker, M.T.; et al. Noncontact, low-frequency ultrasound therapy enhances neovascularization and wound healing in diabetic mice. *Plast. Reconstr. Surg.* **2014**, *134*, 402e–411e. [[CrossRef](#)]
26. Roper, J.A.; Williamson, R.C.; Bally, B.; Cowell, C.A.; Brooks, R.; Stephens, P.; Harrison, A.J.; Bass, M.D. Ultrasonic Stimulation of Mouse Skin Reverses the Healing Delays in Diabetes and Aging by Activation of Rac1. *J. Investig. Dermatol.* **2015**, *135*, 2824–2851. [[CrossRef](#)]
27. Kuo, Y.R.; Wang, C.T.; Wang, F.S.; Chiang, Y.C.; Wang, C.J. Extracorporeal shock-wave therapy enhanced wound healing via increasing topical blood perfusion and tissue regeneration in a rat model of STZ-induced diabetes. *Wound Repair Regen.* **2009**, *17*, 522–530. [[CrossRef](#)] [[PubMed](#)]
28. Yang, G.; Luo, C.; Yan, X.; Cheng, L.; Chai, Y. Extracorporeal shock wave treatment improves incisional wound healing in diabetic rats. *Tohoku J. Exp. Med.* **2011**, *225*, 285–292. [[CrossRef](#)]
29. Hayashi, D.; Kawakami, K.; Ito, K.; Ishii, K.; Tanno, H.; Imai, Y.; Kanno, E.; Maruyama, R.; Shimokawa, H.; Tachi, M. Low-energy extracorporeal shock wave therapy enhances skin wound healing in diabetic mice: A critical role of endothelial nitric oxide synthase. *Wound Repair Regen.* **2012**, *20*, 887–895. [[CrossRef](#)] [[PubMed](#)]
30. Zins, S.R.; Amare, M.F.; Tadaki, D.K.; Elster, E.A.; Davis, T.A. Comparative analysis of angiogenic gene expression in normal and impaired wound healing in diabetic mice: Effects of extracorporeal shock wave therapy. *Angiogenesis* **2010**, *13*, 293–304. [[CrossRef](#)]
31. Smith, J.; Romansky, N.; Vomero, J.; Davis, R.H. The effect of electrical stimulation on wound healing in diabetic mice. *J. Am. Podiatry Assoc.* **1984**, *74*, 71–75. [[CrossRef](#)] [[PubMed](#)]
32. Thawer, H.A.; Houghton, P.E. Effects of electrical stimulation on the histological properties of wounds in diabetic mice. *Wound Repair Regen.* **2001**, *9*, 107–115. [[CrossRef](#)] [[PubMed](#)]
33. Kim, T.H.; Cho, H.Y.; Lee, S.M. High-voltage pulsed current stimulation enhances wound healing in diabetic rats by restoring the expression of collagen, alpha-smooth muscle actin, and TGF-beta1. *Tohoku J. Exp. Med.* **2014**, *234*, 1–6. [[CrossRef](#)]
34. Langoni Cassettari, L.; Colli Rocha Dias, P.; Natalia Lucchesi, A.; Ferraz de Arruda, M.; Veruska Paiva Ortolan, E.; Marques, M.E.; Spadella, C.T. Continuous electrical current and zinc sulphate administered by transdermal iontophoresis improves skin healing in diabetic rats induced by alloxan: Morphological and ultrastructural analysis. *J. Diabetes Res.* **2014**, *2014*, 980232. [[CrossRef](#)] [[PubMed](#)]
35. Yu, W.; Naim, J.O.; Lanzafame, R.J. Effects of photostimulation on wound healing in diabetic mice. *Lasers Surg. Med.* **1997**, *20*, 56–63. [[CrossRef](#)]
36. Danno, K.; Mori, N.; Toda, K.; Kobayashi, T.; Utani, A. Near-infrared irradiation stimulates cutaneous wound repair: Laboratory experiments on possible mechanisms. *Photodermatol. Photoimmunol. Photomed.* **2001**, *17*, 261–265. [[CrossRef](#)]
37. Reddy, G.K.; Stehno-Bittel, L.; Enwemeka, C.S. Laser photostimulation accelerates wound healing in diabetic rats. *Wound Repair Regen.* **2001**, *9*, 248–255. [[CrossRef](#)] [[PubMed](#)]
38. Stadler, I.; Lanzafame, R.J.; Evans, R.; Narayan, V.; Dailey, B.; Buehner, N.; Naim, J.O. 830-nm irradiation increases the wound tensile strength in a diabetic murine model. *Lasers Surg. Med.* **2001**, *28*, 220–226. [[CrossRef](#)] [[PubMed](#)]
39. Al-Watban, F.A.; Andres, B.L. Polychromatic LED therapy in burn healing of non-diabetic and diabetic rats. *J. Clin. Laser Med. Surg.* **2003**, *21*, 249–258. [[CrossRef](#)]
40. Reddy, G.K. Comparison of the photostimulatory effects of visible He-Ne and infrared Ga-As lasers on healing impaired diabetic rat wounds. *Lasers Surg. Med.* **2003**, *33*, 344–351. [[CrossRef](#)] [[PubMed](#)]
41. Whelan, H.T.; Buchmann, E.V.; Dhokalia, A.; Kane, M.P.; Whelan, N.T.; Wong-Riley, M.T.; Eells, J.T.; Gould, L.J.; Hammamieh, R.; Das, R.; et al. Effect of NASA light-emitting diode irradiation on molecular changes for wound healing in diabetic mice. *J. Clin. Laser Med. Surg.* **2003**, *21*, 67–74. [[CrossRef](#)] [[PubMed](#)]
42. Byrnes, K.R.; Barna, L.; Chenault, V.M.; Waynant, R.W.; Ilev, I.K.; Longo, L.; Miracco, C.; Johnson, B.; Anders, J.J. Photobiomodulation improves cutaneous wound healing in an animal model of type II diabetes. *Photomed. Laser Surg.* **2004**, *22*, 281–290. [[CrossRef](#)]
43. Kawalec, J.S.; Hetherington, V.J.; Pfennigwerth, T.C.; Dockery, D.S.; Dolce, M. Effect of a diode laser on wound healing by using diabetic and nondiabetic mice. *J. Foot Ankle Surg.* **2004**, *43*, 214–220. [[CrossRef](#)]

44. Maiya, G.A.; Kumar, P.; Rao, L. Effect of low intensity helium-neon (He-Ne) laser irradiation on diabetic wound healing dynamics. *Photomed. Laser Surg.* **2005**, *23*, 187–190. [[CrossRef](#)] [[PubMed](#)]
45. Vinck, E.M.; Cagnie, B.J.; Cornelissen, M.J.; Declercq, H.A.; Cambier, D.C. Green light emitting diode irradiation enhances fibroblast growth impaired by high glucose level. *Photomed. Laser Surg.* **2005**, *23*, 167–171. [[CrossRef](#)]
46. Al-Watban, F.A.; Andres, B.L. Polychromatic LED in oval full-thickness wound healing in non-diabetic and diabetic rats. *Photomed. Laser Surg.* **2006**, *24*, 10–16. [[CrossRef](#)]
47. Carvalho, P.T.; Mazzer, N.; dos Reis, F.A.; Belchior, A.C.; Silva, I.S. Analysis of the influence of low-power HeNe laser on the healing of skin wounds in diabetic and non-diabetic rats. *Acta Cir. Bras.* **2006**, *21*, 177–183. [[CrossRef](#)] [[PubMed](#)]
48. Rabelo, S.B.; Villaverde, A.B.; Nicolau, R.; Salgado, M.C.; Melo Mda, S.; Pacheco, M.T. Comparison between wound healing in induced diabetic and nondiabetic rats after low-level laser therapy. *Photomed. Laser Surg.* **2006**, *24*, 474–479. [[CrossRef](#)] [[PubMed](#)]
49. Al-Watban, F.A.; Zhang, X.Y.; Andres, B.L. Low-level laser therapy enhances wound healing in diabetic rats: A comparison of different lasers. *Photomed. Laser Surg.* **2007**, *25*, 72–77. [[CrossRef](#)]
50. Houreld, N.; Abrahamse, H. Irradiation with a 632.8 nm helium-neon laser with 5 J/cm² stimulates proliferation and expression of interleukin-6 in diabetic wounded fibroblast cells. *Diabetes Technol. Ther.* **2007**, *9*, 451–459. [[CrossRef](#)]
51. Houreld, N.; Abrahamse, H. In vitro exposure of wounded diabetic fibroblast cells to a helium-neon laser at 5 and 16 J/cm². *Photomed. Laser Surg.* **2007**, *25*, 78–84. [[CrossRef](#)]
52. Houreld, N.N.; Abrahamse, H. Effectiveness of helium-neon laser irradiation on viability and cytotoxicity of diabetic-wounded fibroblast cells. *Photomed. Laser Surg.* **2007**, *25*, 474–481. [[CrossRef](#)]
53. Mirzaei, M.; Bayat, M.; Mosafa, N.; Mohsenifar, Z.; Piryaei, A.; Farokhi, B.; Rezaei, F.; Sadeghi, Y.; Rakhshan, M. Effect of low-level laser therapy on skin fibroblasts of streptozotocin-diabetic rats. *Photomed. Laser Surg.* **2007**, *25*, 519–525. [[CrossRef](#)] [[PubMed](#)]
54. Houreld, N.N.; Abrahamse, H. Laser light influences cellular viability and proliferation in diabetic-wounded fibroblast cells in a dose- and wavelength-dependent manner. *Lasers Med. Sci.* **2008**, *23*, 11–18. [[CrossRef](#)] [[PubMed](#)]
55. Meireles, G.C.; Santos, J.N.; Chagas, P.O.; Moura, A.P.; Pinheiro, A.L. Effectiveness of laser photobiomodulation at 660 or 780 nanometers on the repair of third-degree burns in diabetic rats. *Photomed. Laser Surg.* **2008**, *26*, 47–54. [[CrossRef](#)]
56. Al-Watban, F.A. Laser therapy converts diabetic wound healing to normal healing. *Photomed. Laser Surg.* **2009**, *27*, 127–135. [[CrossRef](#)]
57. Al-Watban, F.A.; Zhang, X.Y.; Andres, B.L.; Al-Anize, A. Visible lasers were better than invisible lasers in accelerating burn healing on diabetic rats. *Photomed. Laser Surg.* **2009**, *27*, 269–272. [[CrossRef](#)] [[PubMed](#)]
58. Dall Agnol, M.A.; Nicolau, R.A.; de Lima, C.J.; Munin, E. Comparative analysis of coherent light action (laser) versus non-coherent light (light-emitting diode) for tissue repair in diabetic rats. *Lasers Med. Sci.* **2009**, *24*, 909–916. [[CrossRef](#)]
59. Gungormus, M.; Akyol, U.K. Effect of biostimulation on wound healing in diabetic rats. *Photomed. Laser Surg.* **2009**, *27*, 607–610. [[CrossRef](#)]
60. Akyol, U.; Gungormus, M. The effect of low-level laser therapy on healing of skin incisions made using a diode laser in diabetic rats. *Photomed. Laser Surg.* **2010**, *28*, 51–55. [[CrossRef](#)]
61. Carvalho Pde, T.; Silva, I.S.; Reis, F.A.; Perreira, D.M.; Aydos, R.D. Influence of ingaalp laser (660 nm) on the healing of skin wounds in diabetic rats. *Acta Cir. Bras.* **2010**, *25*, 71–79. [[CrossRef](#)]
62. Chung, T.Y.; Peplow, P.V.; Baxter, G.D. Laser photobiostimulation of wound healing: Defining a dose response for splinted wounds in diabetic mice. *Lasers Surg. Med.* **2010**, *42*, 656–664. [[CrossRef](#)]
63. Chung, T.Y.; Peplow, P.V.; Baxter, G.D. Laser photobiomodulation of wound healing in diabetic and non-diabetic mice: Effects in splinted and unsplinted wounds. *Photomed. Laser Surg.* **2010**, *28*, 251–261. [[CrossRef](#)]
64. Houreld, N.; Abrahamse, H. Low-intensity laser irradiation stimulates wound healing in diabetic wounded fibroblast cells (WS1). *Diabetes Technol. Ther.* **2010**, *12*, 971–978. [[CrossRef](#)] [[PubMed](#)]

65. Houreld, N.N.; Sekhejane, P.R.; Abrahamse, H. Irradiation at 830 nm stimulates nitric oxide production and inhibits pro-inflammatory cytokines in diabetic wounded fibroblast cells. *Lasers Surg. Med.* **2010**, *42*, 494–502. [[CrossRef](#)] [[PubMed](#)]
66. Jahangiri Noudeh, Y.; Shabani, M.; Vatankhah, N.; Hashemian, S.J.; Akbari, K. A combination of 670 nm and 810 nm diode lasers for wound healing acceleration in diabetic rats. *Photomed. Laser Surg.* **2010**, *28*, 621–627. [[CrossRef](#)]
67. Oliveira, P.C.; Pinheiro, A.L.; Reis Junior, J.A.; de Castro, I.C.; Gurgel, C.; Noia, M.P.; Meireles, G.C.; Cangussu, M.C.; Ramalho, L.M. Polarized light (lambda400-2000 nm) on third-degree burns in diabetic rats: Immunohistochemical study. *Photomed. Laser Surg.* **2010**, *28*, 613–619. [[CrossRef](#)]
68. Santos, N.R.; dos Santos, J.N.; dos Reis, J.A., Jr.; Oliveira, P.C.; de Sousa, A.P.; de Carvalho, C.M.; Soares, L.G.; Marques, A.M.; Pinheiro, A.L. Influence of the use of laser phototherapy (lambda660 or 790 nm) on the survival of cutaneous flaps on diabetic rats. *Photomed. Laser Surg.* **2010**, *28*, 483–488. [[CrossRef](#)]
69. Hegde, V.N.; Prabhu, V.; Rao, S.B.; Chandra, S.; Kumar, P.; Satyamoorthy, K.; Mahato, K.K. Effect of laser dose and treatment schedule on excision wound healing in diabetic mice. *Photochem. Photobiol.* **2011**, *87*, 1433–1441. [[CrossRef](#)] [[PubMed](#)]
70. Oliveira, P.C.; Pinheiro, A.L.; de Castro, I.C.; Reis, J.A., Jr.; Noia, M.P.; Gurgel, C.; Teixeira Cangussu, M.C.; Pedreira Ramalho, L.M. Evaluation of the effects of polarized light (lambda400-200 nm) on the healing of third-degree burns in induced diabetic and nondiabetic rats. *Photomed. Laser Surg.* **2011**, *29*, 619–625. [[CrossRef](#)] [[PubMed](#)]
71. Peplow, P.V.; Chung, T.Y.; Ryan, B.; Baxter, G.D. Laser photobiostimulation of wound healing: Reciprocity of irradiance and exposure time on energy density for splinted wounds in diabetic mice. *Lasers Surg. Med.* **2011**, *43*, 843–850. [[CrossRef](#)]
72. Sekhejane, P.R.; Houreld, N.N.; Abrahamse, H. Irradiation at 636 nm positively affects diabetic wounded and hypoxic cells in vitro. *Photomed. Laser Surg.* **2011**, *29*, 521–530. [[CrossRef](#)] [[PubMed](#)]
73. Ayuk, S.M.; Houreld, N.N.; Abrahamse, H. Collagen production in diabetic wounded fibroblasts in response to low-intensity laser irradiation at 660 nm. *Diabetes Technol. Ther.* **2012**, *14*, 1110–1117. [[CrossRef](#)] [[PubMed](#)]
74. Dadpay, M.; Sharifian, Z.; Bayat, M.; Bayat, M.; Dabbagh, A. Effects of pulsed infra-red low level-laser irradiation on open skin wound healing of healthy and streptozotocin-induced diabetic rats by biomechanical evaluation. *J. Photochem. Photobiol. Bbiol.* **2012**, *111*, 1–8. [[CrossRef](#)]
75. Houreld, N.N.; Masha, R.T.; Abrahamse, H. Low-intensity laser irradiation at 660 nm stimulates cytochrome c oxidase in stressed fibroblast cells. *Lasers Surg. Med.* **2012**, *44*, 429–434. [[CrossRef](#)] [[PubMed](#)]
76. Peplow, P.V.; Chung, T.Y.; Baxter, G.D. Laser photostimulation (660 nm) of wound healing in diabetic mice is not brought about by ameliorating diabetes. *Lasers Surg. Med.* **2012**, *44*, 26–29. [[CrossRef](#)] [[PubMed](#)]
77. Aparecida Da Silva, A.; Leal-Junior, E.C.; Alves, A.C.; Rambo, C.S.; Dos Santos, S.A.; Vieira, R.P.; De Carvalho Pde, T. Wound-healing effects of low-level laser therapy in diabetic rats involve the modulation of MMP-2 and MMP-9 and the redistribution of collagen types I and III. *J. Cosmet. Laser Ther.* **2013**, *15*, 210–216. [[CrossRef](#)] [[PubMed](#)]
78. Fathabadie, F.F.; Bayat, M.; Amini, A.; Bayat, M.; Rezaie, F. Effects of pulsed infra-red low level-laser irradiation on mast cells number and degranulation in open skin wound healing of healthy and streptozotocin-induced diabetic rats. *J. Cosmet. Laser* **2013**, *15*, 294–304. [[CrossRef](#)]
79. He, Y.; Yip, S.L.; Cheung, K.K.; Huang, L.; Wang, S.; Cheing, G.L. The effect of monochromatic infrared energy on diabetic wound healing. *Int. Wound J.* **2013**, *10*, 645–652. [[CrossRef](#)] [[PubMed](#)]
80. Dancakova, L.; Vasilenko, T.; Kovac, I.; Jakubcova, K.; Holly, M.; Revajova, V.; Sabol, F.; Tomori, Z.; Iversen, M.; Gal, P.; et al. Low-level laser therapy with 810 nm wavelength improves skin wound healing in rats with streptozotocin-induced diabetes. *Photomed. Laser Surg.* **2014**, *32*, 198–204. [[CrossRef](#)]
81. Esmaelinejad, M.; Bayat, M.; Darbandi, H.; Bayat, M.; Mosaffa, N. The effects of low-level laser irradiation on cellular viability and proliferation of human skin fibroblasts cultured in high glucose mediums. *Lasers Med. Sci.* **2014**, *29*, 121–129. [[CrossRef](#)]
82. Kilik, R.; Lakyova, L.; Sabo, J.; Kruzliak, P. Effect of equal daily doses achieved by different power densities of low-level laser therapy at 635 nm on open skin wound healing in normal and diabetic rats. *Biomed. Res. Int.* **2014**, *2014*, 269253. [[CrossRef](#)]

83. Sharifian, Z.; Bayat, M.; Alidoust, M.; Farahani, R.M.; Bayat, M.; Rezaie, F.; Bayat, H. Histological and gene expression analysis of the effects of pulsed low-level laser therapy on wound healing of streptozotocin-induced diabetic rats. *Lasers Med. Sci.* **2014**, *29*, 1227–1235. [[CrossRef](#)] [[PubMed](#)]
84. de Loura Santana, C.; Silva Dde, F.; Deana, A.M.; Prates, R.A.; Souza, A.P.; Gomes, M.T.; de Azevedo Sampaio, B.P.; Shibuya, J.F.; Bussadori, S.K.; Mesquita-Ferrari, R.A.; et al. Tissue responses to postoperative laser therapy in diabetic rats submitted to excisional wounds. *PLoS ONE* **2015**, *10*, e0122042. [[CrossRef](#)] [[PubMed](#)]
85. Lau, P.; Bidin, N.; Krishnan, G.; AnaybBaleg, S.M.; Sum, M.B.; Bakhtiar, H.; Nassir, Z.; Hamid, A. Photobiostimulation effect on diabetic wound at different power density of near infrared laser. *J. Photochem. Photobiology. B Biol.* **2015**, *151*, 201–207. [[CrossRef](#)]
86. Firat, E.T.; Dag, A.; Gunay, A.; Kaya, B.; Karadede, M.I.; Kanay, B.E.; Ketani, A.; Evliyaoglu, O.; Uysal, E. The effects of low-level laser therapy on palatal mucoperiosteal wound healing and oxidative stress status in experimental diabetic rats. *Photomed. Laser Surg.* **2013**, *31*, 315–321. [[CrossRef](#)] [[PubMed](#)]
87. Franca, C.M.; de Loura Santana, C.; Takahashi, C.B.; Alves, A.N.; De Souza Mernick, A.P.; Fernandes, K.P.; de Fatima Teixeira da Silva, D.; Bussadori, S.K.; Mesquita-Ferrari, R.A. Effect of laser therapy on skeletal muscle repair process in diabetic rats. *Lasers Med Sci.* **2013**, *28*, 1331–1338. [[CrossRef](#)]
88. Masha, R.T.; Houreld, N.N.; Abrahamse, H. Low-intensity laser irradiation at 660 nm stimulates transcription of genes involved in the electron transport chain. *Photomed. Laser Surg.* **2013**, *31*, 47–53. [[CrossRef](#)] [[PubMed](#)]
89. Park, J.J.; Kang, K.L. Effect of 980-nm GaAlAs diode laser irradiation on healing of extraction sockets in streptozotocin-induced diabetic rats: A pilot study. *Lasers Med. Sci.* **2012**, *27*, 223–230. [[CrossRef](#)] [[PubMed](#)]
90. Lau, P.S.; Bidin, N.; Krishnan, G.; Nassir, Z.; Bahktiar, H. Biophotonic effect of diode laser irradiance on tensile strength of diabetic rats. *J. Cosmet. Laser Ther.* **2015**, *17*, 86–89. [[CrossRef](#)]
91. Wu, X.; Alberico, S.; Saidu, E.; Rahman Khan, S.; Zheng, S.; Romero, R.; Sik Chae, H.; Li, S.; Mochizuki, A.; Anders, J. Organic light emitting diode improves diabetic cutaneous wound healing in rats. *Wound Repair Regen.* **2015**, *23*, 104–114. [[CrossRef](#)]
92. Fekrazad, R.; Mirmoezzi, A.; Kalhori, K.A.M.; Arany, P. The effect of red, green and blue lasers on healing of oral wounds in diabetic rats. *J. Photochem. Photobiol. B Biol.* **2015**, *148*, 242–245. [[CrossRef](#)]
93. Ayuk, S.M.; Abrahamse, H.; Houreld, N.N. The role of photobiomodulation on gene expression of cell adhesion molecules in diabetic wounded fibroblasts in vitro. *J. Photochem. Photobiol. B Biol.* **2016**, *161*, 368–374. [[CrossRef](#)] [[PubMed](#)]
94. Ayuk, S.M.; Houreld, N.N.; Abrahamse, H. Effect of 660 nm visible red light on cell proliferation and viability in diabetic models in vitro under stressed conditions. *Lasers Med. Sci.* **2018**, *33*, 1085–1093. [[CrossRef](#)] [[PubMed](#)]
95. de Loura Santana, C.; de Fatima Teixeira Silva, D.; de Souza, A.P.; Jacinto, M.V.; Bussadori, S.K.; Mesquita-Ferrari, R.A.; Fernandes, K.P.; Franca, C.M. Effect of laser therapy on immune cells infiltrate after excisional wounds in diabetic rats. *Lasers Surg. Med.* **2016**, *48*, 45–51. [[CrossRef](#)]
96. Denadai, A.S.; Aydos, R.D.; Silva, I.S.; Olmedo, L.; de Senna Cardoso, B.M.; da Silva, B.A.K.; de Carvalho, P.T.C. Acute effects of low-level laser therapy (660 nm) on oxidative stress levels in diabetic rats with skin wounds. *J. Exp. Ther. Oncol.* **2017**, *11*, 85–89. [[PubMed](#)]
97. Eissa, M.; Salih, W.H.M. The influence of low-intensity He-Ne laser on the wound healing in diabetic rats. *Lasers Med. Sci.* **2017**, *32*, 1261–1267. [[CrossRef](#)] [[PubMed](#)]
98. Goralczyk, K.; Szymanska, J.; Szot, K.; Fisz, J.; Rosc, D. Low-level laser irradiation effect on endothelial cells under conditions of hyperglycemia. *Lasers Med. Sci.* **2016**, *31*, 825–831. [[CrossRef](#)] [[PubMed](#)]
99. Ranjbar, R.; Takhtfooladi, M.A. The effects of photobiomodulation therapy on Staphylococcus aureus infected surgical wounds in diabetic rats. A microbiological, histopathological, and biomechanical study. *Acta Cir. Bras.* **2016**, *31*, 498–504. [[CrossRef](#)]
100. Tatmatsu-Rocha, J.C.; Ferraresi, C.; Hamblin, M.R.; Damasceno Maia, F.; do Nascimento, N.R.; Driusso, P.; Parizotto, N.A. Low-level laser therapy (904 nm) can increase collagen and reduce oxidative and nitrosative stress in diabetic wounded mouse skin. *J. Photochem. Photobiol. B Biol.* **2016**, *164*, 96–102. [[CrossRef](#)]
101. Huang, Y.-J.; Wu, H.-C.; Tai, N.-H.; Wang, T.-W. Carbon Nanotube Rope with Electrical Stimulation Promotes the Differentiation and Maturity of Neural Stem Cells. *Small* **2012**, *8*, 2869–2877. [[CrossRef](#)]

102. Langelaan, M.L.P.; Boonen, K.J.M.; Rosaria-Chak, K.Y.; van der Schaft, D.W.J.; Post, M.J.; Baaijens, F.P.T. Advanced maturation by electrical stimulation: Differences in response between C2C12 and primary muscle progenitor cells. *J. Tissue Eng. Regen. Med.* **2011**, *5*, 529–539. [[CrossRef](#)]
103. Omar, M.T.; Alghadir, A.; Al-Wahhabi, K.K.; Al-Askar, A.B. Efficacy of shock wave therapy on chronic diabetic foot ulcer: A single-blinded randomized controlled clinical trial. *Diabetes Res. Clin. Pract.* **2014**, *106*, 548–554. [[CrossRef](#)]
104. Isakov, E.; Ring, H.; Mendelevich, I.; Boduragin, N.; Susak, Z.; Kupfert, Y.; Marchetti, N. Electromagnetic stimulation of stump wounds in diabetic amputees. *J. Rehabil. Sci.* **1996**, *9*, 46–48.
105. Peplow, P.V.; Chung, T.Y.; Baxter, G.D. Laser photobiomodulation of wound healing: A review of experimental studies in mouse and rat animal models. *Photomed. Laser Surg.* **2010**, *28*, 291–325. [[CrossRef](#)] [[PubMed](#)]
106. Ud-Din, S.; Bayat, A. Non-animal models of wound healing in cutaneous repair: In silico, in vitro, ex vivo, and in vivo models of wounds and scars in human skin. *Wound Repair Regen.* **2017**, *25*, 164–176. [[CrossRef](#)]
107. Wang, P.H.; Huang, B.S.; Horng, H.C.; Yeh, C.C.; Chen, Y.J. Wound healing. *J. Chin. Med. Assoc.* **2018**, *81*, 94–101. [[CrossRef](#)] [[PubMed](#)]
108. Zhao, G.; Hochwalt, P.C.; Usui, M.L.; Underwood, R.A.; Singh, P.K.; James, G.A.; Stewart, P.S.; Fleckman, P.; Olerud, J.E. Delayed wound healing in diabetic (db/db) mice with *Pseudomonas aeruginosa* biofilm challenge: A model for the study of chronic wounds. *Wound Repair Regen.* **2010**, *18*, 467–477. [[CrossRef](#)] [[PubMed](#)]
109. Zhao, G.; Usui, M.L.; Underwood, R.A.; Singh, P.K.; James, G.A.; Stewart, P.S.; Fleckman, P.; Olerud, J.E. Time course study of delayed wound healing in a biofilm-challenged diabetic mouse model. *Wound Repair Regen.* **2012**, *20*, 342–352. [[CrossRef](#)] [[PubMed](#)]
110. Kilkenny, C.; Parsons, N.; Kadyszewski, E.; Festing, M.F.; Cuthill, I.C.; Fry, D.; Hutton, J.; Altman, D.G. Survey of the quality of experimental design, statistical analysis and reporting of research using animals. *PLoS ONE* **2009**, *4*, e7824. [[CrossRef](#)]



© 2019 by the authors. Licensee MDPI, Basel, Switzerland. This article is an open access article distributed under the terms and conditions of the Creative Commons Attribution (CC BY) license (<http://creativecommons.org/licenses/by/4.0/>).

APPENDIX V

EFFECTS OF PULSED ELECTROMAGNETIC FIELD ON OXYHEMOGLOBIN CONCENTRATION DURING DIABETIC WOUND HEALING

Rachel Lai-Chu Kwan, MPhil; Gladys Lai-Ying Cheing, PhD

Department of Rehabilitation Sciences, The Hong Kong Polytechnic University

In the inflammatory phase of wound healing, the growth of blood vessels results in an increased level of oxyhemoglobin in normal wound. During the late proliferation phase, oxyhemoglobin concentration would drop when angiogenesis stops. However, oxyhemoglobin concentrations in diabetic wound do not decrease like that in the healing of normal wound. The present study examined the effects of pulsed electromagnetic field (PEMF) on restoring oxyhemoglobin concentrations and promoting healing of diabetic wound. Streptozotocin-induced diabetic Sprague-Dawley rat model was adopted. A 6 mm full-thickness circular shaped dermal wound was excised at the posterior aspect of rats' hindlimbs. Diabetic rats were randomly allocated to receive either PEMF or sham PEMF. Twelve rats received PEMF (25 Hz, 2 mT, 60 min daily), 14 rats received the same handling as the PEMF group but exposed to sham PEMF. Assessments on wound size and oxyhemoglobin concentration in the wound bed were conducted on day 3, 5, 7, 10, 14 or 21 post-wounding. Wound size of the PEMF group decreased at a faster rate than that of the sham PEMF group. On day 5, the oxyhemoglobin in the central wound area of the sham PEMF group were significantly higher than that in PEMF group ($P=0.015$). On Day 10, significant higher oxygen saturation at wound edges was found in PEMF group than that of the sham PEMF group ($P=0.037$). PEMF appears to be an effective modality in promoting healing of skin wounds in streptozotocin-induced diabetic rats by restoring oxyhemoglobin concentration.

Word Count: 243

Acknowledgements: This project was supported by the General Research Fund provided by the Research Grants Council of the Hong Kong SAR Government (PolyU151003/14M), China.

REFERENCES

- Centers for Disease Control and Prevention, 2018. *Pseudomonas aeruginosa in Healthcare Settings* [Online]. US: Centers for Disease Control and Prevention. Available: <https://www.cdc.gov/hai/organisms/pseudomonas.html> [Accessed 23 Jan 2019].
- AKBARI, C. M., SAOUAF, R., BARNHILL, D. F., NEWMAN, P. A., LOGERFO, F. W. & VEVES, A. 1998. Endothelium-dependent vasodilatation is impaired in both microcirculation and macrocirculation during acute hyperglycemia. *J Vasc Surg*, 28, 687-94.
- ALAVI, A., SIBBALD, R. G., MAYER, D., GOODMAN, L., BOTROS, M., ARMSTRONG, D. G., WOO, K., BOENI, T., AYELLO, E. A. & KIRSNER, R. S. 2014. Diabetic foot ulcers: Part I. Pathophysiology and prevention. *J Am Acad Dermatol*, 70, 1 e1-18; quiz 19-20.
- ARMSTRONG, D. G., BOULTON, A. J. M. & BUS, S. A. 2017. Diabetic Foot Ulcers and Their Recurrence. *N Engl J Med*, 376, 2367-2375.
- ATHANASIOU, A., KARKAMBOUNAS, S., BATISTATOU, A., LYKOUKDIS, E., KATSARAKI, A., KARTSIOUNI, T., PAPALOUS, A. & EVANGELOU, A. 2007. The effect of pulsed electromagnetic fields on secondary skin wound healing: an experimental study. *Bioelectromagnetics*, 28, 362-8.
- BAO, P., KODRA, A., TOMIC-CANIC, M., GOLINKO, M. S., EHRLICH, H. P. & BREM, H. 2009. The role of vascular endothelial growth factor in wound healing. *J Surg Res*, 153, 347-58.
- BEDIOUI, F., QUINTON, D., GRIVEAU, S. & NYOKONG, T. 2010. Designing molecular materials and strategies for the electrochemical detection of nitric oxide, superoxide and peroxynitrite in biological systems. *Phys Chem Chem Phys*, 12, 9976-88.
- BRUCKDORFER, R. 2005. The basics about nitric oxide. *Mol Aspects Med*, 26, 3-31.
- CALLAGHAN, M. J., CHANG, E. I., SEISER, N., AARABI, S., GHALI, S., KINNUCAN, E. R., SIMON, B. J. & GURTNER, G. C. 2008. Pulsed electromagnetic fields accelerate normal and diabetic wound healing by increasing endogenous FGF-2 release. *Plast Reconstr Surg*, 121, 130-41.
- CHAO, C. Y. & CHEING, G. L. 2009. Microvascular dysfunction in diabetic foot disease and ulceration. *Diabetes Metab Res Rev*, 25, 604-14.
- CHAO, C. Y., ZHENG, Y. P. & CHEING, G. L. 2011. Epidermal thickness and biomechanical properties of plantar tissues in diabetic foot. *Ultrasound Med Biol*, 37, 1029-38.
- CHAO, C. Y., ZHENG, Y. P. & CHEING, G. L. 2012. The association between skin blood flow and edema on epidermal thickness in the diabetic foot. *Diabetes Technol Ther*, 14, 602-9.
- CHEING, G. L., SUN, J., KWAN, R. L. & ZHENG, Y. 2013. The potential influence of diabetic history on peripheral blood flow in superficial skin. *Microvasc Res*, 90, 112-6.
- CHEING, G. L. Y., LI, X., HUANG, L., KWAN, R. L. C. & CHEUNG, K. K. 2014. Pulsed electromagnetic fields (PEMF) promote early wound healing and myofibroblast proliferation in diabetic rats. *Bioelectromagnetics*, 35, 161-9.
- CHIEN, W. Y., YANG, K. D., ENG, H. L., HU, Y. H., LEE, P. Y., WANG, S. T. & WANG, P. W. 2005. Increased plasma concentration of nitric oxide in type 2 diabetes but not in nondiabetic individuals with insulin resistance. *Diabetes Metab*, 31, 63-8.
- CHOI, H. M. C. 2016. *Biomechanical assessment and electromagnetic intervention for diabetic ulcers*. PhD, The Hong Kong Polytechnic University.
- CHOI, H. M. C., CHEING, A. K. K., NG, G. Y. F. & CHEING, G. L. Y. 2018. Effects of pulsed electromagnetic field (PEMF) on the tensile biomechanical properties of diabetic wounds at different phases of healing. *PloS one*, 13, e0191074-e0191074.

- CHOI, M. C., CHEUNG, K. K., LI, X. & CHEING, G. L. Y. 2016. Pulsed electromagnetic field (PEMF) promotes collagen fibre deposition associated with increased myofibroblast population in the early healing phase of diabetic wound. *Arch Dermatol Res*, 308, 21-9.
- COSBY, K., PARTOVI, K. S., CRAWFORD, J. H., PATEL, R. P., REITER, C. D., MARTYR, S., YANG, B. K., WACLAWIW, M. A., ZALOS, G., XU, X., HUANG, K. T., SHIELDS, H., KIM-SHAPIRO, D. B., SCHECHTER, A. N., CANNON, R. O. & GLADWIN, M. T. 2003. Nitrite reduction to nitric oxide by deoxyhemoglobin vasodilates the human circulation. *Nat Med*, 9, 1498-1505.
- DAVIDSON, J. K. 2000. Anesthesia for the diabetic patient. *Clinical Diabetes Mellitus: A Problem-oriented Approach*. 3rd ed. New York: Thieme.
- DELBRIDGE, L., CTERCTEKO, G., FOWLER, C., REEVE, T. S. & LE QUESNE, L. P. 1985. The aetiology of diabetic neuropathic ulceration of the foot. *Br J Surg*, 72, 1-6.
- DOWD, S. E., WOLCOTT, R. D., SUN, Y., MCKEEHAN, T., SMITH, E. & RHOADS, D. 2008. Polymicrobial nature of chronic diabetic foot ulcer biofilm infections determined using bacterial tag encoded FLX amplicon pyrosequencing (bTEFAP). *PLoS One*, 3, e3326.
- FAZLI, M., BJARNSHOLT, T., KIRKETERP-MØLLER, K., JØRGENSEN, B., ANDERSEN, A. S., KROGFELT, K. A., GIVSKOV, M. & TOLKER-NIELSEN, T. 2009. Nonrandom Distribution of *Pseudomonas aeruginosa* and *Staphylococcus aureus* in Chronic Wounds. *Journal of Clinical Microbiology*, 47, 4084-4089.
- FIJALKOWSKI, K., NAWROTEK, P., STRUK, M., KORDAS, M. & RAKOCZY, R. 2015. Effects of rotating magnetic field exposure on the functional parameters of different species of bacteria. *Electromagn Biol Med*, 34, 48-55.
- GIBBONS, G. W. 2003. Lower extremity bypass in patients with diabetic foot ulcers. *Surg Clin North Am*, 83, 659-69.
- GJODSBOL, K., CHRISTENSEN, J. J., KARLSMARK, T., JORGENSEN, B., KLEIN, B. M. & KROGFELT, K. A. 2006. Multiple bacterial species reside in chronic wounds: a longitudinal study. *Int Wound J*, 3, 225-31.
- GOUDARZI, I., HAJIZADEH, S., SALMANI, M. E. & ABRARI, K. 2010. Pulsed electromagnetic fields accelerate wound healing in the skin of diabetic rats. *Bioelectromagnetics*, 31, 318-23.
- GREENMAN, R. L., PANASYUK, S., WANG, X., LYONS, T. E., DINH, T., LONGORIA, L., GIURINI, J. M., FREEMAN, J., KHAODHIAR, L. & VEVES, A. 2005. Early changes in the skin microcirculation and muscle metabolism of the diabetic foot. *Lancet*, 366, 1711-7.
- GUARIGUATA, L., WHITING, D. R., HAMBLETON, I., BEAGLEY, J., LINNENKAMP, U. & SHAW, J. E. 2014. Global estimates of diabetes prevalence for 2013 and projections for 2035. *Diabetes Res Clin Pract*, 103, 137-49.
- GUEST, J. F., VOWDEN, K. & VOWDEN, P. 2017. The health economic burden that acute and chronic wounds impose on an average clinical commissioning group/health board in the UK. *J Wound Care*, 26, 292-303.
- HEDEN, P. & PILLA, A. A. 2008. Effects of pulsed electromagnetic fields on postoperative pain: a double-blind randomized pilot study in breast augmentation patients. *Aesthetic Plast Surg*, 32, 660-6.
- HSIEH, S. T. & LIN, W. M. 1999. Modulation of keratinocyte proliferation by skin innervation. *J Invest Dermatol*, 113, 579-86.

- HURLEY, J. J. 2008. Noninvasive vascular testing in the evaluation of diabetic peripheral arterial disease. *In: BOWKER, J. H. & PFEIFER, M. A. (eds.) Levin and O'Neals's The Diabetic Foot*. 7th ed. Philadelphia: Mosby.
- INHAN-GARIP, A., AKSU, B., AKAN, Z., AKAKIN, D., OZAYDIN, A. N. & SAN, T. 2011. Effect of extremely low frequency electromagnetic fields on growth rate and morphology of bacteria. *International Journal of Radiation Biology*, 87, 1155-1161.
- INSTRON 2009. Bluehill 3 test method development training manual M18-16253-EN Revision A. US: Illinois Tool Works Inc.
- JAMES, P. E., LANG, D., TUFNELL-BARRET, T., MILSOM, A. B. & FRENNEAUX, M. P. 2004. Vasorelaxation by red blood cells and impairment in diabetes: reduced nitric oxide and oxygen delivery by glycated hemoglobin. *Circ Res*, 94, 976-83.
- KAISER, A. B., ZHANG, N. & DER PLUIJM, W. V. 2018. Global prevalence of type 2 diabetes over the next ten years (2018-2028). *Diabetes*, 67, 202-LB.
- KHAN, S. I., BLUMROSEN, G., VECCHIO, D., GOLBERG, A., MCCORMACK, M. C., YARMUSH, M. L., HAMBLIN, M. R. & AUSTEN, W. G., JR. 2016. Eradication of multidrug-resistant pseudomonas biofilm with pulsed electric fields. *Biotechnology and bioengineering*, 113, 643-650.
- KIERNAN, J. A. 2002. Collagen type I staining. *Biotech Histochem*, 77, 231.
- KLEIN, R. 1995. Hyperglycemia and microvascular and macrovascular disease in diabetes. *Diabetes Care*, 18, 258-68.
- KWAN, R. L., CHEING, G. L., VONG, S. K. & LO, S. K. 2013. Electrophysical therapy for managing diabetic foot ulcers: a systematic review. *Int Wound J*, 10, 121-31.
- KWAN, R. L. C., LU, S., CHOI, H. M. C., KLOTH, L. C. & CHEING, G. L. Y. 2019. Efficacy of biophysical energies on healing of diabetic skin wounds in cell studies and animal experimental models: a systematic review. *International Journal of Molecular Sciences*, 20, 368.
- KWAN, R. L. C., WONG, W. C., YIP, S. L., CHAN, K. L., ZHENG, Y. P. & CHEING, G. L. Y. 2015. Pulsed electromagnetic field therapy promotes healing and microcirculation of chronic diabetic foot ulcers: a pilot study. *Adv Skin Wound Care*, 28, 212-9.
- LEVY, R. M., PRINCE, J. M. & BILLIAR, T. R. 2005. Nitric oxide: a clinical primer. *Crit Care Med*, 33, S492-5.
- MAVROGENIS, A. F., MEGALOIKONOMOS, P. D., ANTONIADOU, T., IGOUMENOU, V. G., PANAGOPOULOS, G. N., DIMOPOULOS, L., MOULAKAKIS, K. G., SFYROERAS, G. S. & LAZARIS, A. 2018. Current concepts for the evaluation and management of diabetic foot ulcers. *EFORT Open Rev*, 3, 513-525.
- MILSOM, A. B., JONES, C. J., GOODFELLOW, J., FRENNEAUX, M. P., PETERS, J. R. & JAMES, P. E. 2002. Abnormal metabolic fate of nitric oxide in Type I diabetes mellitus. *Diabetologia*, 45, 1515-22.
- MONCADA, S., PALMER, R. M. & HIGGS, E. A. 1991. Nitric oxide: physiology, pathophysiology, and pharmacology. *Pharmacol Rev*, 43, 109-42.
- MUEHSAM, D., LALEZARI, P., LEKHRAJ, R., ABRUZZO, P. M., BOLOTTA, A., MARINI, M., BERSANI, F., AICARDI, G., PILLA, A. & CASPER, D. 2013. Non-thermal radio frequency and static magnetic fields increase rate of hemoglobin deoxygenation in a cell-free preparation. *PLoS One*, 8, e61752.
- MUSAEV, A. V., GUSEINOVA, S. G. & IMAMVERDIEVA, S. S. 2003. The use of pulsed electromagnetic fields with complex modulation in the treatment of patients with diabetic polyneuropathy. *Neurosci Behav Physiol*, 33, 745-52.

- NEIDRAUER, M., ZUBKOV, L., WEINGARTEN, M. S., POURREZAEI, K. & PAPAZOGLU, E. S. 2010. Near infrared wound monitor helps clinical assessment of diabetic foot ulcers. *J Diabetes Sci Technol*, 4, 792-8.
- NG, G. Y., CHUNG, P. Y., WANG, J. S. & CHEUNG, R. T. 2011. Enforced bipedal downhill running induces Achilles tendinosis in rats. *Connect Tissue Res*, 52, 466-71.
- NG, G. Y., NG, C. O. & SEE, E. K. 2004. Comparison of therapeutic ultrasound and exercises for augmenting tendon healing in rats. *Ultrasound Med Biol*, 30, 1539-43.
- O'BRIEN, P. D., SAKOWSKI, S. A. & FELDMAN, E. L. 2014. Mouse models of diabetic neuropathy. *ILAR J*, 54, 259-72.
- PAPAZOGLU, E. S., WEINGARTEN, M. S., ZUBKOV, L., ZHU, L., TYAGI, S. & POURREZAEI, K. 2006. Optical properties of wounds: diabetic versus healthy tissue. *IEEE Trans Biomed Eng*, 53, 1047-55.
- PAPAZOGLU, E. S., ZUBKOV, L., ZHU, L., WEINGARTEN, M. S., TYAGI, S. & POURREZAEI, K. 2005. Monitoring diabetic wound healing by NIR spectroscopy. *Conf Proc IEEE Eng Med Biol Soc*, 6, 6662-4.
- POSNETT, J. & FRANKS, P. J. 2008. The burden of chronic wounds in the UK. *Nurs Times*, 104, 44-5.
- RODRIGUEZ, P. G., FELIX, F. N., WOODLEY, D. T. & SHIM, E. K. 2008. The role of oxygen in wound healing: a review of the literature. *Dermatol Surg*, 34, 1159-69.
- RUBIN, A. E., USTA, O. B., SCHLOSS, R., YARMUSH, M. & GOLBERG, A. 2018. Selective inactivation of pseudomonas aeruginosa and staphylococcus epidermidis with pulsed electric fields and antibiotics. *Advances in Wound Care*.
- SALMEN, S. H., ALHARBI, S. A., FADEN, A. A. & WAINWRIGHT, M. 2018. Evaluation of effect of high frequency electromagnetic field on growth and antibiotic sensitivity of bacteria. *Saudi J Biol Sci*, 25, 105-110.
- SCHAFFER, M. R., TANTRY, U., EFRON, P. A., AHRENDT, G. M., THORNTON, F. J. & BARBUL, A. 1997. Diabetes-impaired healing and reduced wound nitric oxide synthesis: a possible pathophysiologic correlation. *Surgery*, 121, 513-9.
- SCHAFFER, M. R., TANTRY, U., GROSS, S. S., WASSERBURG, H. L. & BARBUL, A. 1996. Nitric oxide regulates wound healing. *J Surg Res*, 63, 237-40.
- SEGATORE, B., SETACCI, D., BENNATO, F., CARDIGNO, R., AMICOSANTE, G. & IORIO, R. 2012. Evaluations of the effects of extremely low-frequency electromagnetic fields on growth and antibiotic susceptibility of escherichia coli and pseudomonas aeruginosa. *Int J Microbiol*, 2012, 587293.
- SONEJA, A., DREWS, M. & MALINSKI, T. 2005. Role of nitric oxide, nitroxidative and oxidative stress in wound healing. *Pharmacol Rep*, 57 Suppl, 108-19.
- STRAUCH, B., HERMAN, C., DABB, R., IGNARRO, L. J. & PILLA, A. A. 2009. Evidence-Based Use of Pulsed Electromagnetic Field Therapy in Clinical Plastic Surgery. *Aesthetic Surgery Journal*, 29, 135-143.
- STRAUCH, B., PATEL, M. K., NAVARRO, J. A., BERDICHEVSKY, M., YU, H. L. & PILLA, A. A. 2007. Pulsed magnetic fields accelerate cutaneous wound healing in rats. *Plast Reconstr Surg*, 120, 425-30.
- SUMPIO, B. E. 2012. Contemporary Evaluation and Management of the Diabetic Foot. *Scientifica*, 2012, 17.
- TAUBERT, D., ROSENKRANZ, A., BERKELS, R., ROESEN, R. & SCHOMIG, E. 2004. Acute effects of glucose and insulin on vascular endothelium. *Diabetologia*, 47, 2059-71.
- THAWER, H. A., HOUGHTON, P. E., WOODBURY, M. G., KEAST, D. & CAMPBELL, K. 2002. A comparison of computer-assisted and manual wound size measurement. *Ostomy Wound Manage*, 48, 46-53.

- TIE, L., SHI, Y.-D. & LI, X.-J. 2016. Oxidative stress and diabetic wound healing. *The FASEB Journal*, 30, 1b521-1b521.
- TOMPKINS, D. T., PAULOSE, M., GRIMES, C. A., ANDERSON, M. A. & NOGUERA, D. R. 2006. Effects of localised, low-voltage pulsed electric fields on the development and inhibition of *Pseudomonas aeruginosa* biofilms AU - Perez-Roa, Rodolfo E. *Biofouling*, 22, 383-390.
- VALLEJO, S., ANGULO, J., PEIRO, C., NEVADO, J., SANCHEZ-FERRER, A., PETIDIER, R., SANCHEZ-FERRER, C. F. & RODRIGUEZ-MANAS, L. 2000. Highly glycated oxyhaemoglobin impairs nitric oxide relaxations in human mesenteric microvessels. *Diabetologia*, 43, 83-90.
- WEBB, C. Y., LO, S. S. L. & EVANS, J. H. 2003. Prevention of diabetic foot using low frequency magnetotherapy - wound management. *The Diabetic Foot*, 1-14.
- WEINGARTEN, M. S., NEIDRAUER, M., MATEO, A., MAO, X., MCDANIEL, J. E., JENKINS, L., BOURAEE, S., ZUBKOV, L., POURREZAEI, K. & PAPAZOGLU, E. S. 2010. Prediction of wound healing in human diabetic foot ulcers by diffuse near-infrared spectroscopy: a pilot study. *Wound Repair Regen*, 18, 180-5.
- WEINGARTEN, M. S., PAPAZOGLU, E. S., ZUBKOV, L., ZHU, L., NEIDRAUER, M., SAVIR, G., PEACE, K., NEWBY, J. G. & POURREZAEI, K. 2008. Correlation of near infrared absorption and diffuse reflectance spectroscopy scattering with tissue neovascularization and collagen concentration in a diabetic rat wound healing model. *Wound Repair Regen*, 16, 234-42.
- WEINGARTEN, M. S., SAMUELS, J. A., NEIDRAUER, M., MAO, X., DIAZ, D., MCGUIRE, J., MCDANIEL, J., JENKINS, L., ZUBKOV, L. & PAPAZOGLU, E. S. 2012. Diffuse near-infrared spectroscopy prediction of healing in diabetic foot ulcers: a human study and cost analysis. *Wound Repair Regen*, 20, 911-7.
- WEISSMAN, B. A., JONES, C. L., LIU, Q. & GROSS, S. S. 2002. Activation and inactivation of neuronal nitric oxide synthase: characterization of Ca(2+)-dependent [125I]Calmodulin binding. *Eur J Pharmacol*, 435, 9-18.
- WILLIAMS, S. B., GOLDFINE, A. B., TIMIMI, F. K., TING, H. H., RODDY, M. A., SIMONSON, D. C. & CREAGER, M. A. 1998. Acute hyperglycemia attenuates endothelium-dependent vasodilation in humans in vivo. *Circulation*, 97, 1695-701.
- XU, Y., WANG, L., HE, J., BI, Y., LI, M., WANG, T., JIANG, Y., DAI, M., LU, J., XU, M., LI, Y., HU, N., LI, J., MI, S., CHEN, C. S., LI, G., MU, Y., ZHAO, J., KONG, L., CHEN, J., LAI, S., WANG, W., ZHAO, W. & NING, G. 2013. Prevalence and control of diabetes in Chinese adults. *JAMA*, 310, 948-59.
- ZHAO, G., HOCHWALT, P. C., USUI, M. L., UNDERWOOD, R. A., SINGH, P. K., JAMES, G. A., STEWART, P. S., FLECKMAN, P. & OLERUD, J. E. 2010. Delayed wound healing in diabetic (db/db) mice with *Pseudomonas aeruginosa* biofilm challenge: a model for the study of chronic wounds. *Wound repair and regeneration : official publication of the Wound Healing Society [and] the European Tissue Repair Society*, 18, 467-477.
- ZHAO, G., USUI, M. L., UNDERWOOD, R. A., SINGH, P. K., JAMES, G. A., STEWART, P. S., FLECKMAN, P. & OLERUD, J. E. 2012. Time course study of delayed wound healing in a biofilm-challenged diabetic mouse model. *Wound repair and regeneration : official publication of the Wound Healing Society [and] the European Tissue Repair Society*, 20, 342-352.